Earth-Science Reviews 153 (2016) 43–76

Contents lists available at ScienceDirect

Earth-Science Reviews

journal homepage: www.elsevier.com/locate/earscirev

The role of the cryosphere in source-to-sink systems

John M. Jaeger [a,*], Michele N. Koppes [b]

[a] Department of Geological Sciences, University of Florida, Gainesville, FL 32611-2120, USA
[b] Department of Geography, University of British Columbia, 1984 West Mall, Vancouver, BC V6T1Z2, Canada

ARTICLE INFO

Article history:
Received 17 November 2014
Received in revised form 14 September 2015
Accepted 22 September 2015
Available online 25 September 2015

Keywords:
Ice dynamics
Glacial history
Glacigenic sediment
Glacimarine sedimentary processes
High-latitude continental margins
Quaternary stratigraphy

ABSTRACT

Glacial erosion and sediment production are of interest to diverse scientific communities concerned with the interaction of climatic, tectonic and surface processes that influence the evolution of orogens and with the climatic signals archived in glacigenic strata. We review the current state of knowledge on the generation, transfer, and accumulation of glacigenic sediment from land to sea. We draw from geomorphology, marine geology, geochronology, numerical modeling of surface processes and landscape evolution, and experimental and field observations of glacier erosion and deposition, and the interaction of ice with its bed and the ocean boundary. Our primary goal is to examine glacial systems using a holistic source-to-sink approach, with a focus on describing a) how glacial motion produces sediment, b) how the sediments (sink) record the dynamic nature of glacial systems under different climatic (thermal) regimes, c) the challenges in using the sedimentary record to interpret these dynamics in space and time, and d) the approaches still needed to further our understanding of how ice and associated sediment fluxes respond to climatic and other perturbations. The dynamic state of ice, i.e., the ice flux and ice extent, is defined differently between the source and sink communities, reflecting the challenges of establishing a stratigraphic signal that volumetrically constrains glacigenic sediment production as a function of the ice response to climate. Advances in marine geophysics have greatly assisted our understanding of mass transfer pathways and of former ice extents as a measure of ice dynamics, and have identified the primary depocenters and key lithofacies of glacial sinks. Sediment fluxes associated with the dynamic state of the ice are best constrained where sediment volumes derived from key lithofacies and seismic reflection isopachs can be temporally partitioned, of which there are few examples, rather than from discrete point measures of sediment flux that are subject to sediment transfer biases. Forward numerical modeling of sediment fluxes as a function of ice dynamics agree with observational data at the continental-margin scale, but finer time/space scale ice-dynamic models do not yet recreate observed ice extent or flowpaths. Future source-to-sink work in glaciated systems should focus on refining empirical relationships between ice velocity and sediment production, and expand the application of existing methods to develop sediment volumes and fluxes in known depocenters of former and modern ice streams.

Contents

1. Introduction . . . 44
   1.1. Is the modern the key to interpreting the past? . . . 45
2. Signals from the source: the role of glaciers in sediment production . . . 47
   2.1. Ice dynamics: characteristic timescales of response and controls on thermal regime . . . 47
   2.2. The generation of glacigenic sedimentary signals . . . 48
      2.2.1. Theoretical framework . . . 48
      2.2.2. Observations of glacial erosion and sediment production . . . 49
      2.2.3. Modeling erosion and sediment production under conditions of glaciation . . . 51
3. Linking the source to the sink: glacigenic signal transfer . . . 51
4. The sink-fidelity of the glacigenic signal . . . 55
   4.1. Conditions that influence the magnitude of the mass flux signal . . . 57
   4.2. Examples of signal fidelity at various timescales in the glacigenic sink . . . 58

* Corresponding author.
E-mail address: jmjaeger@ufl.edu (J.M. Jaeger).

http://dx.doi.org/10.1016/j.earscirev.2015.09.011
0012-8252/© 2015 Published by Elsevier B.V.

4.2.1. Sub-annual to annual time scales . . . 58
4.2.2. Advance-retreat/surge time scales . . . 58
4.2.3. Post-LGM deglacial timescales . . . 60
4.2.4. Quaternary glacial–interglacial cycles . . . 62
4.3. Modeling ice dynamics and sediment fluxes to the sink . . . 65
5. Conclusions and future directions . . . 67
5.1. Deriving erodibility metrics for landscape evolution . . . 68
5.2. Chronostratigraphic control of geomorphic and seismic stratigraphic features . . . 68
5.3. Deciphering local (autogenic) from regional/global (allogenic) controls on ice dynamics and sediment production . . . 68
5.4. Modern analog approach to glacial source-to-sink studies . . . 69
Acknowledgments . . . 69
References . . . 69

1. Introduction

A principal goal of examining a sediment routing system is to understand how it responds to, and preserves a record of, the dynamic processes that drive sediment production and transfer. This is especially important in settings where the principal geomorphic agent that produced the sediment is no longer present or challenging to work with under modern conditions. Global climate during the Quaternary Era is distinguished by the periodic intensification of glacial conditions on land and along continental margins (Larsen et al., 1994; McKay et al., 2009; Lourens et al., 2010; Jakobsson et al., 2014). The onset of widespread glaciation is viewed as responsible for the global increase in sedimentation that coincided with a change to a cooler and more variable climate beginning ~2–4 Myr ago, creating clastic wedges on continental margins that are up to 5 km thick (Eyles et al., 1991; Vorren et al., 1991; Eidvin et al., 1993; Faleide et al., 1996; Elverhøi et al., 1998a; Solheim et al., 1998; Laberg et al., 2010). The majority of mid- and high-latitude landscapes, from the land to the deep sea, reflect extensive Quaternary glacial influence (Bingham et al., 2010; Champagnac et al., 2014; Pedersen et al., 2014), including large-scale depositional and erosional landforms such as voluminous loess and paraglacial terrestrial deposits (e.g., Derbyshire, 2003), scablands carved by meltwater (e.g., Hanson et al., 2012), ice-gouged seafloors (e.g., Dowdeswell and Bamber, 2007; Dowdeswell et al., 2007; Batchelor et al., 2011; Cofaigh et al., 2012; Dowdeswell et al., 2014), and thick accumulations of glacimarine sediments both on land and in the ocean (e.g., Eyles et al., 1991; Dahlgren et al., 2005; Laberg et al., 2010). Glacial source-to-sink systems consequently are a primary archive of past and present global change.

Glacial erosion and sediment production are of interest to a wide variety of scientific communities concerned with the interaction of climatic, tectonic and surface processes that influence the evolution of mountain ranges, and with the interpretation of climatic and tectonic signals archived in sediments produced by the ice. Glaciated landscapes were one of the first depositional environments where sedimentary signals such as glacial drift, erratics, and moraines were formally interpreted to describe a series of dynamic ice processes that were either absent from or significantly reduced in scale in the current landscape. Since the mid-1800s, glacial chronologies have been developed for many regions where the ice was once more extensive (e.g., Agassiz, 1840; Lyell, 1840; Chorley, 1973), and past global ice volumes have been estimated from the oxygen isotopic record preserved in marine sediments (Imbrie et al., 1984; Lisiecki and Raymo, 2007). While the marine isotope stage (MIS) records have provided broad constraints on the timing of recent and Quaternary glaciations (e.g., Lisiecki and Raymo, 2007; Kawamura et al., 2008), less is known about the internal dynamics of former glaciers and ice sheets and their relationship to climate. Over a century later, we are still grappling with how to link dynamic glacial processes with their sedimentary and geomorphic products.

Landscape modification by ice is profound. Our ability to evaluate how glaciers and glacial erosion shape landscapes, produce sedimentary signals, and reflect climatic (or tectonic) variability is still limited by a dearth of information about what controls the rate of glacial erosion and sediment production. Climate drives a glacier's mass balance, which in turn determines the ice flux that erodes the landscape (e.g., Benn and Evans, 2010; Cuffey and Paterson, 2010). Terrestrial and marine subglacial and proglacial environments are among the most logistically challenging environments to work in, hampering our ability to develop first-order relationships between ice dynamics and sediment production. Moreover, generating a chronology on the timing and magnitude of glacial erosion and deposition has always been challenging (e.g., Balco and Rovey, 2010; Fastook and Hughes, 2013; Ingólfsson and Landvik, 2013; Cofaigh et al., 2014), often requiring multiple approaches (Livingstone et al., 2012; Fastook and Hughes, 2013), but has recently become more robust with evolving geochronometric techniques (e.g., Rosenheim et al., 2008; Balco and Rovey, 2010; Simon et al., 2012).

Glacial source-to-sink systems are unique in that ice, the primary erosional agent, can move through almost the entire length of a system, from the high mountains to the continental shelf edge, during one climatic period and then be entirely absent during others (Fig. 1). Moreover, ice responds to climate by adjusting its spatial extent and its internal flow dynamics (e.g., Raymond, 1987), which vary in space and time its capacity to do geomorphic work and produce sediment. In addition, the potential for ice to recycle its sedimentary record as it advances and retreats through the transfer zone results in an incomplete record of dynamics closest to the ice, and an integrated record beyond the last ice maximum extent (Fig. 1; e.g., Faleide et al., 1996; Hebbeln et al., 1998; Anderson, 1999; Cofaigh et al., 2002; Hemming, 2004). The most complete record often exists in the marine realm, but this setting is subject to its own internal dynamics that mute terrestrial ice signals, and often results in a record that is overprinted by oceanographic processes and tectonic preconditioning of the basin (Figs. 1 and 2; Cofaigh et al., 2002; Nygård et al., 2005; Reece et al., 2011; Andrews and Vogt, 2014; Walton et al., 2014; Romans et al., 2016–this volume). As such, the sedimentary record associated with both ice flux as well as ice sheet growth and decay can reflect both autogenic and allogenic forcing, complicating our ability to directly relate ice dynamics and sediment production to any particular climatic forcing.

Yet, given these limitations, we still are able to develop general conceptual and quantitative models of the role of ice in the production of a sedimentary signal (Figs. 1 and 2). On orbital time scales, the growth and decay of ice has a global signal (Lisiecki and Raymo, 2007; Lourens et al., 2010; Patterson et al., 2014). At higher temporal resolutions, the terrestrial and marine stratigraphic records of glacier and ice sheet dynamics contain a combination of local and regional processes and influences, including the climate, thermal regime of the ice, subglacial hydrology, bedrock lithology, drainage basin topography and size, oceanographic setting, sea level, and tectonic conditioning. For instance, both sediment and meltwater production vary by orders of magnitude over time (e.g., seasonally), as a consequence of the thermal regime of the ice (i.e., temperate versus polar glacial systems), and between

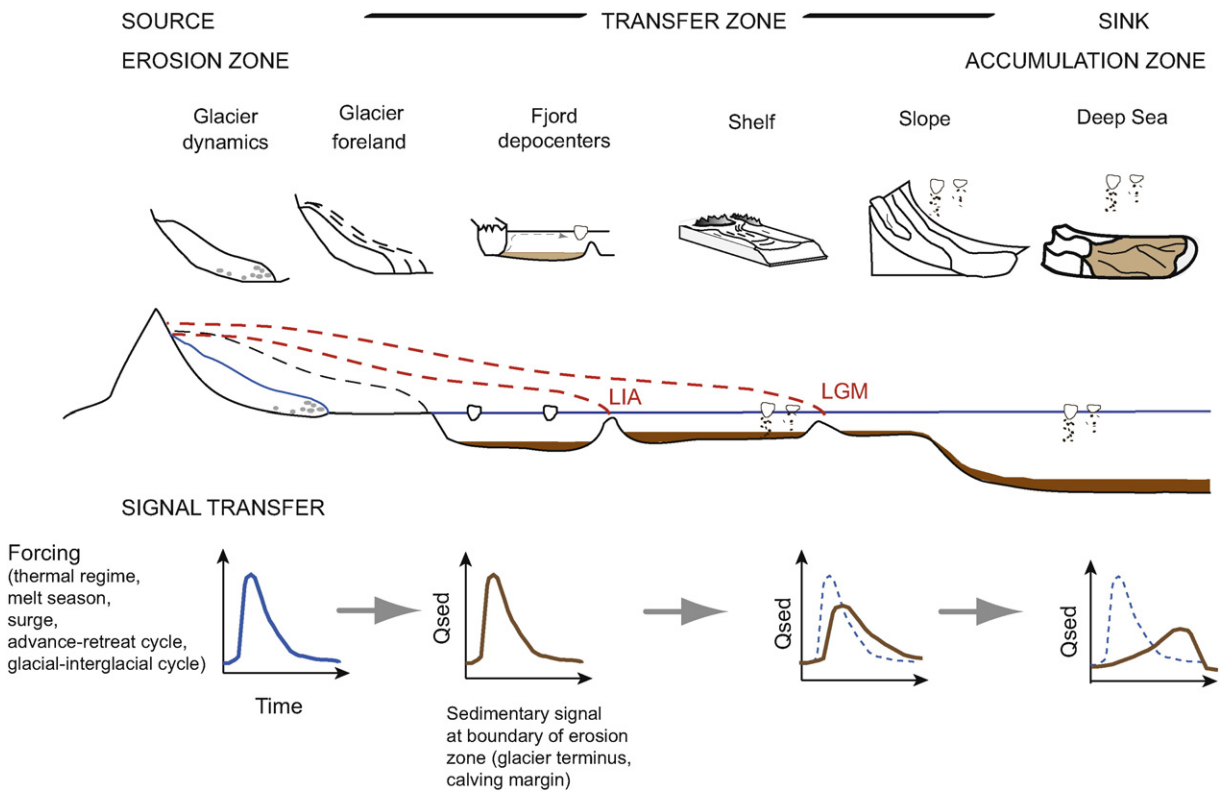

Fig. 1. Overview of glacigenic "signal" production and transfer through a glaciated source-to-sink system. In upper panel, modern high-latitude ice position shown in blue with hypothetical Neoglacial and Pleistocene ice positions shown as orange dashed lines. In lower panel, ice responds to climate forcing (blue curve), eroding the bed and creating a sedimentary signal (brown curve) that is reduced in intensity and is lagged in time as it moves through the transfer zone (fjord, shelf) to ultimately accumulate in the marine sink. Modified from Romans et al. (2016–this volume).

tectonically active and quiescent margins (Koppes and Montgomery, 2009; Koppes et al., 2015). Still, across all thermal and tectonic regimes there are consistent geomorphic and sedimentary signatures that reflect this glacigenic influence, including tills, glacimarine diamicts, ice-rafted debris, moraines, megascale glacial lineations, and grounding zone wedges (e.g., Carlson et al., 1977; Licht et al., 1999; St. John and Krissek, 1999; Stokes and Clark, 2001; Anderson et al., 2002; Cofaigh et al., 2007; Ottesen et al., 2008b; Hambrey and Glasser, 2012; Livingstone et al., 2012; Ingólfsson and Landvik, 2013; Batchelor and Dowdeswell, 2014).

The ultimate goal of studying a glacial sediment routing system is to relate changing boundary conditions including climate, tectonics, ice extent and ice surface topography to the ice response, which in turn generates a mass flux signal. Documenting the relative roles of glacial dynamics and the thermal state of the ice on sediment production and strata formation is the first step (Fig. 1). Developing quantitative models for glacial and glacimarine settings follows, and is paramount for advancing our ability to a) predict how changes in sediment production and transfer are routed through a glacial system, in order to b) interpret the resulting stratigraphic record.

1.1. Is the modern the key to interpreting the past?

How applicable are modern process-based studies for deciphering the Pleistocene landscape? Much of the Quaternary was a significantly colder and more ice-dominant period, yet all of the observations have been made in a distinctively warmer climatic period following the end of the Little Ice Age (LIA; Oerlemans, 2005) and within a relatively warm Pleistocene interglacial period. Decades of field studies have attempted to interpret the modern sedimentary glacigenic record to reconstruct the ice dynamics that create sediment (e.g., Anderson et al., 1980; Powell, 1983; Mackiewicz et al., 1984; Griffith and Anderson, 1989; Powell and Molnia, 1989; Cowan and Powell, 1990; Domack and Williams, 1990; Phillips et al., 1991; Domack and Ishman, 1993; Hunter et al., 1996a; Cowan et al., 1998; Ashley and Smith, 2000; Jaeger, 2002; Hambrey and Glasser, 2012). Does this modern perspective result in a bias in our understanding of the relative magnitude of glacial processes in the past? For example, erosion rates that have been inferred from contemporary sediment yields of temperate tidewater glaciers far surpass those of polar and alpine glaciers (Gurnell et al., 1996; Hallet et al., 1996; Koppes et al., 2015). Moreover, modern (annual to centennial) erosion rates far outpace erosion rates averaged over the long term (10^3–10^6 years) from these same glaciers (Fig. 3; Berger and Spotila, 2008; Delmas et al., 2009; Koppes and Montgomery, 2009; Fernandez et al., 2011). The two- to three-order of magnitude difference in apparent erosional efficiency of these glaciers over annual to million-year timescales brings into question what aspects of modern settings or analogs of processes may be biased by the current "warm" glaciological conditions.

Building on the pioneering 19th century work by Agassiz, Lyell and others, the field of glacial geology has witnessed a wide-ranging effort, from ice sheet summits to deep sea basins, to document and explain how ice shapes the land-ocean–atmosphere interface. Recent recognition that our currently warming climate is accelerating terrestrial ice loss (Rignot et al., 2014), with notable societal impacts (Marzeion et al., 2014), has only heightened our need to understand how ice has responded in the past to climatic perturbations. Here we review the current state of knowledge on the generation, transfer, and accumulation of glacigenic sediment from terrestrial sources to continental-margin sinks (see Fig. 1 for our conceptual approach). We draw on the state of knowledge from various disciplines, including geomorphology, marine geology, geochronology, numerical modeling of surface processes and

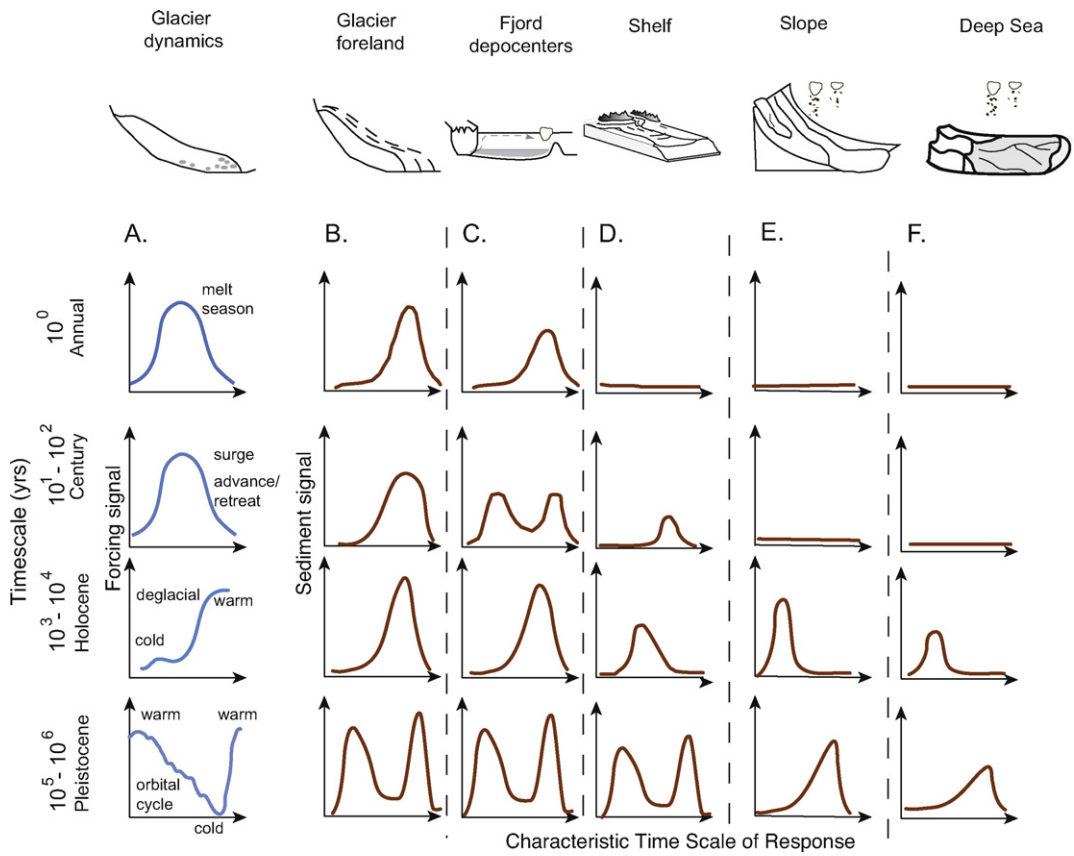

Fig. 2. Several scenarios of glacigenic "signal" transfer through the morphodynamic segments of glacial sediment dispersal systems. Four typical climate-forced scenarios of ice response, from the seasonal to the 100-kyr timescales, are displayed in column A. Relative rates of glacigenic sediment flux as a function of climatic forcing in each dispersal segment are presented in columns B–F, as viewed from a modeling or an observational perspective. The timescale (rows) reflects the characteristic response time for glaciers to difference climatic forcings. The glacigenic depositional signal will vary in space and time depending on the proximity to the ice margin, periodic coverage by flowing ice, and the number of intervening basins to trap the signal. For example, under modern conditions (top row), annual cycles of glacial meltwater discharge are expected to generate an annual sediment pulse that deposits a signal in the glacier foreland and in fjords but is not recorded in open marine conditions. However, signals produced at all timescales have the potential to be recorded in the glacier foreland to the deep sea depending on the relative ice extent within the transfer zone. See text for additional explanation of scenarios.

landscape evolution, experimental and field observations of glacier erosion and deposition, the interaction of ice with its bed, and of meltwater with the ocean, to highlight the processes and controls on glacigenic sedimentary signals from source to sink. Given the long history of glacial studies, comprehensive reviews already exist on the fundamentals of glacial and glacimarine processes and strata formation under the full

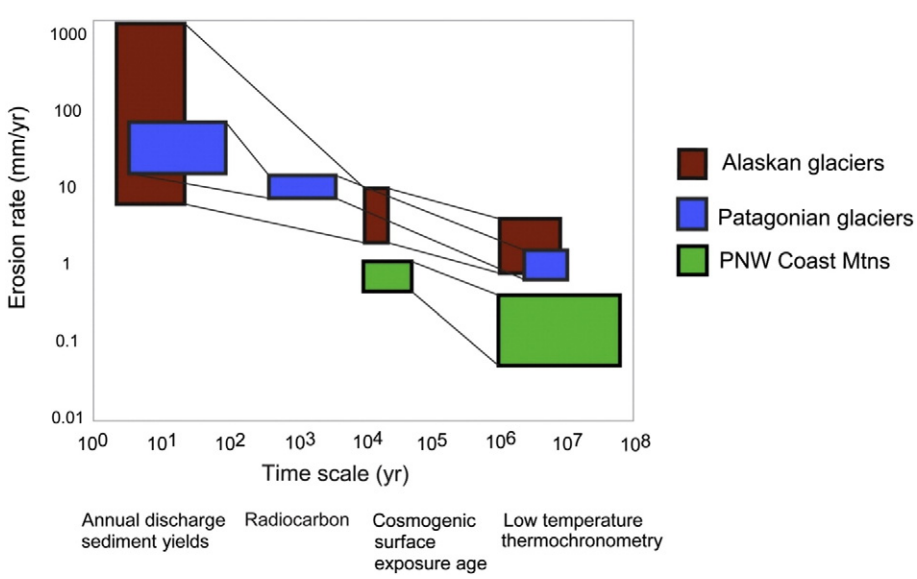

Fig. 3. Comparison of short-term and long-term erosion rates measured using a range of chronometric techniques from the same glaciated basins in Alaska, Patagonia, and the Coast and Cascade Mountains of Washington State and British Columbia. Boxes represent the range of erosion rates, including uncertainty in estimation (height) and timescale of measurement (width). Chronometric techniques used to quantify erosion rate, and the timescales of measurement, are at bottom. Modified from Koppes and Montgomery (2009).

range of climatic conditions (Molnia, 1983; Anderson, 1999; Stokes and Clark, 2001; Bennett, 2003; Benn et al., 2007; Winsborrow et al., 2010; Cook and Swift, 2012; Hambrey and Glasser, 2012; Livingstone et al., 2012; Landvik et al., 2014). Rather, our primary goal here is to examine glacial systems from a synoptic source-to-sink viewpoint, with a focus on describing: a) how glacial motion produces sediment; b) how the sedimentary record (sink) records the dynamic nature of glacial systems under different climatic (thermal) regimes; c) the challenges in using the sedimentary record to interpret these dynamics in space and time; and d) the approaches still needed to further our understanding of how ice and sediment fluxes may respond to future climatic and other perturbations. Fig. 2 serves as our conceptual model of the key spatial and temporal components of a holistic source-to-sink understanding of glacial systems.

2. Signals from the source: the role of glaciers in sediment production

A rigorous understanding of the processes that create the glacigenic sedimentary signal is necessary to infer climatic and glaciological changes from complex stratigraphic records. Climate dictates the ice flux and thus the geomorphic work done by the ice generating the sedimentary mass flux signal. Changes in sedimentary mass flux correspond with seasonal-, annual-, centennial- and millennial-scale ice dynamics that reflect different climate forcings (Fig. 2, column A). Ice extents define the boundary conditions and the magnitude of the spatial response, but do not necessarily elucidate the ice dynamics, i.e., the flux response of the ice to climate drivers. The primary means by which we can interpret the sink in terms of its ability to resolve these ice dynamics is based on observations in modern settings, where the relationship between current ice dynamic states (mass balance, mass transfer, and thermal regime) and the bedforms, strata and mass fluxes generated can be established. The interpretive approach can either be inverse (i.e., using the sedimentary record to infer ice dynamics) or forward (i.e., employing coupled ice–sediment–landscape evolution models) (e.g., Braun et al., 1999; Dowdeswell and Siegert, 1999; Tomkin and Braun, 2002; MacGregor et al., 2009; Herman et al., 2011; Egholm et al., 2012; Yanites and Ehlers, 2012). In this section we review the fundamental controls on glacial erosion and sediment production, starting with the controls on ice dynamics and how they reflect climate, and then address how changes in ice dynamics influence the amount and timing of sediment production and transfer to the terrestrial–marine boundary.

2.1. Ice dynamics: characteristic timescales of response and controls on thermal regime

Glaciers and ice sheets are large, dynamic stores of water, constantly exchanging mass and energy with the atmosphere, the hydrosphere and the lithosphere (Benn and Evans, 2010). The growth of a glacier or ice sheet is dictated by its mass balance, the net accumulation of snow (and its conversion to ice) minus the mass loss by melting and calving, which in turn depend on climate and local topographic factors. At the most basic level, alpine glaciers and terrestrial ice sheets thicken and advance when the overall mass balance (accumulation minus mass loss) is positive, and thin and retreat when the mass balance is negative. Similarly, glacier temperature is a function of the inputs/outputs of energy at the surface and the bed, and controls the rate of ice motion through deformation and sliding (Cuffey and Paterson, 2010). Fluctuations in glacier mass balance and temperatures are therefore strongly coupled responses to climate change. A glacier's climate sensitivity is the magnitude and timing of changes in mass balance in response to a given perturbation in temperature and/or precipitation. The mass balance dictates both the extent of the ice (its growth and decay), the flux of ice and meltwater through the glacial system (i.e., the transfer of mass from accumulation to ablation zones) and the average ice thickness. The ice flux and the ice thickness in turn control the conditions at the glacier bed, primarily the basal water pressure and rate of basal ice motion, which dictate the capacity of the ice to do geomorphic work on the bed (i.e., to erode) (see Fig. 4; Hallet, 1979, 1996; Iverson, 1991, 2012). For a rapidly moving glacier, much of the ice motion is due to basal sliding, which is needed for the ice to erode; in contrast, for a glacier that is slow-moving (i.e., partially frozen to its bed), much of the motion is due to internal deformation of the ice (Fig. 4A). Hence, climatic differences between regions, as well as within a glaciated basin over time, dictate variations in mass balance, basal temperature, availability of meltwater and ice flow in space and time, which in turn influences the sediment yield and the sedimentary signal (e.g., Hallet et al., 1996; Dowdeswell et al., 1998; Koppes and Montgomery, 2009; Herman et al., 2015; Koppes et al., 2015).

To first order, global climate forced by orbital control on insolation has long been recognized as the primary driver for Quaternary glacier and ice sheet mass balance on millennial time scales (Fig. 2, column A); however, interactions with climate are complex and non-linear. For instance, the high albedo of snow and ice acts as a positive feedback on ice sheet mass balance (e.g., Box et al., 2012; Dumont et al., 2014). The presence of a continental-scale ice sheet impacts global and local patterns of air circulation, creating stable high-pressure zones with

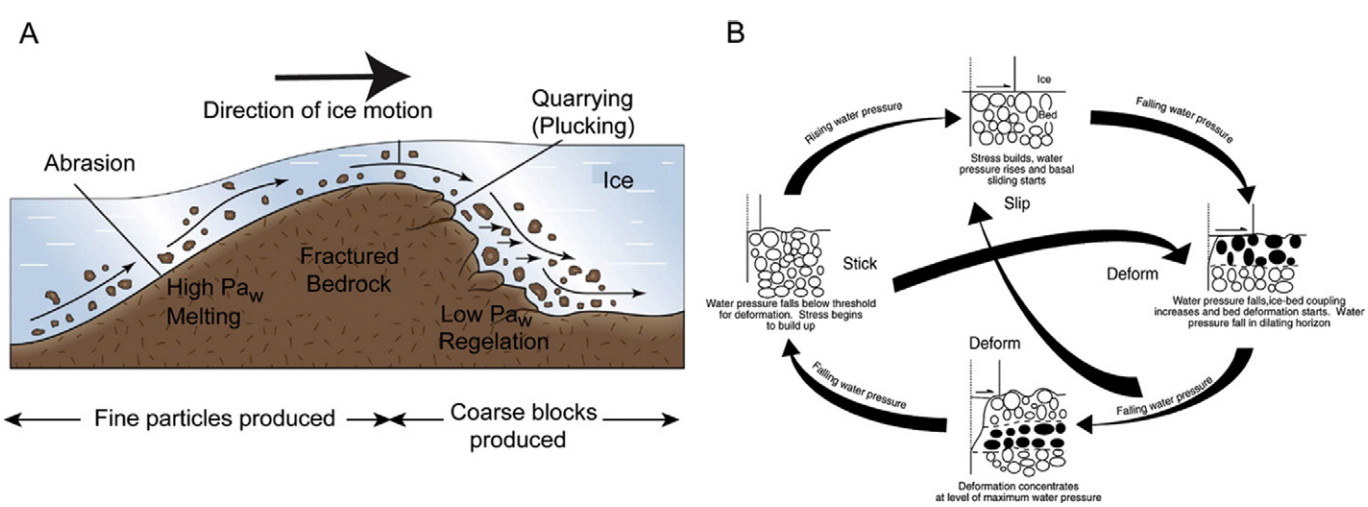

Fig. 4. Modes of glacial erosion, sediment production and sediment transfer. (A) Quarrying (plucking) and abrasion are the dominant mechanical processes of erosion at the glacier bed, and both are a function of ice motion and subglacial water pressure. (B) Stick–slip cycle of basal motion in a deformable bed under an ice stream, showing the importance of the modulation of subglacial water pressure for motion and deformation. From Boulton et al. (2001) and Bennett (2003).

steep pressure gradients that discourage inflow of moist air and enhance buoyancy-driven katabatic winds (e.g., Steffen and Box, 2001; Parish and Bromwich, 2007). Moreover, ice sheets can modify precipitation patterns due to orographic factors, resulting in enhanced accumulation rates nearest the coasts (Roe, 2005).

At the subannual timescale, seasonal melting is the most important driver of ice dynamics, particularly for temperate systems where meltwater can more readily reach the ice-bed interface without refreezing, and help both lubricate the interface to increase ice flux and do geomorphic work on the bed (Alley et al., 1997). Hence, seasonal melt dominates the seasonal-annual sedimentary flux signal (Fig. 2A, B). Water input is known to vary on a daily basis during the summer season, which has an important effect on sliding velocities (e.g., Iken and Bindschadler, 1986; Bartholomaus et al., 2007). Seasonal meltwater fluctuations have strong control on subglacial channel dimensions (Boulton et al., 2007) and sliding velocities (e.g., Iken and Bindschadler, 1986; Bartholomaus et al., 2007; Joughin et al., 2008; Pimentel and Flowers, 2010; Schoof, 2010). In the winter, subglacial water conduits close because of lower water pressures, and any unfrozen water is trapped in a network of linked cavities. Increased melt rates in summer drive higher subglacial water discharge and the formation of larger, more efficient channels, and the subglacial drainage system evolves accordingly. Therefore, it is likely that every year, there is a period when drainage networks shift from sluggish to efficient flow to drain subglacial meltwater. During this shift, subglacial water pressure is large and effective pressure is low, which promotes sliding and erosion, and the linked production of a sediment pulse (Fig. 2B).

On decadal to centennial timescales, such as the Little Ice Age (LIA), several studies have demonstrated a primary relationship between glacier mass balance and inter-annual variability in large-scale atmospheric circulation patterns, variation in solar cycles, and changes in oceanic temperatures and circulation. For instance, a decade of positive mass balance can force temperate glacier surges (Eisen et al., 2001). In the Andes, higher sea-surface temperatures associated with El-Niño events have been linked with persistent negative mass balance of the Peruvian ice caps (Thompson et al., 1984). In western North America, the Pacific Decadal Oscillation drives contrasting patterns of winter snowfall, creating negative mass balances for Pacific Northwest glaciers, but positive mass balance for Alaskan glaciers (Bitz and Battisti, 1999). Across south-central Greenland, a strengthening and warming of the subpolar Irminger current have been linked to increases in submarine melting and the acceleration of the ocean-terminating outlet glaciers of the Greenland ice sheet (e.g. Rignot et al., 2010; Motyka et al., 2011; Straneo and Heimbach, 2013).

Glaciers respond to climatic perturbations that affect their net mass balance by adjusting their width, length, and thickness (Dowdeswell et al., 1995; Eisen et al., 2001; Harrison and Post, 2003; Davis et al., 2009; Menounos et al., 2009; Roe and Baker, 2014). There is a lag in the adjustment of the ice that depends on the response time of the glacier, which is dictated by its geometry (Roe and Baker, 2014). Modern observations of alpine glaciers show response times from several years to decades (Harrison et al., 2001; Oerlemans, 2005; Menounos et al., 2009). Temperate glaciers are known to surge within a few decades following changes in mass balance, releasing large volumes of sediment and meltwater (Fig. 2A, B) (Eisen et al., 2001; Striberger et al., 2011). Alpine glacial termini advanced within a few centuries associated with LIA cooling, and their subsequent retreat occurred within ~50–100 years (Oerlemans, 2005; Barclay et al., 2009). The end of the LIA in Alaska is reflected in increased proglacial sediment accumulation and glacigenic sediment discharge (Fig. 2B; Molnia and Post, 1995; Wiles et al., 1999; Barclay et al., 2009; Crossen and Lowell, 2010; Jaeger and Kramer, 2014). Proxy records of ice retreat associated with the abrupt warming transition at the Bølling interstadial at ~14.8 ka BP indicate a response time within the precision of the chronometer (several hundred years; Praetorius and Mix, 2014).

However, the timing and magnitude of retreat can be unrelated or minimally related to climate forcing, which is particularly true of glaciers in marine-terminating settings. Many modern outlet glaciers terminate in fjords or lakes, and their response to climate is complicated by their sensitivity to non-climatic influences such as terminus geometry, sediment delivery to the terminus, ice-front melt rates, and water depth (Meier and Post, 1987; Powell, 1991; van der Veen, 1996; Warren and Aniya, 1999; Motyka et al., 2003; O'Neel et al., 2005; Pfeffer, 2007; Rignot et al., 2010). Consequently, advance-retreat histories of calving glaciers contain a record both of past climate and of changing ice-front dynamics.

2.2. The generation of glacigenic sedimentary signals

2.2.1. Theoretical framework

According to theory and experimental evidence, the two fundamental mechanical processes that govern the erosion and shaping of landscapes by ice are: a) quarrying of rock blocks from rough edges of the subglacial bed; and b) abrasion of rock that smoothens and polishes the bed (Fig. 4; Boulton, 1979; Hallet, 1979, 1996; Iverson, 1991, 2012). In certain climates and lithologies, abrasion and chemical denudation by meltwater also may play a significant role in erosion; however, less is known about these mechanisms (Anderson and Anderson, 2010). These theories all suggest that subglacial water pressure, and corresponding basal sliding velocity, are the dominant mechanisms that control the tempo of subglacial erosion. Warmer annual temperatures and higher precipitation rates (both rain and snow) favor meltwater production, which is likely to increase the basal water pressure, leading to faster sliding and more erosion (Fig. 2; Iken and Bindschadler, 1986; Bartholomew et al., 2010). High basal water pressures also are thought to promote subglacial erosion by quarrying, especially where they fluctuate frequently (Fig. 4; Hallet, 1996; Iverson, 2012). Indeed, for temperate glaciers, observational data have correlated increases in sliding velocities (inferred from measured increases in glacier surface speeds) with increases in the production and transport of glacial sediment (Fig. 5; e.g., Humphrey and Raymond, 1994; Anderson et al., 2004; Riihimaki et al., 2005; Herman et al., 2015; Koppes et al., 2015).

In polar glaciers and ice sheets where cold-based ice (below the pressure melting point) dominates, glacial erosion and sediment transfer rates decrease significantly (Hallet et al., 1996; Elverhøi et al., 1998a; Cuffey et al., 1999; Koppes et al., 2015). As mean air temperatures drop well below 0 °C, the production of sediment by glacial erosion decreases progressively as surface melt vanishes, because little or no water reaches the bed from the glacier surface to facilitate glacier sliding and erosion. Sediment production is greatly limited once the basal ice temperature drops below the melting point, and erosion rates are then

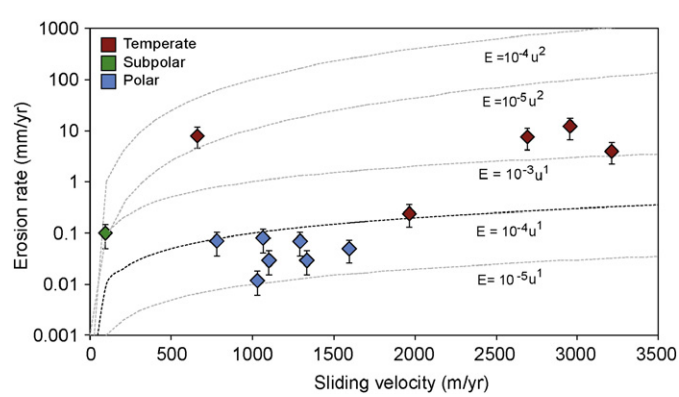

Fig. 5. Erosion rate and basal sliding velocity for 15 outlet glaciers from Patagonia to the Antarctic Peninsula. Dashed lines represent the regression relationship used to define the constants of proportionality used in the 'erosion rule'; black dashed line is the most commonly used form where $n = 1$ and $K_g = 10^{-4}$. Modified from Koppes et al. (2015).

dominated by slow mechanical processes associated with ice deformation (Hallet et al., 1996; Cuffey et al., 1999). The role of glacial meltwater in transporting sediment subglacially also diminishes as the air cools because subfreezing conditions shut off the dominant source of water; the amount generated through frictional heating at or near the glacier bed has little impact on sediment transport (e.g. Cuffey and Paterson, 2010). Under these circumstances, sediment transport under the glacier is presumed to take place primarily in a deforming basal till layer and in basal ice, and not by subglacial or englacial streams (Fig. 4; Griffith and Anderson, 1989; Hooke and Elverhoi, 1996; Powell et al., 1996; Bennett, 2003). However, recent sediment yield data from an outlet glacier in Greenland suggest that efficient subglacial drainage of surface meltwater in the wet snow zone close to the edges of the Greenland ice sheet may create a zone of rapid erosion along the margins of cold-based (polar) ice sheets (Cowton et al., 2012).

Several aspects of the processes and mechanics of glacier erosion remain unconstrained. In contrast to fluvial studies, where the importance of bedrock lithology in fluvial incision rates has been demonstrated (e.g., Stock and Montgomery, 1999), the explicit influence of rock type on glacial erosion is still little understood (Alley et al., 2003). Both chemical weathering rates (Anderson, 2005) and fracture intensity may also influence glacial erosion rates (Dühnforth et al., 2010; Becker et al., 2014). The degree to which the presence of subglacial meltwater and sediment at the bed affects both short-term and long-term glacial erosion is also still debated. For example, glacial hydrology is expected to influence sediment transfer by accelerating sliding, and hence erosion, in the ablation zone where abundant meltwater is available (e.g., Herman et al., 2011; Egholm et al., 2012). Theoretical models for subglacial abrasion highlight the influence of sediments carried by the ice as a driving factor for subglacial erosion (Hallet, 1979, 1996; Iverson, 1991, 2012). Yet, sediments may also act to reduce erosion if allowed to accumulate at the bed and provide a protective cover for the bedrock surface (e.g., Egholm et al., 2012). Moreover, subglacial storage of sediments will also delay the timing between the production of sediment through erosion and its sedimentary signal at the ice front and beyond.

2.2.2. Observations of glacial erosion and sediment production

Quantifying the controls and timing of glacier erosion is central to understanding the role of climate forcing on the development of sedimentary signals in a glacial sediment routing system, yet relationships between these controls are still poorly understood. In part this is due to the difficulty of making direct observations and measurements of glacial erosion beneath or directly in front of active glaciers. There is also a paucity of techniques to measure rates of erosion over both short and long timescales in glacially modified landscapes. Sediment accumulation patterns, rates and volumes near glacier termini in fjords of the northern and southern hemispheres have been examined using sequential bathymetric maps, seismic-reflection surveys, sediment traps and radioisotope analyses (e.g., Molnia, 1983; Cowan and Powell, 1990, 1991; Domack and Ishman, 1993; Hallet et al., 1996; DaSilva et al., 1997; Elverhøi et al., 1998a; Jaeger and Nittrouer, 1999a, 1999b; Koppes and Hallet, 2002, 2006; Koppes et al., 2009, 2010; Szczucinski et al., 2009; Fernandez et al., 2011). Based on these measures of short-term sediment yields, the rapidity with which glaciers erode the bed can be high, in some instances for temperate glaciers, far outpacing the erosion rate of rivers (Fig. 6; Gurnell et al., 1996; Hallet et al., 1996; Koppes and Montgomery, 2009). However, the relationship between the magnitude and timing of sediment yields measured today and of the geomorphic and dynamic processes that produce the erosional signal have received remarkably little attention, and with a few notable exceptions (e.g., Riihimaki et al., 2005; Koppes and Hallet,

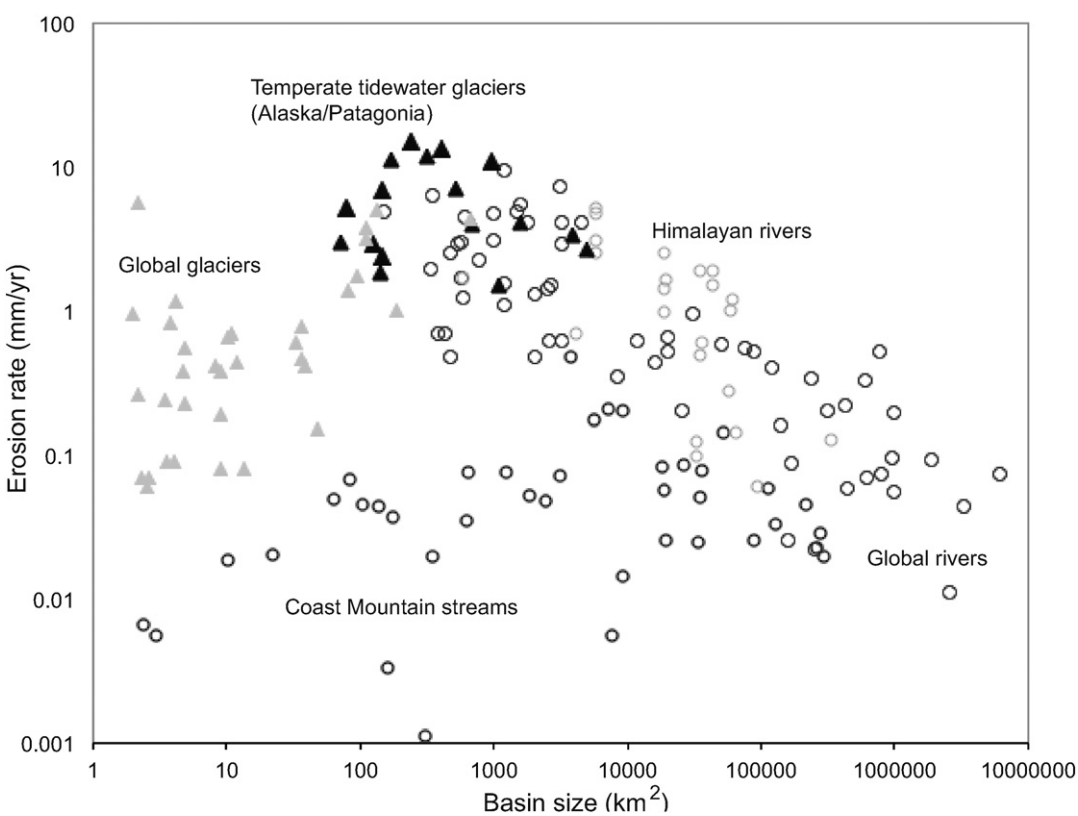

Fig. 6. Comparison of modern (10^0–10^1) glacial erosion rates (triangles) and fluvial erosion rates (circles) derived from sediment yields according to catchment area, revised from data originally compiled by Hallet et al. (1996). Black triangles represent temperate tidewater glaciers from Alaska and Patagonia, gray triangles other alpine and high-latitude glaciers, black open circles are major river basins worldwide (from Milliman and Syvitski, 1992) and mountain basins in British Columbia (from Church and Slaymaker, 1989), and gray open circles are from partially glaciated mountain basins in the high Himalaya. Modified from Koppes and Hallet (2006).

2006; Cowan et al., 2010; Herman et al., 2015; Koppes et al., 2015), are still poorly understood. The importance of ice dynamics on sediment production was first quantitatively demonstrated by studies of Variegated Glacier, Alaska, in the early 1980s, where a two-order-of-magnitude variation in sediment yield was measured over a two-year surge cycle (Humphrey and Raymond, 1994). During this surge event, sliding speeds also increased by two orders of magnitude, but the extent of glacier cover did not change appreciably. Notably, the subglacial discharge increased dramatically at the end of the surge, suggesting that subglacial meltwater flushing may contribute a significant amount of sediment to the proglacial system during distinct (seasonal to interannual) events (Fig. 2B; Merrand and Hallet, 1996). These findings showed that the dynamic nature of a glacier dictates the rate at which it can erode, entrain subglacial sediments and deliver them to the ice front, creating a cryospheric sedimentary signal of changing glacier mass balances.

Given the logistical complexities inherent in establishing subglacial erosion rates quantitatively, a critical component is to determine a chronology for sediment deposition in the glacial foreland and glacimarine realms. Tools developed to understand these depositional processes, and to address the multiple factors that affect sedimentary records created by fluctuating glacial sediment input, include: a) direct measurements of suspended sediment concentrations in fjords and lakes to monitor sediment release and transport mechanisms (e.g., Domack and Williams, 1990; Cowan and Powell, 1991); b) radioisotope analysis and varve counting of seabed samples from shallow cores (e.g., Cowan et al., 1997; Jaeger and Nittrouer, 1999a, 1999b; Cowan et al., 1998; Jaeger, 2002; Ohkouchi and Eglinton, 2008; Rosenheim et al., 2008; Boldt et al., 2013); c) optical and thermoluminesence dating of sediments (Fuchs and Owen, 2008; Berger et al., 2010; Alexanderson and Murray, 2012); d) paleomagnetism (Stoner et al., 2000; Brachfeld et al., 2003; Simon et al., 2012); and e) seismic stratigraphy and facies analyses recorded in strata (e.g., Cai et al., 1997; Elverhøi et al., 1998a; Jaeger et al., 1998; Sheaf et al., 2003; Koppes and Hallet, 2006; Koppes et al., 2009; Cowan et al., 2010; Fernandez et al., 2011). Given the spatial and temporal variability in sediment and meltwater discharge at glacial termini (e.g., Powell and Molnia, 1989; Domack and Ishman, 1993), spot measures in space and/or time of sediment accumulation (a–d) are potentially inadequate to capture the dominant time scale of sediment production, and thus data sets that capture the full flux over space and time (e) are advantageous. However, seismic volumes can only be converted to rates when chronologies and physical properties (e.g., p-wave velocity, bulk density) exist to complement the seismic stratigraphy. Often, only gross assumptions of ages of seismic surfaces can be made, for instance glacial retreat surfaces following LGM or LIA (Elverhøi et al., 1998a; Jaeger et al., 1998; Sheaf et al., 2003; Koppes et al., 2010), which limits our abilities to examine the dynamics of sediment fluxes over time.

Much of what is known about contemporary and centennial sediment yields from glaciers comes from coastal Alaska and Patagonia, where numerous studies have quantified the sediments in the fjords and on the shelf (e.g., Molnia, 1979; Cowan and Powell, 1990, 1991; Powell, 1991; Hallet et al., 1996; DaSilva et al., 1997; Jaeger et al., 1998; Jaeger and Nittrouer, 1999b; Koppes and Hallet, 2002, 2006; Sheaf et al., 2003; Boyd et al., 2008; Koppes et al., 2009, 2010; Cowan et al., 2010). From the measured sediment volumes in fjords and historical records of terminus retreat, Koppes and Hallet (2002, 2006, 2009) modeled the sediment yields of tidewater glaciers in Alaska and Patagonia on an annual basis, based on seismic reflection isopachs, and suggested that the temperate tidewater glaciers in both regions have been unusually dynamic and erosive in the past century since the end of the LIA, when regional warming caused rapid terminus retreat and the drawdown of hundreds of meters of ice. They inferred that the acceleration in ice flow required to evacuate such immense volumes of ice from the basins since the LIA resulted in accelerated basal sliding, and the unusually fast sliding (relative to the typical conditions of the late Pleistocene) produced modern erosion rates (Fig. 2C) that are among the highest known yields worldwide and far exceed those over the long-term (Figs. 3 and 6).

The study by Cowan et al. (2010) stands out for their contribution in terms of documenting sedimentary processes and rates of debris transfer from the glacial source to a fjord. They documented the retreat of Muir Glacier, Alaska and the associated migration of the active depocenter through silled fjord basins at nearly annual resolution for over a century. They concluded that the sediment yield derived from seismic isopachs reflects several sources, and that sediment fluxes measured during retreat should not be considered to represent only bedrock erosion supplied by varying ice flux from Muir Glacier, but also includes contributions from tributary glaciers as well as pre-LIA sediment stored within the deeper basins that is re-eroded by advancing ice. Moreover, sediments are often redistributed from bedrock highs into deep basins. Hence, temporal variations in sediment input from tidewater glaciers represent variations both in production of new debris by erosion as well as in inputs from sediment stored under and in front of the glacier.

Over longer time scales (10–400 ka), averaging several glacial cycles, recent advances in cosmogenic exposure dating have greatly enhanced our ability to define glacial erosion and deposition rates in the terrestrial environment. The use of cosmogenic nuclides has provided a means of directly dating the deposition of subaerial glacial deposits in the absence of any associated organic remains, a common issue for Quaternary deposits (Balco, 2011; Granger et al., 2013). Cosmogenic exposure-age dating, which relies on the measurement of rare nuclides produced in rock surfaces and sediments by cosmic ray bombardment, is now widely used to date both late Pleistocene and Holocene deglaciation ages as well as to quantify subglacial erosion rates via the nuclide concentration in glacially transported boulders and in bedrock exposed during retreat (Balco, 2011). Advances in the use of cosmogenic nuclide isotopes (Miller et al., 2002; Briner et al., 2006; Briner and Kaufman, 2008; Menounos et al., 2009; Balco, 2011; Fastook and Hughes, 2013; Granger et al., 2013; Champagnac et al., 2014; Cofaigh et al., 2014; Hormes et al., 2013; Refsnider et al., 2013; Hodgson et al., 2014; Larter et al., 2014; Lindow et al., 2014; Rother et al., 2014; Winsor et al., 2014) have helped resolve a number of longstanding chronological and process debates in geomorphology, including: topographic relief development (e.g., Tremblay et al., 2014) and the ability of cold-based ice sheets to preserve pre-glacial landscape features (e.g. Stroeven et al., 2002; Briner et al., 2006); complex Holocene glacial exposure–burial histories (e.g. Goehring et al., 2011); and accumulation rates of glacial sediments deposited 0.5 to 3 Ma (e.g., Balco and Rovey, 2010). However, the accuracy of cosmogenic exposure dating remains limited by uncertainties about production-rate calibrations and assumptions about the geologic history of landforms that are difficult to test and may profoundly effect their apparent ages, complicating the glacial and erosional history of landforms and strata (Balco, 2011; Heyman et al., 2011).

Developments in low temperature thermochronometry also have allowed quantification of glacial erosion rates at the million-year timescale appropriate for investigating tectonic–climatic forcing on topographic development. Four low-temperature thermochronometric systems are used: apatite (U–Th)/He, apatite fission track, zircon (U–Th)/He and zircon fission track, which have approximate closure temperatures of ~60–90 °C, 110 °C, 180 °C and 250 °C, respectively. Taken together, these thermochronometers enable the tracking of bedrock erosion from shallow crustal depths of about 8–10 km up to the Earth's surface (e.g., Herman et al., 2013). These temperatures and bedrock cooling histories correspond to the glacial–interglacial phase of topographic denudation (e.g, Shuster et al., 2005). For instance, recent low temperature thermochronometric studies along the glaciated coasts of Alaska, British Columbia and in the Patagonian Andes support the notion of rapid glacial erosion at altitudes near the snowline (Fig. 3) (Shuster et al., 2005; Berger and Spotila, 2008; Thomson et al., 2010; Herman et al., 2013). One notable drawback

to this method is that bedrock cooling ages can only be established where samples can be collected, which precludes sampling under modern ice streams that may be the locus of erosion over LGM time scales (Berger et al., 2008b; Enkelmann et al., 2010; Headley et al., 2013). One alternative is to use detrital thermochronometery on grains collected from glacial outwash. Where this has been accomplished from modern glaciers, the results are ambiguous in terms of the exhumation rates under the glaciers, which may reflect decadal-scale variability in subglacial sediment storage and transfer that influences the cooling age spectra of grains sampled from outwash (Headley et al., 2013).

2.2.3. Modeling erosion and sediment production under conditions of glaciation

Increasingly, the effects of glacial erosion on geomorphic development of topography and the production of a sedimentary signal are being studied using landscape evolution models, which provide numerical simulations of both ice flux and glacier erosion over periods spanning multiple glaciations. The geomorphic signatures of glacial landscapes, such as U-shaped valley cross-sections, low-sloping longitudinal profiles punctuated by steep steps, overdeepened bedrock basins and fjords, cirques, and hanging valleys, clearly demonstrate differences in the erosional capacity of fluvial and glacial systems (e.g. Harbor et al., 1988; Braun et al., 1999; Kessler et al., 2008; MacGregor et al., 2009; Pedersen and Egholm, 2013). However, there has been slow progress directed toward quantitatively understanding the development of these geomorphic features, quantifying the timescale of their formation, or determining the rates of glacigenic sediment production. Most recent numerical modeling efforts have focused on reproducing the processes that produce the hypsometric signature of a glaciated landscape, including erosion by glacial sliding and isostatic landscape uplift caused by erosional unloading (e.g., MacGregor et al., 2009; Yanites and Ehlers, 2012; Pedersen and Egholm, 2013).

Central to these glaciated landscape evolution models is the need for a simple index that relates the glacial erosion rate, i.e., sediment production rate, to glaciological or climatic variables. Most models assume that erosion rates are proportional to the ice sliding velocity at the bed, and reach a peak at the equilibrium line altitude (ELA) (e.g., Harbor, 1992; Braun et al., 1999; Tomkin and Braun, 2002; Egholm et al., 2009; MacGregor et al., 2009; Tomkin, 2009; Herman et al., 2011). Some models assume that glacial erosion can be approximated by the integrated ice discharge (Anderson et al., 2006, Kessler et al., 2008; Headley et al., 2012). Although treatments of glacier flow in these models have become increasingly sophisticated (e.g., Herman et al., 2011; Egholm et al., 2012), the constraints placed on the erosion rate have remain unchanged, and most apply a bedrock erosion (E) rule of the form:

$$E = K_g u_s{}^n$$

where u_s is the glacier sliding speed, K_g is a constant representing bedrock erosion susceptibility, and n is a constant normally assumed to be 1 (e.g., Harbor, 1992; Tomkin, 2007, 2009; Herman and Braun, 2008; Egholm et al., 2009; MacGregor et al., 2009; Herman et al., 2011; Yanites and Ehlers, 2012). In nearly all of these cases, the two constants of proportionality used have been tuned to a single empirical study in which both the sediment flux and ice motion were measured during a surge of Variegated Glacier in Alaska (Humphrey and Raymond, 1994). Recent findings at Franz Josef Glacier in New Zealand (Herman et al., 2015) and temperate outlet glaciers in Patagonia (Koppes et al., 2015) suggest that the relationship between erosion rate and sliding is non-linear, i.e., $n = 2$ (see Fig. 5).

While field studies and some of the most recent modeling studies have shown that water plays a major role in modulating sliding (Herman et al., 2011; Egholm et al., 2012), with important implications for enhanced erosion, the impact it may have on sediment yields and erosion rates is still unclear. Beaud et al. (2014) found that variations in seasonal subglacial drainage pattern, sliding speeds, and the form of the erosion rule used resulted in significant differences in predicted erosion rates. Thus, improved empirical data on the patterns and development of subglacial hydrology, and on the role of hydrology in modulating erosion and sediment production, are still needed.

Documenting the timing of subglacial sediment generation at the source and transfer to the sink also is complicated by paraglacial changes in erosional and transport pathways throughout glacial advance–retreat cycles. For example, DeWinter et al. (2012) modeled the change in erosion and sediment generation to the glacial foreland during deglaciation, and found a distinct time lag between glacier warming and retreat, and a corresponding increase in erosion and sediment production. They attributed this lag to rising concentrations of abrasive agents (i.e. sediment) in the basal ice and an increase in sliding. They also noted that the lag between warming (and deglaciation) at the glacier source and the increase in sediment delivery to the proglacial sinks may be complicated by sediment storage in the terrestrial and fluvial transfer domains, creating a pulse of paraglacial reworked sediments in the proglacial foreland following deglaciation (Church and Ryder, 1972; Church and Slaymaker, 1989; Ballantyne, 2002).

3. Linking the source to the sink: glacigenic signal transfer

A primary source-to-sink (S2S) goal is to determine the mass dispersal processes by which glacigenic sediment is transferred from the locus of production (i.e., the glacial source) to the locus of accumulation (i.e., the glacimarine sink), and how these dispersal pathways are controlled by ice dynamics and related controls such as sea level. In contrast with river systems that are persistent on the landscape over millions of years, a primary question for glacial S2S systems is how the signal is transferred, especially when the glaciers are no longer present in the landscape.

Sediment is transferred from where it is eroded within the source zone to the terminus (the source/transfer zone boundary) (see Fig. 1) through several well-documented processes, including superglacial and englacial rafting within the ice, transport in a deformable till or debris-laden basal ice layer at the ice-bed interface, or carried in the subglacial hydrologic system (Fig. 4; Alley et al., 1997). The dominant sediment transfer process will depend on the thermal state of the ice. In temperate, meltwater-dominated systems, the primary mode of sediment transfer is through subglacial meltwater conduits (Lawson, 1993; Alley et al., 1997). Superglacial meltwater feeding the subglacial system can rapidly advect sediment through the glacier, and subglacial flow can flush all available sediment stored beneath the ice (Alley et al., 1997; Hunter et al., 1996a; Swift et al., 2005). In colder systems such as in Antarctica, basal melting is greatly reduced, and meltwater discharge is minimal (Alley et al., 1997; Griffith and Anderson, 1989; Koppes et al., 2015).

Subglacial sediment transport also can occur by deformation of till at the glacier bed, and may be the dominant mode of transport under ice streams (Fig. 4B; Kristoffersen et al., 2000; Bennett, 2003). Characteristic basal sediment thicknesses of less than 0.5 m have been measured beneath temperate Alaskan tidewater glaciers (e.g., Kamb et al., 1985; Humphrey et al., 1993). The few observations of these deformable till layers from boreholes suggest they are no more than a few meters thick at most (Engelhardt et al., 1990; Truffer et al., 1999). Transport also occurs by freezing to the sole of the glacier, resulting in thick zones of debris-rich basal ice where regelation and freeze-on from supercooled subglacial water is prevalent (Alley et al., 1997; Creyts et al., 2013). Sediment fluxes associated with ice streams range from 10^2 to 10^3 m^3 yr^{-1} per meter ice width (Alley et al., 1987; Alley, 1989; Hooke and Elverhøi, 1996; Tulaczyk et al., 2001; Shipp et al., 2002; Dowdeswell et al., 2004; Anandakrishnan et al., 2007; Laberg et al., 2009; Christoffersen et al., 2010). To generate and sustain such a large sediment flux, subglacial sediment transfer near the ice margins

must be dominated by thick zones of deforming till (Alley et al., 1989; Anandakrishnan et al., 2007; Livingstone et al., 2012) or debris-rich basal ice layers (Christoffersen et al., 2010).

Local geology and basin topography dictate how much mass wasting occurs, shedding sediment onto the ice surface, and hence the relative amount of supraglacial and englacial debris transported by the ice (e.g., Alley et al., 1997). The magnitude of the sediment transported directly by ice is, however, considered a minor contributor to the overall flux. For instance, Hunter et al. (1996a) found that, for three relatively "dirty" Alaskan tidewater glaciers where bedrock erodibility was relatively high and where small but significant portions of the basins were above the ice surface and available to contribute superglacial debris, the superglacial and englacial debris entrained in the ice amounted to no more than 10% of the total sediment yield.

Changes in subglacial hydrology and subglacial storage also may influence transfer of sediment along dispersal pathways within the glacier 'source' zone, adding complexity to the sedimentary record in the ice-proximal sink. Subglacial basins can act to temporarily store both sediment and water (Cook and Swift, 2012). Any change in the sediment-transport capacity of the subglacial hydrologic system, such as caused by a decrease in bed slope due to subglacial sediment storage or an increase in surface slope as the glacier thins, can evacuate stored sediment (Alley et al., 1987; Motyka et al., 2006; Cuffey and Paterson, 2010; Cook and Swift, 2012). Hence, the sedimentary signal at the ice-ocean boundary is not a simple record of changes in the sediment production rate due to changes in climate or erosion rate. Because changes in subglacial hydrology and storage may dominate the sediment flux to certain ice-proximal settings, a simple interpretation of sediment fluxes as a metric of ice flux is challenging, as subglacial hydraulics are arguably the least understood component of the glacier system.

In contrast, a substantial set of investigations into the physical processes in fjords has provided a conceptual framework for modeling the flux and fate of glacial sediment that enters marine waters (e.g., Elverhøi, 1984; Powell, 1984; Syvitski et al., 1987; Cowan and Powell, 1990, 1991; Domack and Williams, 1990; Domack and Ishman, 1993; Domack et al., 1994; Harris et al., 1999; Ashley and Smith, 2000; Gilbert et al., 2003). While some glacimarine sedimentary dispersal processes such as turbid meltwater plumes have been measured in situ, or inferred from fjord sedimentary deposits, the specific transport mechanisms, especially near the terminus, can only be inferred from geophysical or acoustic sampling (e.g., Powell, 1990; Domack et al., 1994; Goff et al., 2012). However, rare is the situation where termini are subareally exposed following retreat to allow documentation of the full range of transport processes (Smith et al., 1990; Phillips et al., 1991).

In glacimarine environments, most glacially derived sediment enters proglacial fjords via subglacial meltwater discharge, and to a much lesser extent by direct melting of the calving front and of icebergs (Figs. 1, 7, and 8; e.g., Powell and Molnia, 1989; Cowan and Powell, 1991; Hunter et al., 1996b). The majority of sediment is thought to be delivered to temperate fjords via subglacial and englacial meltwater channels (Hunter et al., 1996a); at the terminus, subglacial discharge generally rises as a turbulent plume that mixes with ambient seawater (Fig. 8 inset; Powell and Molnia, 1989; Syvitski, 1989). Some of the highest sediment accumulation rates measured worldwide occur near the grounding line of temperate glaciers, and reach up to meters per year (Powell, 1981, 1983, 1990, 1991; Goff et al., 2012). Empirical studies of proglacial sedimentation rates in front of temperate-polythermal tidewater glaciers all suggest that they decrease exponentially with distance from the ice front, reflecting rapid sediment deposition (hours–days) of suspended sediment (Syvitski, 1989; Cowan and Powell, 1991; Dowdeswell et al., 1998; Hill et al., 1998; Jaeger and Nittrouer, 1999b). Such rapid sedimentation processes have been quantitatively (Powell, 1990) and numerically (Mugford and Dowdeswell, 2011; Salcedo-Castro et al., 2013) modeled and are highly dependent upon the time-evolving jet dynamics at the subglacial conduit and suspended-sediment flocculation dynamics in the water column (Hill et al., 1998).

The dominant sediment-transport process in meltwater-dominated fjord depends strongly on the subglacial meltwater sediment concentration. For sediment-laden freshwater to exceed the density of the ambient fjord seawater, the suspended-sediment concentration needs to exceed ~30 g l^{-1} (Mulder and Syvitski, 1995). At concentrations <30 g l^{-1}, subglacial meltwater plumes become buoyant and travel along the water surface, as sediment flocculates and settles to the seabed (e.g., Cowan et al., 1988; Hill et al., 1998; Curran et al., 2004). If the plume is hyperpycnal (>30 g l^{-1}), high-concentration gravity flows can carry sediment along the fjord seabed great distances from the source (e.g., Prior et al., 1987; Syvitski et al., 1987; Willems et al., 2011). Gravity flows, including hyperpycnal flows, disperse highly mobile sediment along a flat seabed; gravity-flow strata are a significant component of the sedimentary facies accumulating proximal to the ice (Fig. 7; Syvitski, 1989; Willems et al., 2011; Hambrey and Glasser, 2012). Secondary meltwater input from tributary glacifluvial sources can add to mass fluxes and also result in gravity flows and turbidite deposition (Fig. 8; Dowdeswell and Vásquez, 2013). Sinuous turbidity–current channels are common to temperate fjords influenced by highly variable discharge from glacifluvial braided rivers (Prior et al., 1986; Syvitski et al., 1987; Dowdeswell and Vásquez, 2013).

Sediment delivery into polar fjords is controlled primarily by calving and ice rafting, with most of the sediment accumulating directly at the ice front (Fig. 7A; Domack and Ishman, 1993; Hambrey and Glasser, 2012). Broad variations in the amount of sediment produced and in the role of meltwater facilitating glacial sediment transport are evident from several studies across the Antarctic Peninsula. For example, biogenic sediments are dominant in polar fjords in Antarctica indicating relatively minimal terrigenous input (Domack and Williams, 1990), whereas the subpolar bays of the Antarctic Peninsula receive greater fluxes of terrigenous sediment (Griffith and Anderson, 1989; Domack and Ishman, 1993; Anderson, 1999; Boldt et al., 2013), thought to be delivered by suspended-sediment plumes and influenced by currents (Domack and Williams, 1990; Domack et al., 1994; Yoon et al., 1998; Harris et al., 1999; Ashley and Smith, 2000). Bottom and intermediate plumes, which appear to originate at the grounding line, transport the majority of suspended sediment in polar and subpolar settings (Fig. 7A) (e.g., Domack et al., 1994). Observed temporal variability of these plumes suggests time-varying subglacial discharge as the dominant control. However, the mechanisms generating these plumes, for instance tidal action or meltwater discharge, remain poorly understood (Domack and Williams, 1990; Domack et al., 1994; Domack and Harris, 1998). Sediment transfer by turbidity currents, debris flows, rain-out debris, and meltwater-derived sediments also has been interpreted as occurring in sub-iceshelf environments in the vicinity of the grounding line of polar ice sheets (Fig. 7; Anderson, 1999; Domack et al., 1999; Licht et al., 1999; Evans and Pudsey, 2002; Hillenbrand et al., 2005).

Iceberg rafting of sediment can also be a volumetrically significant transfer mechanism, especially in polythermal and polar settings (Fig. 7). Ice-rafted debris (IRD) accumulation is commonly assumed to indicate that the marine terminating ice flux was high, supplying enough mass to allow for wide dispersal of coarse-grained sediment (Ruddiman, 1977; Molnia, 1983; Powell and Molnia, 1989; Krissek, 1995; Cowan et al., 1997; Anderson, 1999; St. John and Krissek, 1999; Clark and Pisias, 2000; Hemming, 2004; Tripati et al., 2008; Forwick and Vorren, 2009; Marcott et al., 2011; Cofaigh, 2012; Patterson et al., 2014). The amount of IRD transferred along the dispersal system also depends on the amount of material entrained in the ice, the amount of time it takes icebergs to transit the transfer zone, and the melting rate along this transit (Andrews, 2000). Time-varying fluxes of IRD to a specific site have been used as evidence of the dynamic extent of the ice (Hebbeln et al., 1998; Solheim et al., 1998; Stokes et al., 2005; Patterson et al., 2014), but the interpretation of IRD concentrations as

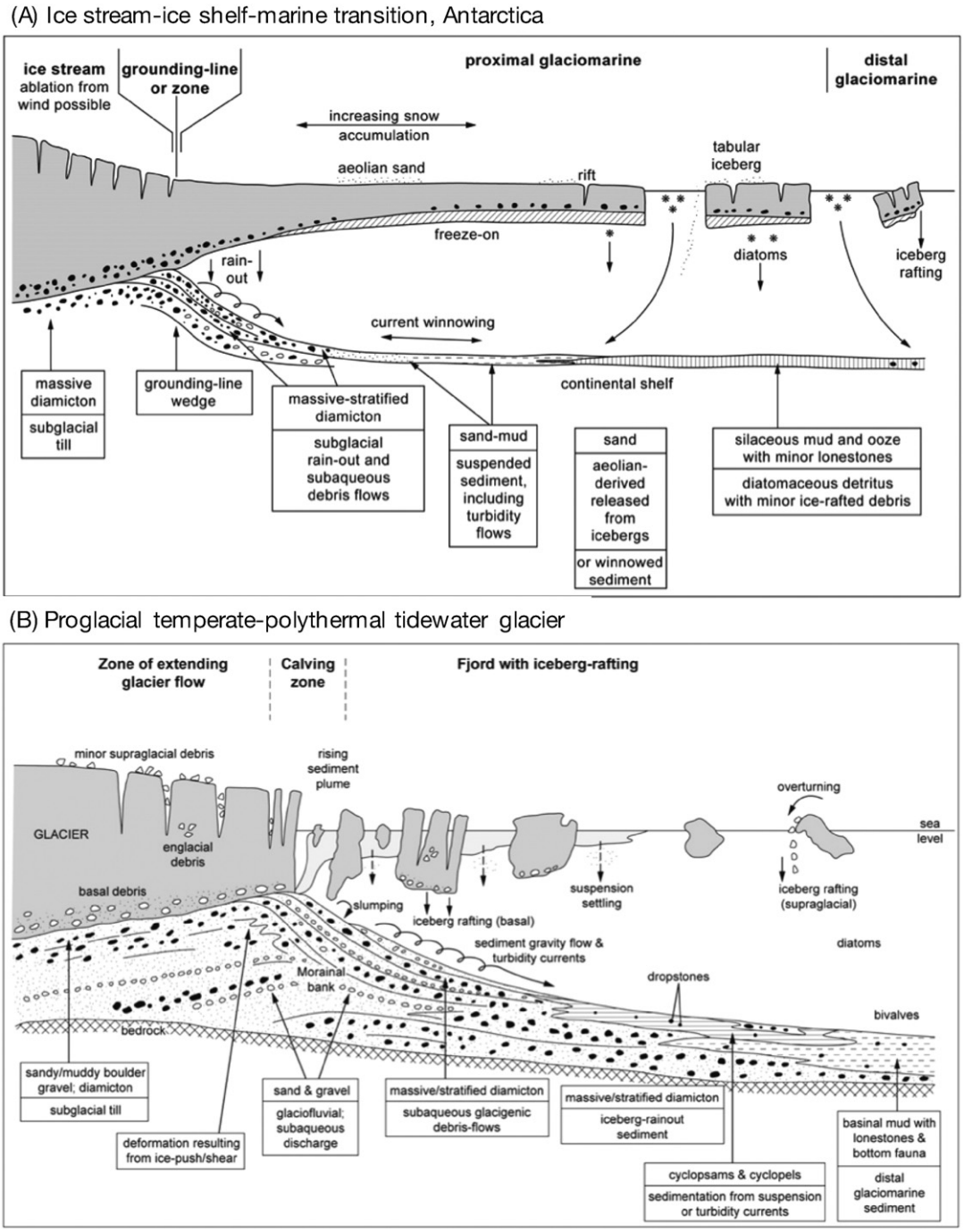

Fig. 7. Conceptual model for proglacial depositional processes and characteristic lithofacies in fjords and on continental shelves. Top panel (A) represents a polar, ice stream-influenced continental-shelf environment. Bottom panel (B) represents a temperate-polythermal tidewater glacier environment. From Hambrey and Glasser (2012).

simply a proxy for ice margin stability has been questioned (St. John and Krissek, 1999; Andrews, 2000; Clark and Pisias, 2000). In the iceberg-dominated margins of East Greenland (Dowdeswell et al., 1998), higher concentrations of IRD are assumed to represent major periods of calving associated with a retreat of the ice front (Elverhøi et al., 1998a; Funder et al., 1998). In Antarctica, IRD concentrations in open marine sediments do not appear to be related to ice sheet dynamics, but rather reflect relative winnowing of fines by strong bottom currents (Cofaigh et al., 2001b; Cofaigh, 2012) and other deepwater sediment reworking processes over the past million years. In temperate glacial settings, higher concentrations of IRD have been associated with ice margin retreat on continental shelves (Hendy and Cosma, 2008), but may also reflect seasonally varying suspended-sediment concentrations in fjords (Cowan et al., 1997). Regional oceanography can also have a major impact on IRD dispersal patterns, varying greatly over short distances (Solheim et al., 1998). For example, two ODP cores taken 75 km apart on the East Greenland shelf showed a significant seaward decrease in IRD content, likely influenced by the East Greenland Current, which has kept icebergs closer to the margin and prevented eastward transport to the outer shelf (Larsen et al., 1994).

Continental shelves impacted by glacial processes share a common set of characteristics that reveal the dynamics of ice and sediment transfer over a larger range of time scales (Figs. 1 and 2D). Ice streams flowing from ice masses of all sizes are the predominant transfer mechanism of ice, meltwater, and sediment to and across continental shelves (Figs. 9 and 10; Bentley, 1987; Cofaigh et al., 2003; Cofaigh et al., 2008;

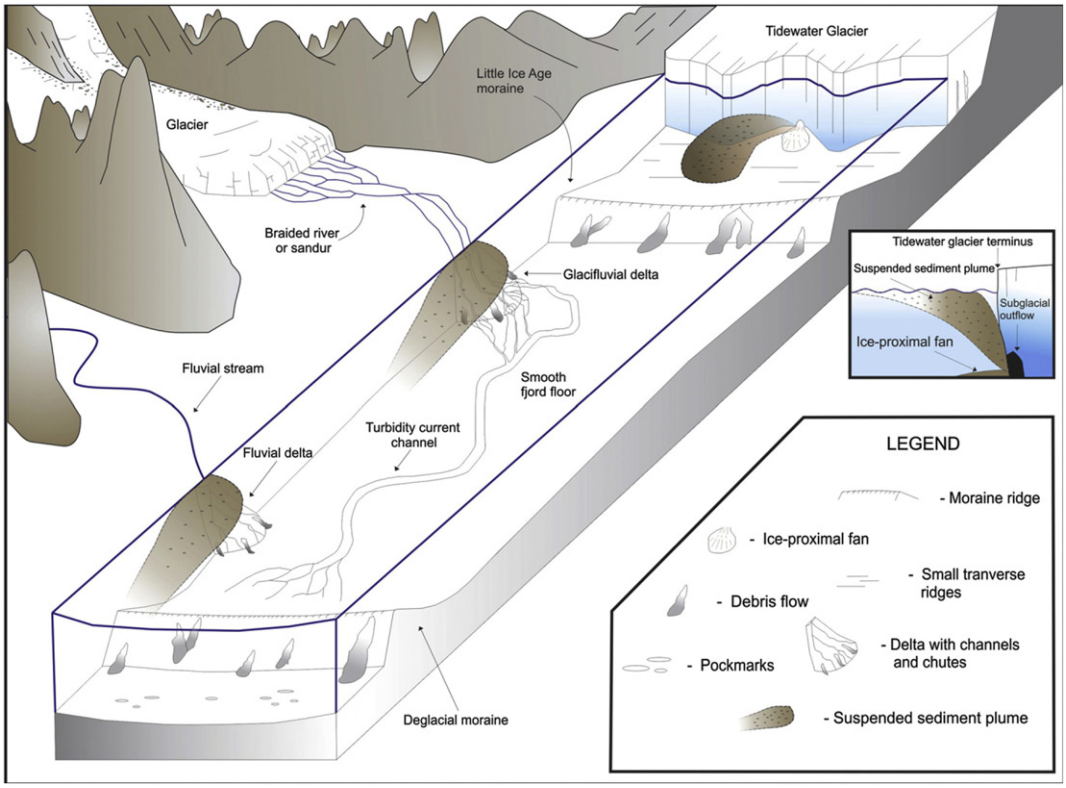

Fig. 8. A schematic landform-assemblage model for temperate, meltwater-dominated fjords subject to relatively mild climatic and oceanographic conditions, such as the fjords of Patagonia or Alaska. Inset shows the efflux of a subglacial meltwater channel at the tidewater glacier terminus and the plume of turbid sediment and ice-proximal fan produced beyond the subglacial outflow mouth. From Dowdeswell and Vásquez (2013).

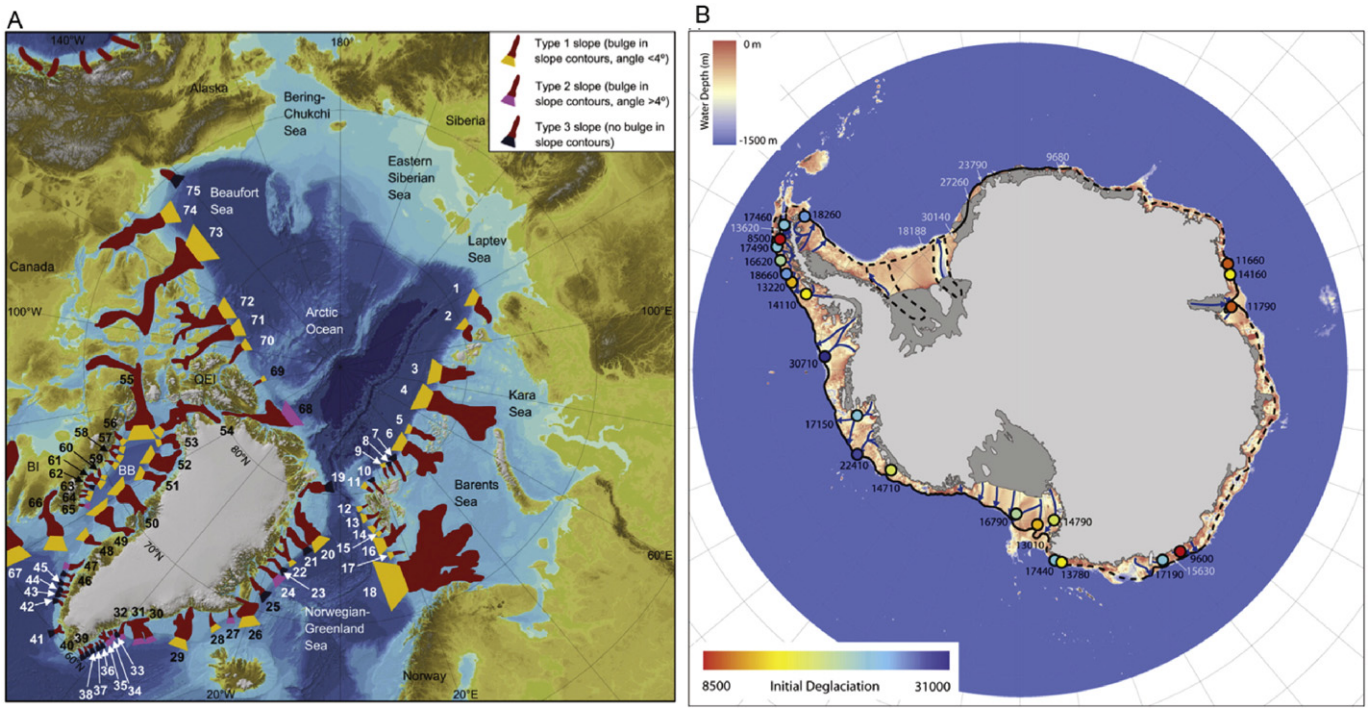

Fig. 9. Location of paleo-ice streams and cross-margin troughs in the Arctic and Antarctic. (A) Locations of circum-Arctic cross-shelf troughs (red; Batchelor and Dowdeswell, 2014) displayed on IBCAO bathymetric data (Jakobsson et al., 2012). Three types of continental slopes are shown. Numbers refer to specific ice streams discussed in Batchelor and Dowdeswell (2014). Approximate locations of cross-shelf troughs in Gulf of Alaska shown in red (after Carlson et al., 1982). (B) Location (blue arrows) and chronology of initial deglaciation (colored dots) for Antarctic paleo-ice streams. Dates (in black) represent initial retreat of the palaeo-ice streams; dates in gray refer to initial retreat of the ice sheet margin. The black line shows the reconstructed position of grounded ice at the LGM. The dashed line indicates approximate grounding-line positions due to a paucity of data. From Livingstone et al. (2012).

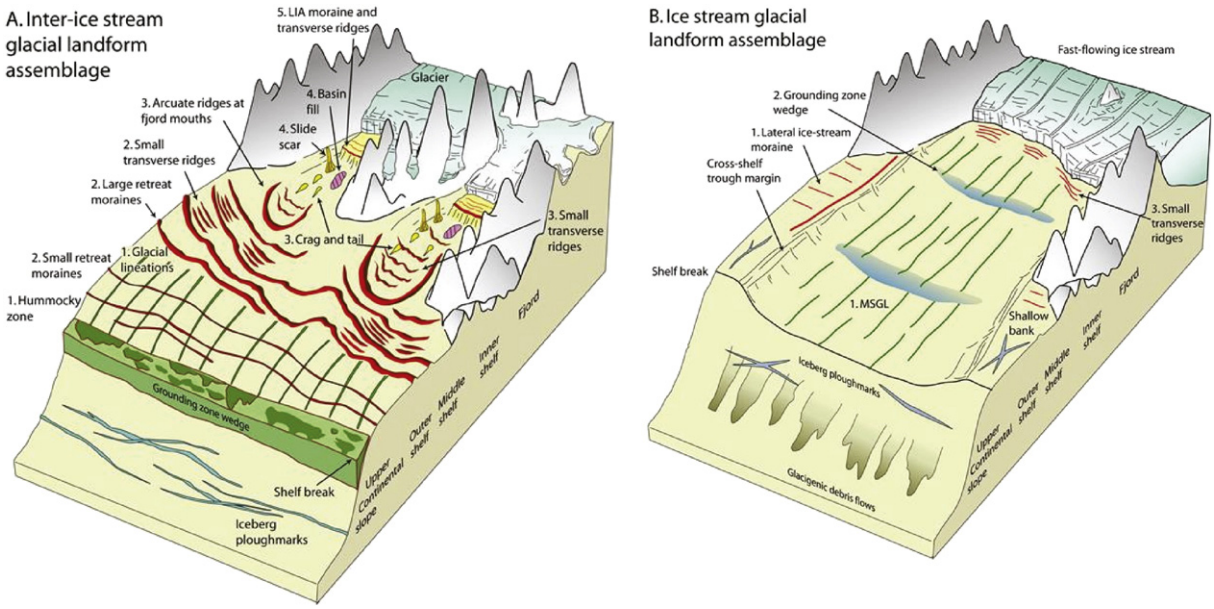

Fig. 10. Assemblages of submarine landforms on continental shelves typical of inter-ice-stream (A) and paleo ice-stream (B) sedimentary environments. From Dowdeswell et al. (2008b) and Ottesen and Dowdeswell (2009).

Stokes and Tarasov, 2010; Livingstone et al., 2012; Batchelor and Dowdeswell, 2014; Dowdeswell et al., 2014; Landvik et al., 2014). Deep (100–2000 m) cross-shelf troughs are the geomorphic signature of paleo-ice streams, interpreted to represent the main ice routes across the continental shelf, often to the shelf break (Fig. 10). These troughs link up with major sediment depocenters and dispersal systems on continental slopes (Bentley, 1987; Cofaigh et al., 2003; Dowdeswell et al., 2008a; Reece et al., 2011; Livingstone et al., 2012; Batchelor and Dowdeswell, 2014; Dowdeswell et al., 2014; Landvik et al., 2014; Larter et al., 2014; Walton et al., 2014). Between ice streams, slower flowing ice transfers less mass but is primarily recognizable from a depositional record of nested arcuate moraines marking the positions of former ice margins (Fig. 10; Dowdeswell et al., 2002; Landvik et al., 2005; Ottesen et al., 2007; Ottesen and Dowdeswell, 2009; Cofaigh et al., 2012; Landvik et al., 2014).

Continental slopes and the adjacent deep basins are the ultimate sink for glacigenic sediment that has been supplied to the glacimarine transfer zone, reworked, and advected to the more distal part of the system (Figs. 1 and 2E, F). Sediment cores and seismic facies in the deep sea reveal that gravity flows and hemipelagic settling are the main transfer mechanisms to these sinks (Figs. 1 and 11; Dowdeswell et al., 1996; Dowdeswell et al., 1998; Wilken and Mienert, 2006; Reece et al., 2011; Cofaigh, 2012; Garcia et al., 2012; Batchelor and Dowdeswell, 2014; Walton et al., 2014). Debris flows are ubiquitous on continental slopes seaward of cross-shelf troughs that were occupied by ice streams (Figs. 10 and 11; Laberg and Vorren, 1996; King et al., 1998; Taylor et al., 2002a; Batchelor and Dowdeswell, 2014; Dowdeswell et al., 2014; Rebesco et al., 2014). Deposition of debrites results in the formation of trough mouth fans, the primary depositional landform on many northern hemisphere margins (Vorren et al., 1998; Dahlgren et al., 2002; Elverhøi et al., 2002; Taylor et al., 2002a; Cofaigh et al., 2003; Dahlgren et al., 2005; Nielsen et al., 2005; Batchelor and Dowdeswell, 2014; Rebesco et al., 2014). Trough mouth fans occur wherever slopes are <4° (Cofaigh et al., 2003; Batchelor and Dowdeswell, 2014); on steeper slopes, gravity flows supply sediment to deep submarine basins via large submarine channels (Dobson et al., 1998; Reece et al., 2011; Garcia et al., 2012; Walton et al., 2014). Although gravity flows transfer large volumes of glacigenic sediment onto slopes and into deepwater basins (Reece et al., 2011; Garcia et al., 2012; Walton et al., 2014), suspended sediment settling from turbid surface and intermediate water depth plumes dominates the temporal record in these settings (Taylor et al., 2002c). At shelf margins in Antarctica and NE Greenland, trough mouth fans are rare to absent (Livingstone et al., 2012; Batchelor and Dowdeswell, 2014), and the prevalent gully morphology suggests that density flows drive near-bed sediment transport to deeper basins (Nielsen et al., 2005; Dowdeswell et al., 2008b; Noormets et al., 2009; Livingstone et al., 2012; Gales et al., 2013). The lack of trough mouth fans in these settings may either reflect steeper continental shelf breaks or lower sedimentation rates than are required to construct a low-angle slope (Livingstone et al., 2012; Gales et al., 2013). This observation suggests that reduced sediment fluxes from polar ice sheets influence continental slope morphology at the highest latitudes.

4. The sink-fidelity of the glacigenic signal

The major objective of studying a sediment routing system from source to sink is to establish the fidelity of the stratigraphic record in capturing the dynamics of the geomorphic processes creating sediment, the drivers of those processes, and the internal routing dynamics. Relating dynamic ice fluxes (i.e., velocity) to strata formation in glacial S2S systems requires quantification of glacigenic sediment accumulation rates, which depends on resolving the sedimentary record at timescales equal to or better than the characteristic timescale of the ice response in question (Fig. 2; Cofaigh et al., 2002). This is most easily accomplished in modern temperate, meltwater-dominated glacial systems, because sediment production is elevated and thus signal generation is the strongest, resulting in higher mass fluxes that produce the accumulation rates necessary to resolve the recent or short-timescale ice response function (Cowan et al., 1997; Dowdeswell et al., 1998; Dowdeswell and Siegert, 1999; Jaeger and Nittrouer, 1999a; Jaeger, 2002; Andresen et al., 2012; Pedersen et al., 2013). For modern iceberg-dominated systems, reduced production and flux of sediment to the sink limits our ability to quantify the relationship between ice flux (velocity) and the stratigraphic signal for short (sub-annual to decadal) timescales (Harden et al., 1992; Domack and McClennen, 1996; Lowe and Anderson, 2002; Hillenbrand et al., 2010a; Kirshner et al., 2012; Boldt et al., 2013). Consequently, the greatest advances in linking ice dynamics at modern to Quaternary advance-retreat time scales to sedimentary signal preservation exist for meltwater-dominated systems (Fig. 2).

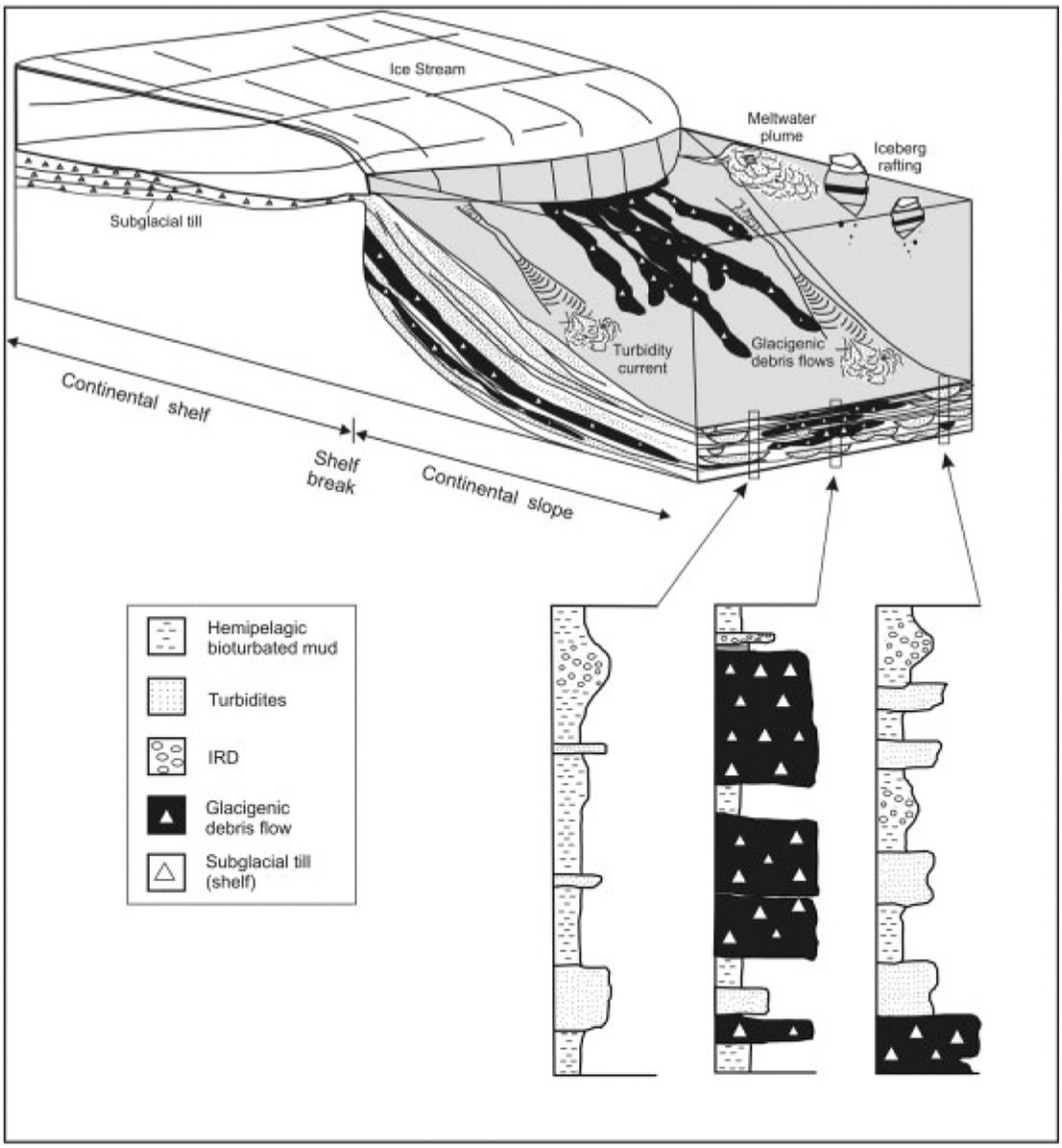

Fig. 11. Conceptual model of glacigenic sedimentation on a high-latitude trough-mouth fan. Dominant sediment transfer mechanisms include gravity flows, meltwater discharge plumes and iceberg rafting. Idealized lithofacies assemblages across the fan are shown. From Cofaigh et al. (2013).

Establishing links between lithostratigraphy and glacial geomorphology requires identifying the genesis of the sedimentary signal, which is most easily accomplished in currently glaciated settings. Interpreting the ice influence on strata formation depends on recognizing distinctive lithofacies and/or seismic-facies assemblages characteristic of glacial settings (e.g., Svendsen et al., 1992; Faleide et al., 1996; Dowdeswell et al., 1998; Licht et al., 1999; Anderson et al., 2002; Powell and Cooper, 2002; McKay et al., 2009; Cowan et al., 2010; Dowdeswell and Fugelli, 2012; Hambrey and Glasser, 2012; Hogan et al., 2012; Kirshner et al., 2012; Batchelor et al., 2014; Dowdeswell et al., 2014; Larter et al., 2014; Rebesco et al., 2014). Many diagnostic lithofacies criteria for recognizing glacigenic processes depend on examination of clast fabric, grain orientation, physical properties, and biofacies (Powell, 1983; Powell and Molnia, 1989; Eyles and Eyles, 1992; Dowdeswell et al., 1998; Wellner et al., 2001; Cofaigh et al., 2007; Garcia et al., 2011; Cowan et al., 2012, 2014; Hambrey and Glasser, 2012; Kirshner et al., 2012; Larter et al., 2014). Lithofacies information from point sources (e.g., cores) reveals local temporal changes, whereas marine geophysics are often used to capture the spatial variability in glacigenic strata formation. Even then, individual, acoustically-stratified seismic facies interpreted as glacigenic, such as suspended sediment deposition, are not unique to ice-dominated settings. The most powerful combination for establishing the extent of glacigenic influence in the sink is to relate seismic facies to lithofacies within a chronostratigraphic context (Anderson et al., 2002; Barrie and Conway, 2002; Dahlgren et al., 2002; Cofaigh et al., 2004; Nygård et al., 2007; Laberg et al., 2009; Hogan et al., 2010).

Sedimentation associated with a moving terminus within the transfer zone leaves behind a record of ice extent, which is a secondary signal of ice dynamics, but it cannot be used to quantify the relationship between ice sliding velocity and sediment produced (Figs. 1 and 5). Documenting this sedimentation is the most common approach used to relate the stratigraphic record with ice dynamics (extent) for glacial S2S systems. In this way, the glacial sedimentary record is treated as a binary (on/off) signal reflected in the deposition of characteristic glacigenic lithologic, geochemical, and/or seismic facies (e.g., Rebesco et al., 2006; Anderson et al., 2014; Cofaigh et al., 2014; Hogan et al., 2010; Larter et al., 2014; Patterson et al., 2014; Reyes et al., 2014; Dowdeswell et al., 2014; Simon et al., 2014). However, the drawback to this approach is that the depositional record (e.g., diamict; laminated

or massive mud; graded beds; chaotic or transparent seismic reflectors) observed in modern glacial environments are not unique to a particular thermal regime (Powell and Molnia, 1989; Dowdeswell et al., 1998; Licht et al., 1999; Evans and Pudsey, 2002; Garcia et al., 2011; Cofaigh and Dowdeswell, 2001; Cofaigh et al., 2001a). Proper discrimination of the climatic setting from a binary signal depends on holistically describing facies assemblages/distributions (Cofaigh et al., 2013; Garcia et al., 2011; Cofaigh and Dowdeswell, 2001; Cofaigh et al., 2001a). Even then, similar lithofacies assemblages (e.g., diamict to laminated mud to massive mud) can accumulate under widely varying climatic regimes (Garcia et al., 2011; Cofaigh et al., 2001a). Only by establishing the geomorphic context and sediment accumulation rates is it possible to differentiate between lithofacies associated with meltwater- versus iceberg-dominated systems, and thus capture the association between changes in ice flux and sediment production (Smith and Andrews, 2000; Desloges et al., 2002).

Observations of the dynamic response of ice to external forcing at various timescales allow us to generate hypothetical sediment mass flux response functions (Fig. 2). The challenge in using field data to derive a response function is placing time constraints on the sedimentary record. The most robust examples are those where accumulation rates can be coupled with unambiguous facies or morphologic indicators of glacigenic sources. As noted, establishing temporal control relies on a chronostratigraphy commensurate with the response time of the perturbation (Kroon et al., 2000). Consequently, the number of studies that establish absolute rates of glacimarine processes and accumulation rates is most numerous for short-term (seasonal-centennial) processes. As the timescales of interest expand into the late Pleistocene, the available chronometers have uncertainties greater than 10^2 yrs. (Austin et al., 1995; Davies-Walczak et al., 2014; Hall, 2009), which is greater than the ice response time seen in the late Holocene (Nesje et al., 2008; Oerlemans, 2005; Wiles et al., 2008). In instances where chronologies are lacking, sedimentary, geomorphic, and geophysical proxies such as IRD, laminated mud and diamict lithofacies, seabed morphology, grounding zone wedges (GZW), and/or mega-scale glacial lineations (MSGL) have been used to infer an ice-dynamic relationship to the stratigraphic signature. Rates of landform formation derived from modern analogs are provided wherever possible (Anderson, 1999; Andrews and Principato, 2002; Anderson et al., 2014; Andreassen and Winsborrow, 2009; Batchelor and Dowdeswell, 2014; Batchelor et al., 2013; Cai et al., 1997; Cofaigh et al., 2008; Cofaigh et al., 2005; Cowan et al., 1997, 2010; DaSilva et al., 1997; Domack, 1990; Dowdeswell et al., 2000; Hambrey and Glasser, 2012; Hogan et al., 2010; Jaeger and Nittrouer, 1999b; Larter et al., 2014; Livingstone et al., 2012; Mackiewicz et al., 1984; Molnia, 1983; Ottesen et al., 2005; Ottesen et al., 2008a, 2008b; Phillips et al., 1991; Powell and Cooper, 2002; Powell and Molnia, 1989; Shipp et al., 2002; Wellner et al., 2006; Willems et al., 2011).

Examples of using glacigenic stratigraphy to resolve ice flux dynamics range from fjords to the deep sea, and from sub-annual to the Pleistocene timescales (Figs. 1 and 2). Given the complexity and breadth of these records, we chose to focus this review on continental-margin settings, as they contain the volumetric bulk of the glacigenic sedimentary record (Fig. 2B–F). For processes operating at the decadal to century timescale (e.g., surges; Fig. 2A), we provide examples primarily from modern fjords where glaciers currently terminate, but recognize that a sedimentary record of similar processes may also exist on shelves, slopes, and in the deep sea whenever ice advanced through the transfer zone (e.g., LGM, Fig. 1). We also only focus on the record where sediment is supplied directly by ice, as this provides the clearest illustration of the ability of these records to resolve ice dynamics. We explicitly ignore glaciofluvial discharge from former ice sheets that dominated North America, Europe, and Asia during the late Pleistocene, as well as the transfer of this sediment from the glacial foreland to the ocean, because determining terrestrial residence times and fluxes are hampered by limited chronologies in terrestrial settings, as well as by the influence of eustasy in modulating fluxes from terrestrial storage basins into the marine realm (e.g., Blum et al., 2000).

4.1. Conditions that influence the magnitude of the mass flux signal

Observations from glaciated basins identify the relative processes that transfer the sedimentary signal of ice flux or ice extent (Section 3), but they also illustrate processes that can introduce complexity in the interpretation of the sedimentary record. Establishing a glacigenic sediment flux requires chronometric control that is most often established in sediment cores, but spatial variability in dispersal processes will influence the flux to that point location. For meltwater-dominated systems, spatial and temporal changes in delivery from the terminus affect point measures in sediment accumulation rates. In temperate settings, sediment fluxes to individual locations (e.g., core sites) will be highly dependent on the residence time of the terminus near that location, because the absolute sediment flux to the seabed often decreases exponentially from the ice-front source (Cowan and Powell, 1991; Powell and Domack, 1995; Syvitski and Shaw, 1995; Gilbert et al., 1998). Where there is rapid deposition at the terminus, the frequency and magnitude of downslope gravity flows will affect accumulation rates (Cofaigh et al., 2013; Taylor et al., 2002a). Without additional spatial data (e.g., seismic reflection profiles), it is challenging to place point measures of accumulation rates into the broader context of dispersal processes to address potential biases (e.g., Willems et al., 2011).

For iceberg-dominated sinks, the sediment flux to any one location is dependent upon the path and residence time of floating ice through the dispersal system. Where icebergs become trapped by sea ice, the overall sediment flux to individual locations might be low because a large component of subglacial and englacial sediment had previously melted out at the terminus (Syvitski et al., 1996; Smith and Andrews, 2000; Mugford and Dowdeswell, 2010). When sea-ice breaks up, there is an increase in iceberg flux through the system and a corresponding increase in the sediment flux. For example, iceberg drift in Baffin Bay is strongly modulated by seasonal sea ice limits, and by longer-term variations in the extent and duration of sea ice cover (Deser et al., 2002; Andrews et al., 2014). For iceberg-dominated sinks covered by floating ice shelves (e.g., the Ross Sea), the sediment flux will be low at sites distal to the grounding line. However, absolute sediment accumulation rates may increase as the ice sheet breaks up and retreats and this leaves open water allowing for increased biogenic fluxes (Licht et al., 1996; Milliken et al., 2009; Maddison et al., 2005, 2006; Leventer et al., 2006).

The size of the depocenter also can influence localized sediment accumulation rates. For meltwater systems with high englacial/subglacial sediment fluxes, sediment dispersal in meltwater plumes or turbidity currents will transfer material to deeper basins, thereby distributing the mass over a larger area (Reece et al., 2011; Taylor et al., 2002b; Walton et al., 2014). As sediment dispersal becomes increasingly distal from the source, sedimentation rates decrease, allowing for secondary processes such as bioturbation to influence the stratigraphic record, creating non-glacial "noise" in the system (Cofaigh et al., 2002; Romans et al., 2016–this volume).

The sediment flux to a particular location also depends on the bedrock type and morphology over which the ice flux does its geomorphic work. For many shelf systems, there is a transition from crystalline rock on the inner shelf to sedimentary (often glacimarine) on the outer shelf (Batchelor and Dowdeswell, 2014; Batchelor et al., 2011; Cofaigh et al., 2004; Livingstone et al., 2012; Nielsen et al., 2005; Wellner et al., 2001; Ottesen et al., 2005). Over comparable periods of erosion and sediment transfer to the sink, the flux signal will be larger for a glacier that occupies more easily erodible bedrock (Hogan et al., 2012; Swift et al., 2008). For example, higher erosion rates at Disko Bay, Greenland are in part related to the high erodibility of the basaltic bedrock (Desloges et al., 2002). Troughs between bedrock highs can also focus sediment

accumulation (Hogan et al., 2012; Lowe and Anderson, 2002; Graham et al., 2010; Jakobsson et al., 2012; Kirshner et al., 2012; Larter et al., 2014) producing a point measure of sediment accumulation that may reflect time spent in constrained bathymetry rather than the volume of subglacially eroded material.

Lastly, autogenic factors can influence glacigenic sediment accumulation rates that are independent of any external climatic forcing on ice flow and erosion. These influences can complicate the ability to use the sedimentary record to inversely determine ice dynamics. The duration of the terminus at any point on the shelf depends on the stability of the grounding line (Powell, 1991; Alley et al., 2007). In Antarctica, it is observed that retreat began earlier for ice streams in deeper troughs than those in shallower troughs, suggesting that water depth influences retreat dynamics (Livingstone et al., 2012), although Larter et al. (2014) suggest that local bathymetric "bottle-necks" also influence ice stream retreat rates. A positive feedback may exist where sediment accumulation is high enough to create a grounding-zone wedge that further stabilizes the grounding line allowing for additional focused deposition. This may allow the grounding line to remain in the same location even as sea level is changing (Powell, 1991; Warren et al., 1995; Van der Veen, 1996; Fischer and Powell, 1998). Also, the accumulation rate used to determine sediment fluxes depends on the available accommodation. Net sediment accumulation may be low even under high sediment input from the glacier terminus if accommodation is low. This may exist where accommodation is reduced due to rapid sediment accumulation (Powell and Molnia, 1989; Powell, 1990; Plink-Bjorklund and Ronnert, 1999), glacioisostatic loading creates a pro-glacial forebulge (Barrie and Conway, 2002), active tectonic uplift (Powell and Cooper, 2002), or the low shelf gradients typical of divergent (passive) margins (Cofaigh et al., 2003). Conversely, sediment accumulation rates in fjords or on the continental shelf and slope may be low if accommodation is high and marine dispersal is efficient. This may be the case wherein higher slopes favor gravity flows that redistribute sediment to deeper basins (Powell, 1991; Dobson et al., 1998; Cofaigh et al., 2003).

4.2. Examples of signal fidelity at various timescales in the glacigenic sink

4.2.1. Sub-annual to annual time scales

Seasonal air temperature fluctuations result in changes in meltwater production and in ice flux (Fig. 2A, B). In temperate systems, increased meltwater production in the summer lubricates the bed, and is associated with increased sliding velocity (Bartholomew et al., 2010; Cuffey and Paterson, 2010). The sliding speed for tidewater glaciers also is dependent on the presence of sea ice that buttresses the terminus in the winter months and breaks up in spring, facilitating faster flow (Mugford and Dowdeswell, 2010). In polar settings where meltwater generation is restricted, the sediment supply comes from direct melting of the calving face and is driven by ocean temperatures for marine-terminating ice (Domack and Ishman, 1993). Consequently, a sub-annual to annual sedimentary signal is more prevalent in temperate settings with higher meltwater fluxes (Fig. 2B).

For the vast majority of modern high-latitude continental margins, marine-terminating ice is present only in fjords or on the inner shelf in Antarctica (Batchelor and Dowdeswell, 2014; Livingstone et al., 2012). Modern glacigenic sediment delivery and measurements of accumulation are generally limited to these settings (Figs. 1, 7, and 8; Powell and Molnia, 1989; Powell and Domack, 2002; Anderson, 1999). Sediment-trap measurements in temperate and subpolar fjords support a temporally varying sediment flux throughout the year (Fig. 2C; Cowan and Powell, 1991; Ashley and Smith, 2000; Svendsen et al., 2002; Phillips et al., 1991) driven by seasonal variability in meltwater production (Kempf et al., 2013; Svendsen et al., 2002; Griffith and Anderson, 1989; Domack and Ishman, 1993; Yoon et al., 1998; Ashley and Smith, 2000). Sedimentation rates can be as high as 10 cm d^{-1} and 10 m yr^{-1} near the terminus of temperate tidewater glaciers (Molnia, 1983; Cowan and Powell, 1991). Similarly, reduced sediment deposition rates in the winter have been documented using short-lived radioisotopes (Jaeger, 2002; Muñoz et al., 2014). Interstratified mud in temperate fjords has been interpreted as annual varves, with the interstratification of sand, coarse silt and mud created by fluctuations in meltwater discharge and interactions with tidal currents to produce monthly and bimonthly cycles (Cowan et al., 1998; Jaeger, 2002). Massive and stratified diamicts accumulate in the winter, when IRD is not diluted by meltwater-driven sediment input, and the residence time of icebergs in the fjords increases (Syvitski, 1989; Mackiewicz et al., 1984; Cowan et al., 1997, 1999; Dowdeswell and Cromack, 1991).

Accordingly, the sedimentary proxy of seasonal changes in meltwater and sediment input in a meltwater-dominated, ice-proximal setting is an IRD–diamict interstratified mud couplet (varve). The preservation of interannual stratification depends on sedimentation rates, which are in turn dependent upon distance from the ice front. When rates drop below 4 cm yr^{-1}, bioturbation homogenizes the record (Jaeger and Nittrouer, 1999b). In contrast to glaciolacustrine sinks, where an empirical relationship has been shown to exist between meltwater input and varve thickness (e.g., Chutko and Lamoureux, 2008), this approach has yet to be conclusively demonstrated for temperate fjords (Pedersen et al., 2013), which may reflect the greater number of variables influencing sediment transfer from ice front to sink (Gilbert et al., 2002; Cofaigh and Dowdeswell, 2001).

In modern polar fjords, seasonal variability in sediment flux from the ice exists, but relatively high biogenic fluxes and low glacigenic sediment fluxes (~few mm yr^{-1}) often results in a homogenous fjord lithofacies (sandy mud with dispersed clasts) greatly impacted by bioturbation (Leventer et al., 1993, 2006; DeMaster et al., 1991; Powell and Domack, 2002; Hillenbrand et al., 2010b; Maddison et al., 2005, 2006; McClintic et al., 2008). For example, at Jakobshavn Isbræ in eastern Greenland, seasonal variation in calving rates due to changes in ice velocity results in winter advance and summer retreat of the terminus (Joughin et al., 2012), yet no annual signal from this process is recorded in the sediments, likely due to low sedimentation rates relative to bioturbation rates (Cofaigh and Dowdeswell, 2001). Laminated facies can be preserved, but they may reflect both increases in seasonal productivity, as well as sediment resuspension during calving events and tidal influences (Ashley and Smith, 2000; Domack, 1990; Powell and Domack, 2002).

Given that most modern marine-terminating ice is restricted to fjords, there are few examples of annual glacigenic strata formation on continental shelves or slopes (Jaeger and Nittrouer, 1999b; Figs. 1 and 2D, E). Although there may be seasonal increases in glacigenic sediment discharge to some shelves (e.g., Merrand and Hallet, 1996; Jaeger and Nittrouer, 1999b), the sedimentation rate is generally not high enough to overcome homogenizing effects from bioturbation to allow for preservation of a distinct annual signal (Fig. 2D; Cofaigh et al., 2002; Jaeger and Nittrouer, 2006; Cofaigh and Dowdeswell, 2001).

4.2.2. Advance-retreat/surge time scales

The ice dynamics of the past 10–1000 years are characterized in many settings by episodic advance-retreat events that can span from a year, i.e., a surge (e.g., Raymond, 1987) to hundreds of years, such as the Little Ice Age (Oerlemans, 2005; Dowdeswell et al., 1991). These events are often observed in temperate and polythermal glacial settings, including Alaska, Svalbard, and Chile (Kempf et al., 2013; Hagen et al., 1993; Dowdeswell et al., 2000; Dowdeswell et al., 1991). Each event can be a consequence of a change in mass balance (Svendsen and Mangerud, 1997; Ottesen and Dowdeswell, 2006; Plassen et al., 2004; Kempf et al., 2013; Oerlemans, 2005; Huybers and Roe, 2009; Jiskoot et al., 2000; Kamb et al., 1985; Molnia and Post, 2010; Murray et al., 2003; Muskett et al., 2008; Ottesen et al., 2008a; Pritchard et al., 2005; Raymond, 1987), or be independent of climate forcing (Murray et al., 2003; Nick et al., 2007). The ice flux is expected to increase during the advance phase (Fig. 2A; Lingle and Fatland, 2003; Moon et al., 2012;

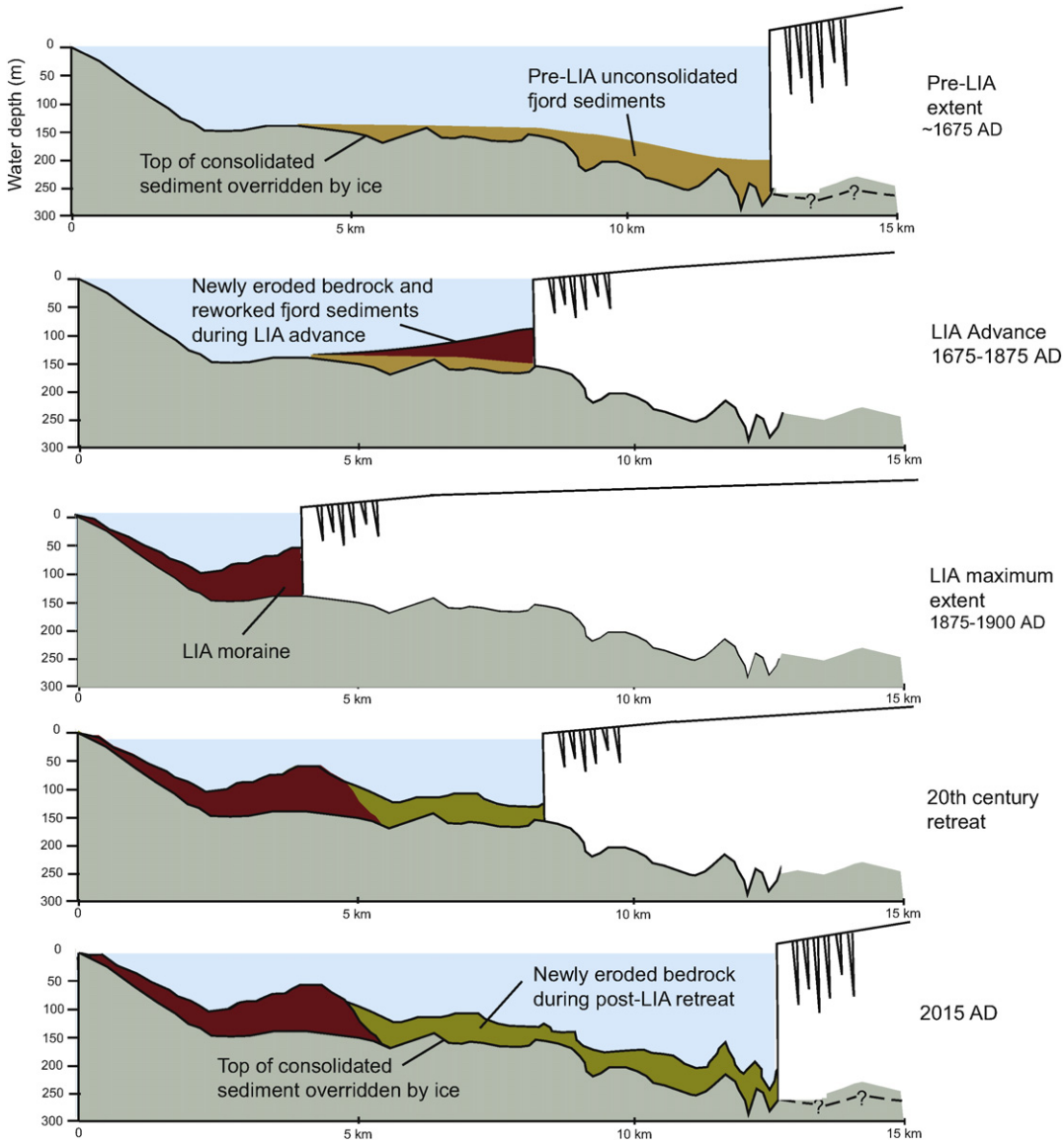

Fig. 12. Cartoon interpretation of the seismic stratigraphic record of the LIA advance and subsequent retreat of San Rafael Glacier, North Patagonian Icefield, and the associated sedimentary sequences found in Laguna San Rafael, the ice-proximal fjord. Pre-LIA unconsolidated sediment deposited by turbid meltwater plumes and IRD before the start of the LIA advance event (<1675 AD) and subsequently reworked by advancing ice in tan. Newly generated sediment from the glacier catchment and fjord sediments remobilized and redeposited during LIA advance and maximum extent in burgundy. Newly generated sediments eroded during 20th century retreat in olive. Duration of LIA advance, maximum stillstand and retreat are derived from early navigational maps and aerial photography. Gray indicates top of eroded and reworked pre-LIA sediment consolidated by overriding ice during LIA advance-retreat cycle, noted in seismic profiles as a strong subbottom reflector. Modified from Koppes et al. (2010).

Murray et al., 2003), and also during the retreat phase (O'Neel et al., 2005; Koppes et al., 2009), which could hypothetically generate two sediment pulses per event (Fig. 2B, C). As with annual signals, the magnitude of this glacigenic sediment signal is expected to be highest in temperate, meltwater-dominated settings (Fig. 6) (Merrand and Hallet, 1996; Hallet et al., 1996; Jaeger and Nittrouer, 1999b).

The ability to constrain the onset and termination of each surge event presents one challenge for documenting the duration of an advance/retreat event using sediment accumulation rates. For the timescale of the LIA, historical maps of termini positions, where available, can constrain the event duration (e.g., Fig. 12) (Ottesen et al., 2008b; Koppes et al., 2010; Cowan et al., 2010). However, in most locations, resolving the duration of LIA and Neoglacial events in the sedimentary record is challenging because of the imprecision of radiocarbon and other geochronometers over these centennial response timescales (Austin et al., 1995; Hall, 2009; Dowdeswell et al., 2000).

The sedimentary signal produced by surges and advance-retreat events is mostly observed in fjords where modern glaciers reside (Fig. 2C). For example, Gilbert et al. (2002) captured the sediment flux associated with a short, five-year surge event in Disko Fjord, West Greenland. The higher meltwater input during the surge resulted in the deposition of diurnal laminated mud that accumulated up to 30 times faster than the long-term, pre-surge ^{14}C-derived accumulation rates. Additionally, Kempf et al. (2013) examined the changing lithofacies and sediment fluxes associated with episodic "surge" events lasting for ~200 years in Spitsbergen, and found clast-rich, sporadically stratified glacimarine mud close to the morainal bank, which decreased in accumulation rate by an order of magnitude following each event. The cores did not have the temporal resolution to test for a hypothetical increase in sediment flux at the onset of each event (Fig. 2C). Szczucinski et al. (2009) also documented a substantial increase in sediment flux following the LIA in Billefjorden, Svalbard, and inferred that

post-LIA increases in temperature and negative glacier mass balance resulted in larger meltwater discharges both eroding subglacial sediment stores and transferring considerable amounts of sediment from the glaciers. Notably, the properties of the fjord sediments (grain size, IRD, coarse-fraction composition, clay mineralogy) showed no distinct differences between those of the LIA advance and the 20th century retreat.

Under certain conditions, centennial-scale advance/retreat events provide perhaps the best opportunity to document how changing ice flux over an advance-retreat cycle impacts sediment production. Establishing the chronology and duration of the event is critical to document the changing sediment flux and can best be achieved when historical or terrestrial chronologies of the event exist (e.g., Cowan et al., 2010; Koppes et al., 2010). Whereas point measurements (sediment cores) provide a measure of time-varying flux to local portions of the depocenter, the inherent dynamics of sediment dispersal may result in a biased record of overall flux from the ice (Gilbert et al., 2002). To overcome this, the delineation of sediment/seismic volumes into discrete advance/retreat phases allows for capturing the total sediment produced through various dispersal processes. The ideal setting to test this is in a constrained basin where the total or majority of the sediment flux of the event can be captured (Fig. 12) (Koppes et al., 2010).

Time-varying sediment fluxes associated with the retreat of the Muir Glacier, Glacier Bay Alaska, from its LIA maximum were established with seismic-reflection volumes constrained by historic termini positions (Cowan et al., 2010; Koppes and Hallet, 2002, 2006). Cowan et al. (2010) found that the sediment flux decreased in time with decreasing drainage basin area. Sediment input was established to be both from the retreating Muir Glacier but also from tributary sources and gravity flows shed from the sides of basins. Consequently, the temporal sediment-flux record associated with event-related ice dynamics must account for the time-varying extent of the ice volume. The ability to quantify fluxes over the full cycle of an event is challenging, because the advance phase removes some portion of the existing record within the basin (Cowan et al., 2010) and deposits it down-flow, often in wider distal basins where it accumulates with sediment from other sources. Because of this, most sediment-flux records of an event capture only the retreat phase. One exception to this was documented for Laguna San Rafael, Chile (Koppes et al., 2010). The use of historical navigational maps and aerial photos, coupled with bathymetric mapping and subbottom profiles allowed for the reconstruction of sediment volumes that were deposited during the advance, maximum LIA-standstill, and post-LIA retreat of the San Rafael Glacier (Fig. 12). The sediment fluxes were normalized to glacial basin area to derive an erosion rate, with the highest rates occurring at the start of the retreat phase, and steadily decreasing as retreat continued. Erosion rates were more than 4 times lower during the glacial advance phase than during the retreat phase.

In polar fjord settings, the sedimentary record of advance/retreat events is less clear. For example, Jennings and Weiner (1996) and Dowdeswell et al. (2000) documented the accumulation of stratified diamict and laminated mud during the LIA in Nansen Fjord, East Greenland and attributed the accumulation of this lithofacies to dynamic sea conditions that prevented IRD accumulation, providing another example of how changes in accumulation rates might reflect an autogenic response in the basin rather than a direct measure of glacigenic sediment flux. Conversely, Milliken et al. (2009) interpreted the ~14-ky-long multiproxy record from the SHALDRIL drill core retrieved from Maxwell Bay in the Antarctic Peninsula, and found several oscillations in ice extent in the proxy record but no distinctive intervals that reflect LIA or other late Holocene climatic fluctuations.

On the continental shelf and in deeper water, the sedimentary record of decadal- to centennial-scale ice dynamics is poorly documented. Moreover, the deposition of non-glacigenic sediment at these time scales in high-latitude open water settings is expected to dominate the signal, and reflect basin-scale changes in water-column productivity or local bottom current strength (Fig. 2D–F; Cofaigh et al., 2002; Kroon et al., 2000; Radi and de Vernal, 2008; Taylor et al., 2002c). One notable exception is the LIA advance and retreat of the Bering Glacier in Alaska, which was recorded on the adjacent continental shelf and constrained onshore by dendrochronology (Wiles et al., 1999). Jaeger and Kramer (2014) found sediment accumulation rates doubled during the period of maximum ice extent, but due to uncertainty in marine reservoir ages/atmospheric production rates on ^{14}C ages, changes in sediment flux over the complete LIA cycle could not be established.

One indirect depositional proxy of episodic advance-retreat events on the continental shelf is the isolated hummocks and ridges found in many fjords or inner continental shelves, which are interpreted as push moraines during advance or morainal banks formed by bedload dumping at the terminus during retreat (Figs. 1 and 10; Dowdeswell and Vásquez, 2013; Landvik et al., 2014; Molnia, 1983; Ottesen and Dowdeswell, 2006; Ottesen et al., 2008a; Hald et al., 2001; Kristensen et al., 2009; Plassen et al., 2004; Kempf et al., 2013; Dowdeswell, 1995; Dowdeswell et al., 2014). For the last LIA event, recent terminus retreat and lower post-LIA sedimentation rates allow for these landforms to be observed and mappable in swath bathymetry (Ottesen et al., 2008a). As noted by Boulton and Hagdorn (2006), such lobate landform features must be a consequence of local, fast ice streaming, where the response time of the ice dictates whether these features reflect a short-term surge event or a long-term occupation of the fjord by an ice stream. The challenge in using these features to quantify glacigenic sediment production during an event cycle is partitioning sediment that was previously deposited and has been remobilized and reworked into the morainal bank during the advance from newly-produced sediment that reflects the contemporaneous basal ice conditions and accounts for variable bedrock lithology (Fig. 12; Koppes et al., 2010).

4.2.3. Post-LGM deglacial timescales

Over the period of the Last Glacial Maximum (LGM), large ice sheets dominated by ice streams were the major dispersal system generating and transferring sediments from land to ocean. However, the large variability in spatial extent of the ice during this period, which at times extended across the entire transfer zone (Fig. 1), presents a distinct challenge in preserving a sedimentary record in the sink. To depict glacigenic sediment production at LGM time scales (Fig. 2B), we postulate changes in sediment fluxes based on observations of modern ice advance-retreat dynamics. For instance, from observations of one the few contemporary examples of a glacier advance at Taku Glacier in SE Alaska (Motyka et al., 2006) we can hypothesize that sediment flux to the terminus will be highest as the ice advances across the transfer zone (foreland, fjord, shelf, slope) under a cooling climate (Fig. 2A), because higher flux results from both the recycling of existing deposits in the transfer zone and increased bedrock erosion associated with the larger area of ice cover. Given observations of modern dynamics, we also can postulate that at the maximum stillstand associated with the coldest ocean and air temperatures, meltwater production, ice velocities and sediment transfer rates all would be lower (Fig. 2B). During deglaciation, sediment transfer to glacial termini would be expected to increase as a result of ice acceleration during retreat and drawdown (e.g., Koppes et al., 2010).

The global withdrawal of ice sheets from their LGM maximum extents provides examples of the sedimentary flux associated with the late-Pleistocene to Holocene deglaciation phase (Henriksen et al., 2014; Landvik et al., 1998; Ottesen et al., 2005; Evans et al., 2002; Kempf et al., 2013; Lekens et al., 2005). However, with the exception of examples from West Greenland, little is known about concurrent changes in the internal dynamics of the ice during this deglaciation. The hypothetical spatio-temporal sediment flux associated with this LGM-Holocene transition will reflect the duration and extent of the ice in each segment of the S2S system (Figs. 1 and 2C–F). For instance, ice streaming and sediment erosion in fjords and in shelf troughs during the LGM will transition to net accumulation as the

terminus retreats past a given point. Moreover, once deglaciation commences, glacigenic sediment accumulation on the continental slope and deep sea is rapidly reduced as the ice margin retreats landward (Fig. 2E–F).

In a landmark paper, Elverhøi et al. (1998b) interpreted seismic reflection isopachs to establish glacigenic sediment production in Svalbard during the LGM-Holocene transition. They used changes in seismic facies associated with LGM retreat and dated episodic surge events in fjords to establish a chronology for the isopachs, and found that glacigenic sediment yields (i.e., mass/drainage basin area/time) varied by more than an order of magnitude over the Holocene. The highest rates were associated with deglaciation, decreasing from the Early Holocene to a Mid Holocene low, corresponding to the regional climatic optimum. Sediment yields increased again during the Late Holocene reflecting ice readvance; they interpreted this increase in flux to reflect both increased subglacial erosion and redistribution of paraglacial sediment that had been stored in the proglacial basin during the middle Holocene.

In contrast, in West Greenland, marine records of LGM-Holocene glacigenic sediment fluxes in the fjords and on the shelf are relatively few, but recent field data have added substantial information about ice dynamics in this region (Roksandic, 1979; Kuijpers et al., 2007; Hogan et al., 2011; Schumann et al., 2012; Dowdeswell et al., 2014; Hogan et al., 2012; Cofaigh et al., 2013). During the LGM, ice streams from western Greenland extended to the shelf edge through Uummannaq and Disko troughs, and retreated episodically after 14.8 kya (Cofaigh et al., 2013; Dowdeswell et al., 2014). Sediment accumulation rates from cores collected from the shelf troughs decreased by a factor of 5–10 from the start of deglaciation to the present (Cofaigh et al., 2013). Hogan et al. (2012) used seismic reflection isopachs to quantify sediment volumes and demonstrated that the highest sediment accumulation rates occurred during deglaciation, comparable to the highest modern rates from temperate environments (e.g., Hallet et al., 1996; Koppes and Montgomery, 2009). Whereas the fjords of West Greenland currently exhibit relatively low glacigenic sediment fluxes (Lloyd et al., 2005; Lloyd, 2006; Desloges et al., 2002; Cofaigh et al., 2013), the high sediment accumulation rates during deglaciation suggest higher meltwater and sediment inputs, and thus higher ice fluxes, during this period (Hogan et al., 2012).

Other examples of elevated sediment fluxes during deglaciation exist in high-latitude fjords. Laberg et al. (2009) determined that the glacigenic sediment accumulation rate during the LGM retreat of the Vestfjorden paleo-ice stream, part of the northwestern Fennoscandian ice sheet, was significantly elevated relative to overall Holocene rates, with calculated bedrock erosion rates of >1 mm yr^{-1}, equivalent to rates from Svalbard and other Fennoscandian ice streams (Elverhøi et al., 1998b). The SHALDRIL drill core retrieved from Maxwell Bay in the Antarctic Peninsula recorded glacigenic sedimentation rates that decreased from 31 mm yr^{-1} during the LGM-Holocene transition to 4 mm yr^{-1} in the late Holocene, reflecting significant warming and grounding line retreat at the end of the LGM (Milliken et al., 2009).

On continental slopes that received sediment directly from the former LGM ice sheets in Svalbard, Alaska, and British Columbia, individual cores record the deglaciation transition as an order of magnitude decrease in sediment flux that reflects terminus retreat and substantial contraction of ice (Fig. 13; Barrie et al., 1991; Hendy and Cosma, 2008; Davies et al., 2011; Lekens et al., 2005; Vorren et al., 1998). Higher glacigenic sediment fluxes during the initial deglacial period are recognized both in terms of ^{14}C- or δ^{18}O-established chronologies and also from lithofacies proxies (e.g., laminated glacimarine mud). Importantly, these higher fluxes can be directly related to the dynamics of the ice through meltwater events interpreted from planktonic foraminiferal δ^{18}O records associated with destabilization of the ice sheets (Evans et al., 2002; Hendy and Cosma, 2008; Davies et al., 2011; Lekens et al., 2005).

On continental margins, sediment accumulation rates of hemipelagic, IRD, and gravity flow deposits also reflect temporal changes associated with LGM ice extents (Fig. 13B). In East Greenland, ice advance across the shelves to the LGM maximum extent is revealed by increased mass accumulation rates on the continental slope (Funder et al., 1998; Evans et al., 2002). Subsequent decreased glacigenic sediment accumulation and IRD fluxes to the slope likely indicate ice retreat from the shelf (Funder et al., 1998), which is supported by increasing glacigenic sediment accumulation rates on the inner shelf (Fig. 13B). However, Funder et al. (1998) noted that the IRD flux signal on the East Greenland shelf must be carefully interpreted in terms of ice dynamics, as high IRD fluxes can occur under both colder conditions (ice advance to shelf edge) or warmer conditions (no sea ice present to trap icebergs).

Along the Antarctic margin, the sedimentary record of ice dynamics has been predominantly used to determine the maximum extent at the LGM and the subsequent history of deglaciation, especially of the West Antarctic Ice Sheet (WAIS). This region is currently experiencing accelerated volume loss due to increased ice velocities of the many outlet glaciers and ice streams (Anderson et al., 2014; Hillenbrand et al., 2014; Larter et al., 2014; Rignot et al., 2014). In many respects, this region serves as a key example of how marine geophysics, sedimentology, and cosmogenic dating can be used to establish ice extent and dynamics, as is thoroughly discussed in several comprehensive review papers (Anderson et al., 2014; Cofaigh et al., 2014; Hillenbrand et al., 2014; Hodgson et al., 2014; Larter et al., 2014; Mackintosh et al., 2014). Ice extent and dynamics in the Antarctic marine realm are determined from dating subglacial to glacimarine to open-marine lithofacies transitions (see Anderson et al., 2014; Cofaigh et al., 2014; Hillenbrand et al., 2014; Hodgson et al., 2014; Larter et al., 2014; Mackintosh et al., 2014 for cited studies). Because of the scarcity of calcareous fossils in Antarctic shelf sediments, it is particularly challenging to use marine ^{14}C to develop constraints on the timing of deglaciation and the accompanying sediment flux (Anderson et al., 2002; Andrews et al., 1999; Hall, 2009; Hillenbrand et al., 2010a; Larter et al., 2014; Licht and Andrews, 2002). In light of these dating challenges, the ability to recognize the large-scale regional controls on ice extent (e.g., shelf bathymetry, oceanographic forcing) is easiest when all chronological controls are synoptically summarized (Anderson et al., 2014; Cofaigh et al., 2014; Hillenbrand et al., 2014; Larter et al., 2014). Doing so reveals that the maximum extent of the WAIS at the LGM was variable across the shelf. Initial deglaciation was asynchronous, and deglaciation was variable in space, particularly on the inner shelf (Bentley et al., 2014). Although chronologies can be established for ice retreat along the Antarctic margin, the record is not well enough resolved to establish the variability of sediment fluxes associated with retreat (Leventer et al., 2006; Licht et al., 1996).

In summary, the fast terminus retreat and rapid drawdown of ice associated with the retreat phase of modern tidewater glaciers suggest that ice fluxes and corresponding sediment fluxes should be elevated during deglaciation (Humphrey and Raymond, 1994). Examination of temperate and polar sedimentary records reveals high sediment accumulation rates at various points along the retreating ice margin during deglaciation. This decreased substantially over time, with a few instances of increased accumulation in the late Holocene associated with periods of renewed ice advance (Davies et al., 2011; Evans et al., 2002; Kempf et al., 2013). Sediment isopach thicknesses vary as a function of retreat rate, but in several examples the total sediment flux during deglaciation derived from isopachs argues for greatly elevated flux during retreat relative to the present (Hogan et al., 2012). For many marine-terminating systems from Alaska to East Greenland, the sedimentary record does support the hypothesis that retreat of the ice margin results in elevated glacigenic sediment production that may reflect an increased ice flux during deglaciation. For polar iceberg-dominated systems of Antarctica, where sediment fluxes

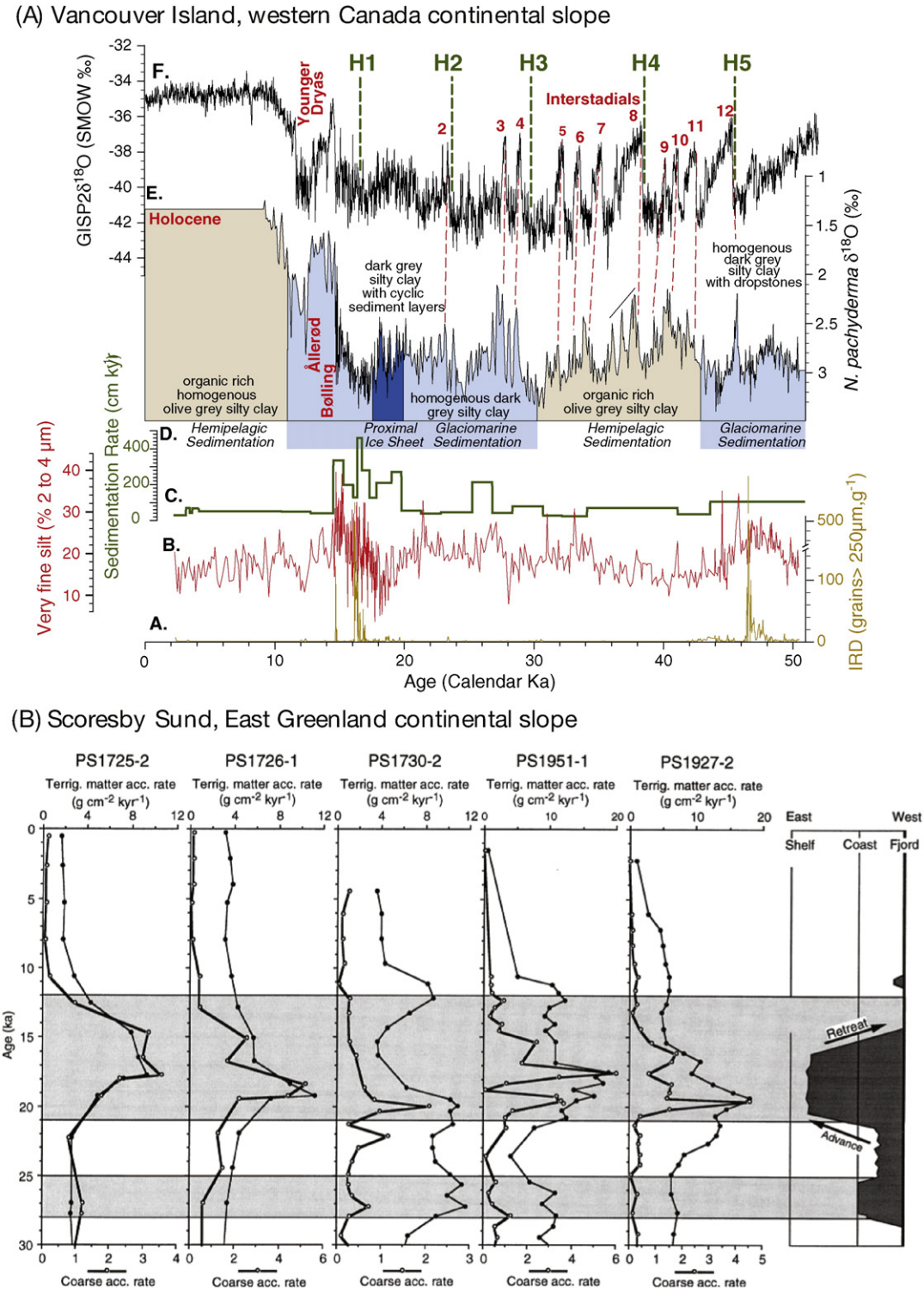

Fig. 13. Two examples of continental slope sedimentary records of LGM ice extent. (A, Top) Comparison of North Pacific/Cordilleran ice extent with the North Atlantic, from Hendy and Cosma (2008). A = ice-rafted debris or IRD, B = percent of terrigenous sediment, 2–4 μm (red), C = sedimentation rate (cm ka^{-1}), D = core lithology and interpretation, E = N. pachyderma $\delta^{18}O$ (MD02-2496, Vancouver Island), F = comparison with GISP2 $\delta^{18}O$ from the Greenland ice sheet. Major climate events correlate between the core and GISP2 (interstadials dashed red line; North Atlantic Heinrich events (H1-H5) dashed green lines). (B, Bottom) Terrigenous and IRD accumulation rates from the continental slope east of Scoresby Sund, East Greenland, from Funder et al. (1998). Amount of IRD and flux rates of terrigenous sediment plotted versus reservoir-corrected radiocarbon ages. Shaded intervals indicate timing of major pulses of IRD discharge associated with maximum ice extent and subsequent retreat.

are modulated by floating ice shelves and/or sea ice, there are relatively insufficient data at this time to quantitatively resolve how deglaciation influences glacigenic sediment production and sediment release at the grounding line.

4.2.4. Quaternary glacial–interglacial cycles

The distinctive trough-bank morphology of high latitude continental shelves is a testament to prevalence of ice in shaping glacigenic sinks over Pleistocene timescales. Ice streaming and rapid calving maintain

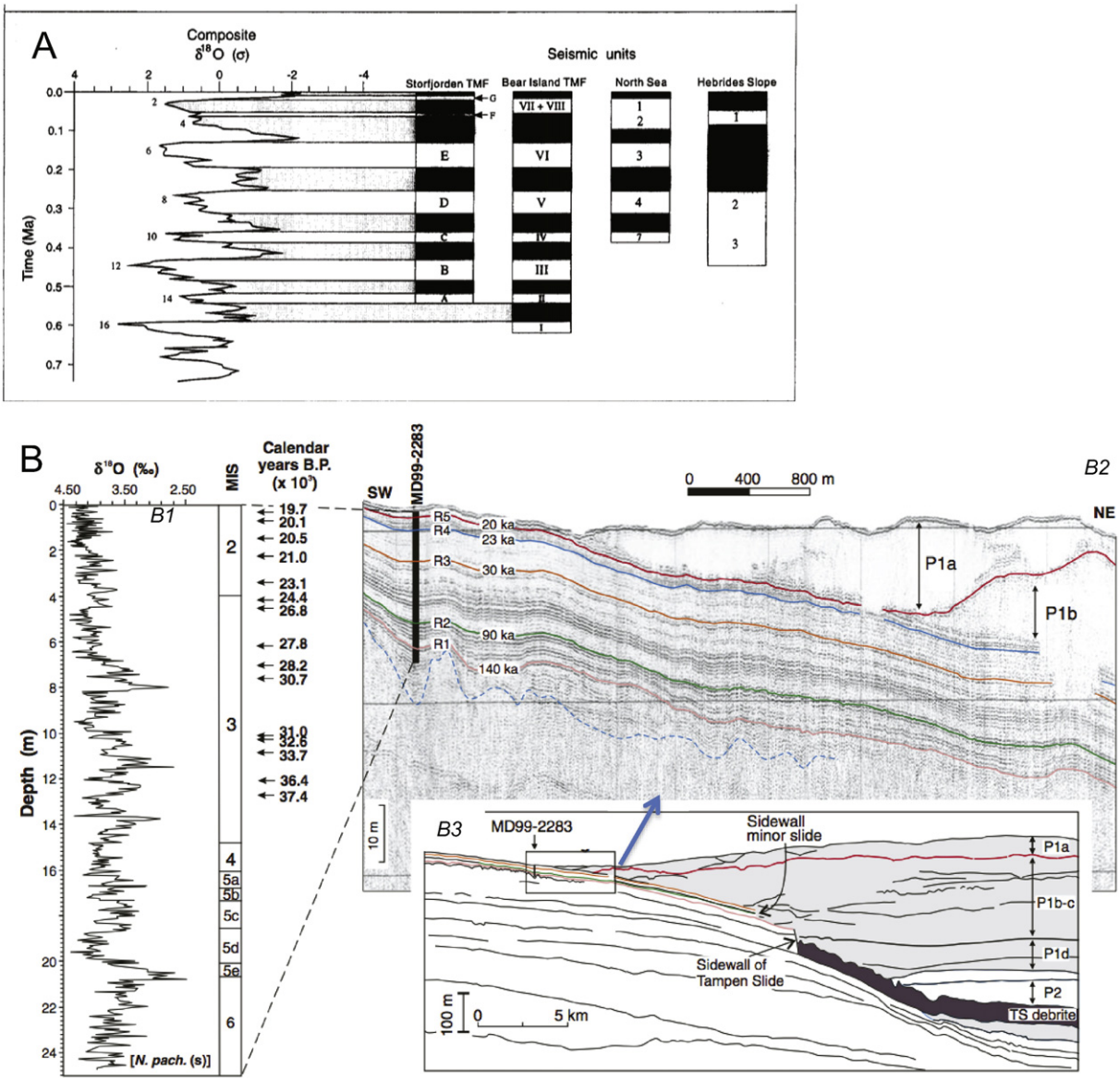

Fig. 14. Two examples of chronostratigraphic control of seismic reflection data. (A, Top) Correlation of seismic units (debris flow units) in the trough-mouth fans of northeastern Atlantic/Barents Sea margin with MIS (marine isotope stages) from global oxygen isotopic stratigraphy. Debris flows are assumed to occur during periods of maximum ice extent across shelves. From Vorren and Laberg (1997). (B, Bottom) Integrated seismic and core stratigraphy, Norwegian Channel Ice Stream, from Nygård et al. (2007). B1: Oxygen isotope ($\delta^{18}O$) profile [*N. pach.* (*s*)] and calibrated radiocarbon ages of core MD99-2283; B2: Along-slope deep-tow boomer profile with interpreted reflectors R1–R5, showing position of core MD99–2283; B3: Interpreted single airgun profile shot alongside boomer profile, showing regional stratigraphy. Light gray shading indicates glacigenic debris flows; dark gray indicates slide debrites; white background represents layered sediments of hemipelagic origin.

a high ice flux through the S2S system that is capable of eroding and reshaping both bedrock and glacigenic strata (Livingstone et al., 2012). Advances in marine geophysics and swath bathymetry have allowed us to map at high spatial resolution the flow of ice across these regions, documenting the dispersal pathways from source to sink over orbital timescales (Section 3). Establishing glacial sediment fluxes over the same timescales has proven more challenging, however, because ice advance through the transfer zone removes prior strata (Berger et al., 2008a; DaSilva et al., 1997; Powell and Cooper, 2002; Wellner et al., 2006). Consequently, the most complete stratigraphic record of glacial–interglacial ice dynamics is found beyond the continental shelf break. To first order, former ice extents can be determined from the binary, proxy sedimentary records found in gravity-flow deposits and IRD accumulating on the continental slope and in deeper basins (Auffret et al., 2002; Cofaigh et al., 2004; Hendy and Cosma, 2008; Davies et al., 2011; Dowdeswell et al., 1998; Nielsen et al., 2005; Rebesco et al., 2006; Patterson et al., 2014; Simon et al., 2014). Further establishing the ice flux dynamics from glacigenic sediment volumes requires spatially distributed seismic reflection data linked to a chronology that is based on a long drill-core record (e.g., Fig. 14; Dowdeswell et al., 2010; Nygård et al., 2007; Reece et al., 2011; Vorren and Laberg, 1997).

The sedimentary record of ice extent on Quaternary time scales is commonly established from IRD and other sedimentologic/geophysical proxies (Section 3). The challenges associated with developing glacial–interglacial chronologies in high-latitude sediments can be overcome by the combined use of multiple chronometers (Fig. 15; Alexanderson and Murray, 2012; Fuchs and Owen, 2008; Hillenbrand et al., 2010b; Simon et al., 2012; Brachfeld et al., 2003; Stoner et al., 2000; Hendy and Cosma, 2008; Davies et al., 2011; Praetorius and Mix, 2014). Where distinctive bedrock geology is present, the relative contributions of glacially eroded sediments from different ice sources can be established through temporal analyses of sediment provenance (Andrews et al., 2014; Andrews and Vogt, 2014; Cook et al., 2014; Reyes et al., 2014; Simon et al., 2014; Pierce et al., 2014; Flowerdew

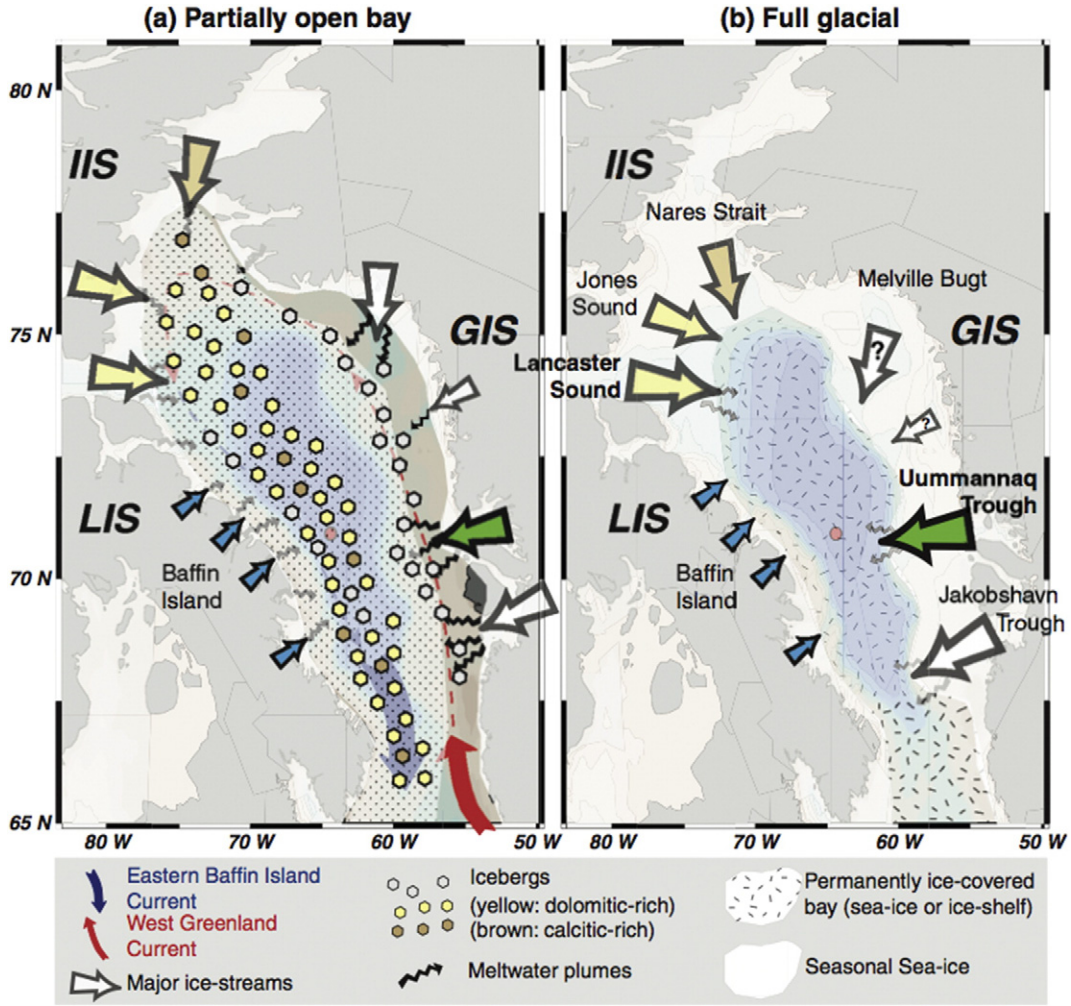

Fig. 15. Simplified Baffin Bay paleogeography during the last glacial cycle. (a) Partially open bay characterized by IRD sediments originating from the northern ice streams (yellow, brown arrows), and by meltwater plumes from Baffin Island ice streams (blue arrows). West Greeland Current traps GIS IRD along coast. (b) Full glacial mode characterized by Greenland and Baffin Island diamicts corresponding to a permanently ice-covered bay, and by extended fast-flowing ice streams feeding an ice shelf in the bay. From Simon et al. (2014).

et al., 2012, 2013; Bailey et al., 2013). For example, several attempts have been made to integrate the numerous glacigenic, seismic reflection, and proxy records of ice sheet extent in the Barents–Kara sea region (Ingólfsson and Landvik, 2013; Jakobsson et al., 2014a; Mangerud et al., 1998; Svendsen et al., 2004). Synthesizing many different datasets with their own temporal and spatial resolution results in a glacial history that is a compromise and often does not match with local stratigraphic records, but the benefit of this approach is that the driving mechanisms of ice dynamics (climate, oceanography, sea level) can be explored and tested against observations (Ingólfsson and Landvik, 2013; Jakobsson et al., 2014b).

In contrast, a more simplified view of ice dynamics can be developed from a single, central location that integrates the spatial and temporal variability of Quaternary ice sheet dynamics, such as that done by Simon et al. (2014) in Baffin Bay (Fig. 15). Using a multiproxy approach from one distal, deep basin, they document variable glacigenic sediment production from the northeastern Laurentide, southern Innuitian and western Greenland ice margins over the last 115 ka. Contrary to the hypothesized high (glacial advance)–low (glacial maximum)–high (glacial retreat) sediment flux expected over a full glacial–interglacial cycle (Fig. 2B), the highest sediment accumulation rates were found during the MIS 1-2 deglacial transition, associated with elevated input from the Laurentide and southern Innuitian ice sheets, while sediment delivery from the fast-flowing ice stream in the Uummannaq Trough dominated the LGM period from ~32 to ~16 ka.

It can be argued that a temporal examination of sediment fluxes at a single site may not capture the total sediment flux generated from the source because of variable sediment routing to the sink (Jerolmack and Sadler, 2007; Gilbert et al., 2002). Adequately testing the high-low-high sediment flux scenario for a full glacial–interglacial cycle requires a) chronologically constrained seismic reflection data and b) a closed-system sink (i.e., all sediment delivered to the sink can be accounted for) over the timescale of interest. However, glaciated continental-margin settings present tremendous logistical and analytical challenges for collecting such geophysical data. It is difficult to recover sediment from diamicts by conventional drilling or to develop chronologies from barren sediments. Accordingly, there are few examples where even parts of the glacial–interglacial cycle can be examined at a temporal resolution equal to the response time of the ice.

The predominance of cross-margin troughs on high-latitude margins suggests that ice streams are the principal mass dispersal pathways, and offer some of the best geographic locations to quantify mass fluxes over full glacial cycles (Vorren and Laberg, 1997). One notable example of attempting to quantify such a system is the work by Nygård et al. (2007), who used a dense seismic reflection network with millennial-scale age control to document the sediment flux at the outlet of the Norwegian Channel ice stream, within the 100-kyr cycle (Fig. 15). Extremely high sediment yields of up to 1.1 Gt yr^{-1} (equivalent to yields from the largest modern rivers) from glacigenic debris flows persisted for a short time between ~20 to 19 ka, suggesting that the

ice stream was highly dynamic during this period. Estimated ice stream velocities associated with this high flux were 1.3–2.7 km yr^{-1}. Assuming a transport distance from source to sink of 300–600 km, the potential transfer time of the signal from the upper reaches of the source was equal to, or slightly faster than, the duration of the event (Nygård et al., 2007).

Another notable example of integrating geophysical, sedimentological, and chronstratigraphic approaches to establish the erosive dynamic state of ice is by Laberg et al. (2009). They examined the sedimentary record produced in Vestfjorden, a former major ice stream of the northwestern Fennoscandian ice sheet (Boulton et al., 2001; Ottesen et al., 2005). The chronostratigraphy is relatively well established for the latest glacial cycle (~35–10 ka; Andersen, 1975; Lauritzen, 1991; Olsen et al., 2001; Baumann et al., 1995; Dahlgren and Vorren, 2003; Bergstrøm et al., 2005). Significant erosion of >100 m of unconsolidated sediments was observed in the outer part of the fjord during the LGM, and it is believed that the majority of erosion occurred under temperate bed conditions in the lower tributaries of the ice stream (Stroeven et al., 2002). The resultant sediment volume that accumulated between 26 and 18 kya (the limit of their temporal resolution) equates to an average erosion rate of 1.7 mm yr^{-1} and a glacigenic sediment discharge of $>10^8$ t yr^{-1}, which is comparable to modern glacifluvial systems in Alaska (Jaeger et al., 1998) yet an order of magnitude less than that observed by Nygård et al. (2007). The lack of a high-temporal-resolution chronostratigraphy directly tied to the seismic-reflection dataset in the Laberg et al. (2009) study precluded the ability to determine if the sediment flux was limited to a very short time period during the maximum ice extent, as was done by Nygård et al. (2007) (e.g., Fig. 14).

The studies by Nygård et al. (2007) and Laberg et al. (2009) illustrate the need to capture and date the full seismic volume associated with an ice stream cycle from source to sink if the goal is to use sediment fluxes as a means of partitioning glacigenic sediment production through time (Fig. 14). While these two studies document sediment fluxes within a 100-kyr glacial–interglacial cycle with relatively high temporal fidelity, additional examples integrating seismic-and chrono stratigraphy exist where sediment fluxes have been determined at lower temporal resolution for the LGM (Dahlgren et al., 2005; Knies et al., 2009; Dowdeswell et al., 2010; Laberg et al., 2010; Laberg and Vorren, 1996; Nielsen et al., 2005; Vorren et al., 1988).

Although the stratigraphic record over a glacial cycle has the potential to be more volumetrically complete in deep sea basins than in shelf and fjord settings (Elverhøi et al., 1998b; Laberg et al., 2009), care must be taken in interpreting changes in sediment volumes as a reflection of the dynamic state of the ice. Seismic isopachs from glacially influenced deep-water basins can be interpreted to track the mode of dispersal and its relation to ice extent (Fig. 16; Taylor et al., 2002b). In the Norwegian and Lofoten deep-sea basins during the LGM (30–10 ka), sediment fluxes were dominated by large-scale submarine mass failures eroding pre-Quaternary strata (Fig. 16; Dowdeswell et al., 1996; Vorren et al., 1998; Dowdeswell and Siegert, 1999; Taylor et al., 2002b). Although pelagic, hemipelagic, and glacimarine processes were active over a glacial–interglacial cycle, they represented only 10% of the total deep-water sediment volume. In these settings, large-scale mass failure deposits may dominate the stratigraphic record, but the smaller glacigenic debris flows and glacimarine fluxes that could be used to constrain ice flux dynamics (e.g., Nygård et al., 2007) comprise a greatly reduced fraction of the record (Figs. 11 and 15; Taylor et al., 2002b; King et al., 1998).

In addition to core-based sediment accumulation rates or seismic reflection isopachs on continental shelves and slopes, subaqueous landforms provide another high-resolution record of ice dynamics. Transverse ridges and/or morainal banks found from temperate to polar settings are interpreted as seasonal/annual re-advances of the terminus (Fig. 10), and the spacing of these features provides a proxy for the rate of terminus retreat (Domack et al., 1999; Baeten et al., 2010; Boulton, 1986; Boulton et al., 1996; Ottesen and Dowdeswell, 2006, 2009; Ottesen et al., 2008a; Kempf et al., 2013; Livingstone et al., 2012; Shipp et al., 2002; Dowdeswell et al., 2008b; Cofaigh et al., 2008). Some grounding zone wedges are observed in Antarctic troughs where retreat rates during deglaciation were estimated to be rapid, and thus the sediment flux to the terminus must have been correspondingly high for them to form (Livingstone et al., 2012; Kilfeather et al., 2011). Perhaps the best-constrained record of the variability between ice dynamics and sediment fluxes on Antarctic shelves is from the eastern Ross Sea, where Bart and Owolana (2012) were able to develop a detailed chronology of sediment fluxes for a prominent grounding zone wedge (Fig. 17). Fluxes were partitioned between sediment recycled during re-advance and sediment contemporaneously eroded from the drainage basin, with the highest sediment fluxes during the penultimate interglacial and in the LGM.

4.3. Modeling ice dynamics and sediment fluxes to the sink

The logistical and chronological challenges of data collection in high-latitude margins currently limit our ability to relate ice flux dynamics

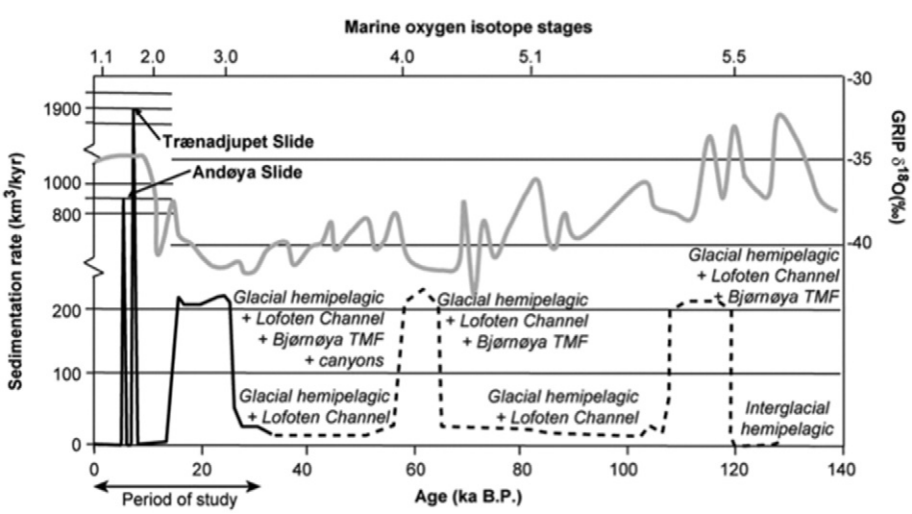

Fig. 16. Measured (solid) and hypothesized (dashed) sedimentation rates for the Lofoten Basin, Norwegian Sea based on seismic stratigraphic interpretation. Gravity flows (large mass failures and glacigenic debris flows) are the volumetrically dominant sediment transfer mechanism for this glacier-influenced margin during at least the last 30–100 ka. Notable contrasts exist between glacial and interglacial sedimentation rates associated with the mode of sediment supply, with the majority of sediments accumulating in a short time span during glacial periods. Variations in rates reflect the time varying sediment input to the Bjørnøya trough mouth fan, the Lofoten Channel and elevated glacial hemipelagic rates. Note breaks in sedimentation rate scale. Smoothed GRIP $\delta^{18}O$ record (in gray) and marine oxygen isotope stages for timescale. From Taylor et al. (2002b).

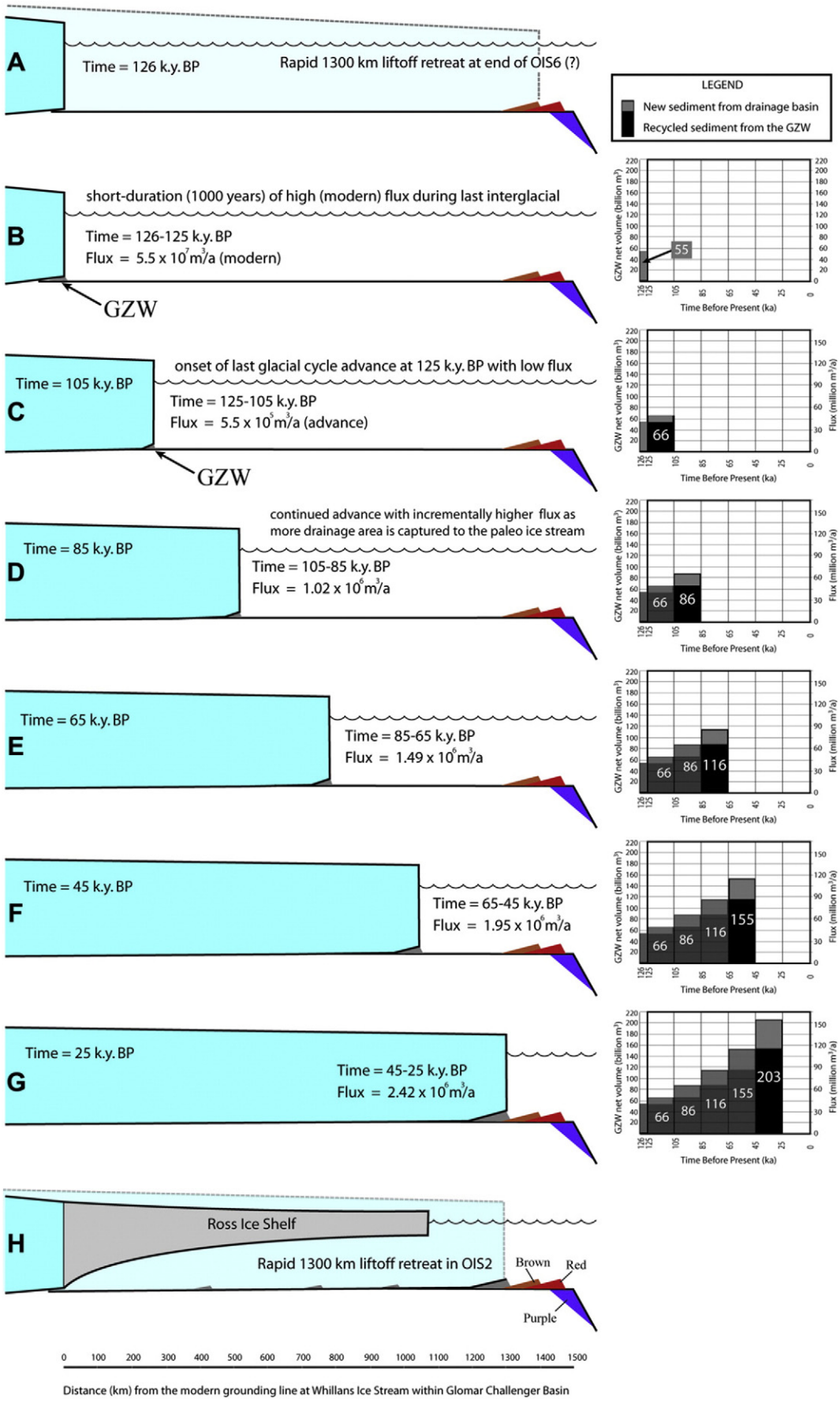
A
Time = 126 k.y. BP
Rapid 1300 km liftoff retreat at end of OIS6 (?)
LEGEND
New sediment from drainage basin
Recycled sediment from the GZW
B
short-duration (1000 years) of high (modern) flux during last interglacial
Time = 126-125 k.y. BP
Flux = 5.5 x 10^7 m^3/a (modern)
GZW
55
C
Time = 105 k.y. BP
onset of last glacial cycle advance at 125 k.y. BP with low flux
Time = 125-105 k.y. BP
Flux = 5.5 x 10^5 m^3/a (advance)
GZW
66
D
Time = 85 k.y. BP
continued advance with incrementally higher flux as more drainage area is captured to the paleo ice stream
Time = 105-85 k.y. BP
Flux = 1.02 x 10^6 m^3/a
66
86
E
Time = 65 k.y. BP
Time = 85-65 k.y. BP
Flux = 1.49 x 10^6 m^3/a
66
86
116
F
Time = 45 k.y. BP
Time = 65-45 k.y. BP
Flux = 1.95 x 10^6 m^3/a
66
86
116
155
G
Time = 25 k.y. BP
Time = 45-25 k.y. BP
Flux = 2.42 x 10^6 m^3/a
66
86
116
155
203
H
Ross Ice Shelf
Rapid 1300 km liftoff retreat in OIS2
Brown
Red
Purple
0 100 200 300 400 500 600 700 800 900 1000 1100 1200 1300 1400 1500
Distance (km) from the modern grounding line at Whillans Ice Stream within Glomar Challenger Basin
GZW net volume (billion m^3)
Flux (million m^3/a)
Time Before Present (ka)
126 125 105 85 65 45 25 0

and sediment production. Accordingly, a forward modeling approach similar to the numerical models used to quantify glacial erosion rates and topographic development (Section 2.2.3) provides another means to assess the potential for the sedimentary record to contain a signal of ice dynamics and to establish testable hypotheses that can be constrained with future field programs.

The leading example to date of a model relating climate, ice dynamics, and sediment production from source to sink is the one developed for a 30-kyr glacial cycle in the Barents–Kara Sea region as part of the European Science Foundation's QUEEN (Quaternary Environment of the Eurasian North) program (Dowdeswell and Siegert, 1999; Siegert et al., 1999; Siegert and Dowdeswell, 2002, 2004). The Siegert model is based on empirically established relationships between ice stream flow and deformation, and transport of water-saturated basal sediment (Alley, 1989). The model assumes that the topography at the start of the model run at 30 kya is analogous to the modern topography, and the model accounts for the time-evolution of topography and sea level due to ice loading. Global estimates of eustatic sea-level (Fairbanks, 1989; Shackleton, 1987) are used to modify local sea-level at the calving front (Siegert and Dowdeswell, 1995) and empirically derived relationships are used to model calving rates (Pelto and Warren, 1991; Hughes, 1992). Ice dynamics in the model depend on air temperature and precipitation as a function of geographic location and altitude. The regional climate dynamics described by Pelto et al. (1990) are used to drive net surface mass balance of the ice sheet, and the ELA is related to temperature through a regional adiabatic lapse rate (Fortuin and Oerlemans, 1990). Temporal changes in regional air temperature are assumed to empirically follow global proxies of climate, with the atmospheric CO_2 concentration used as the proxy of choice; little difference occurs if sea level or oxygen isotopic forcing functions are used instead (Siegert, 1993; Siegert and Dowdeswell, 1995). The validity of the ice dynamics output from the model is tuned using an inverse approach by adjusting the climatic input to best match the known extent of ice over the 30-kyr period and to the glacio-isostatic response (Siegert et al., 1999; Landvik et al., 1998; Svendsen et al., 1999). The validity of the resulting sediment fluxes, however, remains unconstrained.

The model predicts spatial and temporal evolution of sediment flux to the margin (Fig. 18). In it, ice streams transported sediments to the margin from 27 to 16 ka at a relatively constant rate, with maximum delivery around ~15 ka associated with rising sea level that stimulated increased ice velocity and sediment transfer rate within the ice streams to the trough mouths (Fig. 18). Sediment volumes produced by the model compare favorably with the total volume inferred from seismic records of the Bear Island and Storfjorden fans. Sensitivity experiments show that adjustments to model environmental inputs or dynamics of sediment generation at the bed using the chosen empirical relationships do not significantly affect their sediment flux results.

Higher spatial resolution models have been attempted with variable success in matching known ice dynamics. Kirchner et al. (2011b) modeled ice dynamics within the subdomain of Svalbard using a zero-order force balance where the ice surface velocities are proportional to the ice surface gradient and the ice thickness. They compared their results of ice velocity to the reconstructions of Svalbard paleo-ice streams by Ottesen et al. (2007). In contrast to the simpler Siegert model, ice streams were created where expected under full LGM conditions depending on whether LGM or present topography is used as a boundary condition. However, a high-resolution (5 km) numeric ice-sheet model constraining past ice dynamics in the Antarctic Peninsula was able to recreate both the ice sheet thickness and the flow directions of the major outlets and ice streams (Golledge et al., 2013; Cofaigh et al., 2014). For most other modeling studies of glaciated regions, however, the coupling of Global Circulation Models (GCMs) with 3D thermomechanical ice sheet models to reconstruct paleo-ice sheet dynamics has failed to reproduce the geologic evidence of former ice extent, because ice sheet dynamics appear to be highly sensitive to the downscaling of global climate to the "local" ice sheet (Kirchner et al., 2011a). Improving coupled GCM-ice sheet dynamics is clearly needed, and requires developing higher-spatial-resolution ice sheet models with bidirectional ice sheet-atmosphere feedbacks, improved treatment of the surface mass balance, and more precise regional climate data and paleoclimate reconstructions (Kirchner et al., 2011a).

5. Conclusions and future directions

The ultimate goal of studying a glacial source-to-sink system is to relate changing boundary conditions with the ice response and the sedimentary record. Documenting the impact of ice on the landscape is a fundamental component of Quaternary geomorphology. Yet, modern glacial environments remain among the most logistically challenging environments in which to try to study the processes that generate and transfer sediment from the landscape to its sink and to provide a modern analog for Quaternary landscape change. However, some of these processes are well enough constrained that predictive relationships can be demonstrated. In this review, we have highlighted those processes of sediment generation and transfer that are well understood in both time and space, and those that remain poorly constrained and where further focus is needed. We recognize that the dynamic state of the ice is viewed differently between the communities studying the source (i.e., glaciology and glacial geomorphology communities) and the sink (i.e., Quaternary and marine geology communities). For the former, the ice flux and mass response to climate change are of most interest, while for the latter, the emphasis has been on documenting temporal and spatial changes in ice extent, which defines the boundary conditions that influence ice sheet development, but does not necessarily elucidate the ice flux.

Observations from contemporary glaciated systems, primarily through marine geophysics (swath bathymetry, seismic), geochronology, and advances in sedimentary provenance, have proven instrumental in establishing genetic relationships. However, to interpret the dynamic state of the ice, the sedimentary signal must be resolved in terms of mass fluxes of characteristic glacial facies. Doing so requires chronological control at the timescale of the ice response function, which fundamentally limits the types of climate forcing that can be evaluated. Establishing absolute rates of sediment transfer is easiest at annual timescales in modern ice-proximal settings, but becomes increasing difficult for the Pleistocene because of reduced chronometric precision. Moreover, to isolate the glacial/climatic signal in the sink record, it is necessary to account for transfer mechanisms from ice-proximal (fjord) to ice-distal (deep sea) locales that complicate the signal, e.g., mass redistribution, gravity flows, ice rafting, and ocean circulation.

Advancements in our understanding of the mechanics of glacial source-to-sink systems will be predicated upon the collection and examination of additional sedimentary records that were deposited under a variety of climatic and ice flux boundary conditions to establish sediment fluxes that can be tied to evolving ice dynamics. Documenting the relative roles of the glacier thermal regime and ice dynamics on sediment production and strata formation should be a fundamental goal of future research in Quaternary geomorphology, glaciology, and glacial sedimentology. We conclude by offering some

Fig. 17. Cartoon of flux of glacigenic sediment over a 100-kyr glacial cycle on a high-latitude continental shelf and slope, Great Challenger Basin, Antarctica. Sediment volumes derived from seismic isopachs and a long drill-core record. Sediment at the shelf edge (right panel) is partitioned into new sediment generated by glacial erosion in the drainage basin (gray) and sediment reworked and recycled in prograding grounding zone wedge (GZW) (black). Average position of the ice margin at 20 ky time slices, and average sediment flux for each time slice, are highlighted. From Bart and Owolana (2012).

potential avenues for future studies that can advance the field in the coming decade.

5.1. Deriving erodibility metrics for landscape evolution

A major challenge in understanding the role of glacial erosion in modifying the earth's surface, and in producing sediment, is the tuning of an 'erosion rule' for given climatic inputs that is applicable over the long periods required for the development of topography. We know that climate dictates the ice flux and thus the geomorphic work done by the ice generating the sedimentary mass flux signal, and that the most work occurs in fast moving ice and in the presence of meltwater, through temperate outlet glaciers and ice streams. However, while glaciers wax and wane, the degree to which subglacial regions are subject to fast ice flow and erosion is still debated. Moreover, the proportion of glacier motion due to basal sliding, which depends on a number of factors including bed type, water pressure fluctuations at the bed, and ice temperature, will vary significantly over both time and space, and likely varies by orders of magnitude over glacial–interglacial cycles. Additional measurements of glacial sediment yields over a range of climatic settings and parameters including varying substrate lithology, ice flux, ice temperature and meltwater discharge rates are required to better constrain the erosion parameter space and its evolution over glacial cycles. These can help address the outstanding question as to the erosive versus protective nature of ice.

5.2. Chronostratigraphic control of geomorphic and seismic stratigraphic features

Remotely sensed data have greatly expanded our view of the role of ice in shaping Quaternary landscapes. Radar-based ice thickness measurements, LIDAR, and multibeam bathymetry have revolutionized the mapping of glacigenic morphologic features. High-resolution multichannel seismic reflection and higher-resolution CHIRP/TOPAS 3.5 kHz reflection profiles give detailed subsurface images of glacimarine strata. For both surface and subsurface mapping, chronostratigraphic control is frequently lacking, often due to inability to collect long cores or develop chronologies for collected strata. Sampling that provides more precise chronological control of stratigraphic horizons is required to address the glacial response to external forcing. New developments in scientific drilling (e.g., ANDRILL, SHALDRIL, IODP) have made fundamental advances in recovery of these challenging strata. Novel chronologic tools have been developed for microfossil-barren strata, offering the potential for improved age control to maximize interpretation of existing geophysical data.

5.3. Deciphering local (autogenic) from regional/global (allogenic) controls on ice dynamics and sediment production

Regional topography is influenced by tectonics, glacioisostacy, and the balance between erosion and deposition. Topography in turn influences local climate, ice fluxes, accommodation for sediment

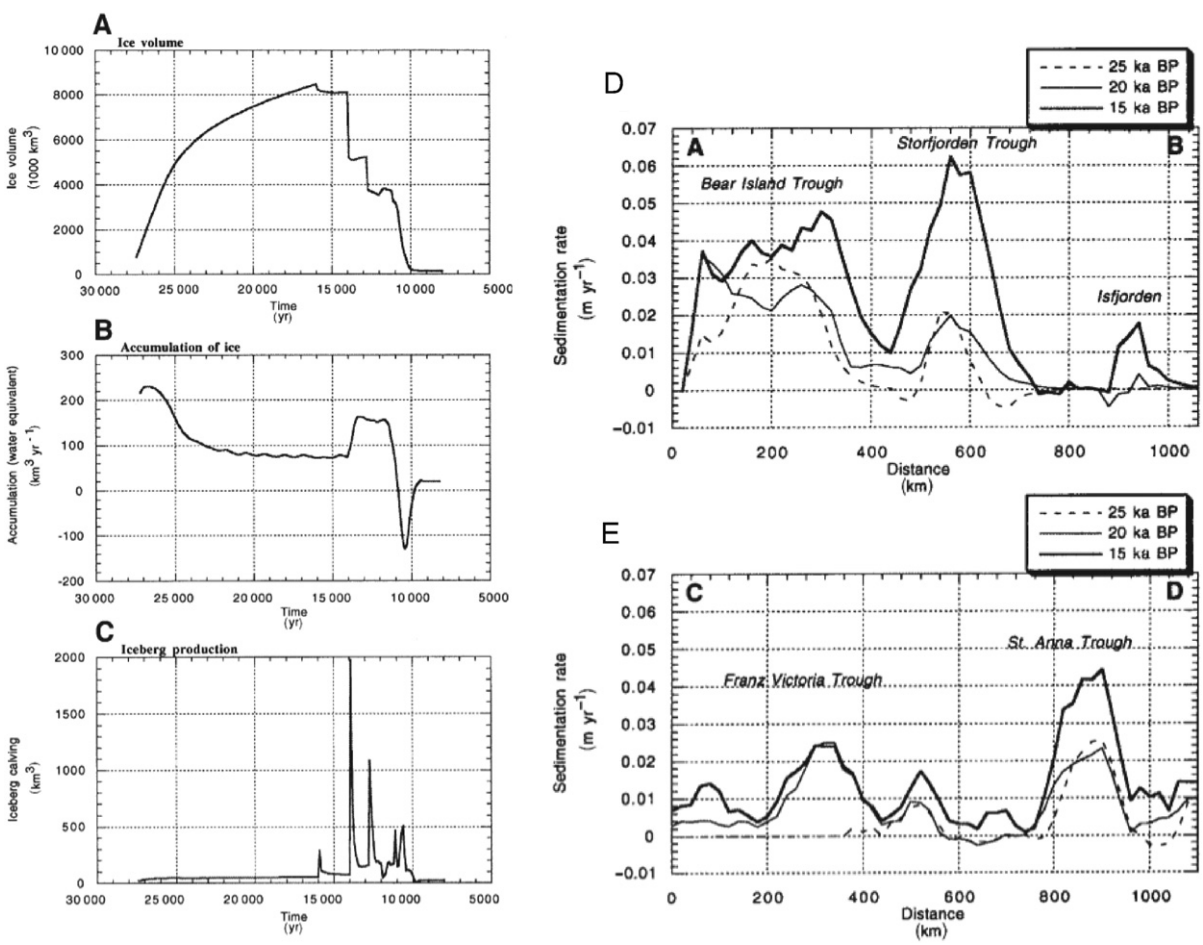

Fig. 18. Modeled changes in predicted ice-sheet parameters and sedimentation rates over the past 30 k.y. for the Barents–Kara and Scandinavian ice sheets, derived from the QUEEN ice-sheet-landscape model. (A) Ice sheet volume, in 10^3 km^3. (B) Annual winter mass balance of ice sheet (ice accumulation), in km^3 yr^{-1}. (C) Annual volume of iceberg calving, in km^3. (D–E) The rate of model-predicted sediment delivery along transects across the western and northern Eurasian continental margin, for (D) Barents Sea–Svalbard margin and (E) Arctic Ocean margin between Svalbard and Severnaya Zemlya. The sedimentation rate, in m yr^{-1}, is given for time slices at 25, 20, and 15 ky. The highest sedimentation rates are associated with collapse of the ice streams. From Dowdeswell and Siegert (1999).

accumulation, and sediment dispersal pathways. The relative importance of these different local influences on topography will vary in space and time. A major challenge is to interpret the signal of these influences from geophysical and sedimentary records. Examples of identifying allogenic climate signals from the sedimentary record exist for local basins, where all glacigenic sediment can be accounted for in mass budgets. A larger challenge is to scale up in space and time to address fundamental questions about the ability of the glacial sedimentary record to capture ice dynamics in light of potential autogenic controls. Recent and proposed scientific drilling of Pleistocene strata that establishes chronologies for interpreted seismic volumes and sediment dispersal pathways and rates will help address these challenges.

5.4. Modern analog approach to glacial source-to-sink studies

Our observational dataset of active glacial processes has been collected entirely within a time of rapid climate change following a major Neoglacial (LIA) period. Short-lived interglacial periods such as the one we are experiencing today are atypical relative to the majority of the Pleistocene. Most Quaternary glacial landscapes likely formed under conditions quite different from the present. If the physics of glacial erosion and glacigenic sedimentation can be well established, particularly in polar settings that have not yet experienced rapid climate warming, this information should be transferrable to the past if the appropriate climatic boundary conditions are known. There is a need for more mechanistic-level studies that integrate the principal processes governing ice–sediment–ocean interactions over both short and long time periods, with the appropriate temporal resolution to examine the various response time functions. These processes should include subglacial sediment production and evacuation and how both water and sediment are routed through each component of a source-to-sink system.

Acknowledgments

The final manuscript benefited greatly from patient, critical, and insightful reviews by Ellen Cowan, Roger LeB. Hooke, Edward King, and J.P. Walsh. J.M.J. recognizes the National Science Foundation (Grants OPP-0326926, OCE-0351043, OCE-1434402) for support of research in the topics of glacimarine sedimentation. M.N.K. was supported by National Science Foundation Grant OPP-0338371 and National Science and Engineering Research Council (NSERC) operating grants for research on glacial erosion.

References

Agassiz, L., 1840. Etudes sur les Glaciers. Neuchâtel, Switzerland.
Alexanderson, H., Murray, A.S., 2012. Luminescence signals from modern sediments in a glaciated bay, NW Svalbard. Quat. Geochronol. 10, 250–256.
Alley, R.B., 1989. Water-pressure coupling of sliding and bed deformation. 2. Velocity–depth profiles. J. Glaciol. 35, 119–129.
Alley, R.B., Blankenship, D.D., Bentley, C.R., Rooney, S.T., 1987. Till beneath ice stream-B. 3. Till deformation — evidence and implications. J. Geophys. Res. Solid Earth Planets 92 (B9), 8921–8929.
Alley, R.B., Blankenship, D.D., Rooney, S.T., Bentley, C.R., 1989. Water pressure coupling of sliding and bed deformation. 3. Application to ice stream B, Antarctica. J. Glaciol. 35, 130–139.
Alley, R.B., Cuffey, K.M., Evenson, E.B., Strasser, J.C., Lawson, D.E., Larson, G.J., 1997. How glaciers entrain and transport basal sediment: physical constraints. Quat. Sci. Rev. 16, 1017–1038.
Alley, R.B., Lawson, D.E., Larson, G.J., Evenson, E.B., Baker, G.S., 2003. Stabilizing feedbacks in glacier-bed erosion. Nature 424, 758–760.
Alley, R.B., Anandakrishnan, S., Dupont, T.K., Parizek, B.R., Pollard, D., 2007. Effect of sedimentation on ice-sheet grounding-line stability. Science 315, 1838–1841.
Anandakrishnan, S., Catania, G.A., Alley, R.B., Horgan, H.J., 2007. Discovery of till deposition at the grounding line of whillans ice stream. Science 315, 1835–1838.
Andersen, B.G., 1975. Glacial geology of northern Nordland, north Norway. Nor. Geol. Unders. 320, 1–74.
Anderson, J.B., 1999. Antarctic Marine Geology. Cambridge University Press, Cambridge 289 pp.
Anderson, S.P., 2005. Glaciers show direct linkage between erosion rate and chemical weathering fluxes. Geomorphology 67, 147–157. http://dx.doi.org/10.1016/j.geomorph.2004.07.010.
Anderson, R.S., Anderson, S.P., 2010. Geomorphology: The Mechanics and Chemistry of Landscapes. Cambridge University Press 637 pp.
Anderson, J.B., Kurtz, D.D., Domack, E.W., Balshaw, K.M., 1980. Glacial and glacial marine-sediments of the Antarctic continental-shelf. J. Geol. 88, 399–414.
Anderson, J., Shipp, S., Lowe, A., Wellner, J.S., Mosola, A.B., 2002. The Antarctic ice sheet during the Last Glacial Maximum and its subsequent retreat history: a review. Quat. Sci. Rev. 21, 49–70.
Anderson, R.S., Anderson, S.P., MacGregor, K.R., Waddington, E.D., O'Neel, S., Riihimaki, C.A., Loso, M.G., 2004. Strong feedbacks between hydrology and sliding of a small alpine glacier. J. Geophys. Res. 109 (F3), 1–17. http://dx.doi.org/10.1029/2004JF000120.
Anderson, R.S., Molnar, P., Kessler, M.A., 2006. Features of glacial valley profiles simply explained. J. Geophys. Res. Earth Surf. 111 (F1), F01004. http://dx.doi.org/10.1029/2005JF000344.
Anderson, J.B., Conway, H., Bart, P.J., Witus, A.E., Greenwood, S.L., McKay, R.M., Hall, B.L., Ackert, R.P., Licht, K., Jakobsson, M., Stone, J.O., 2014. Ross sea paleo-ice sheet drainage and deglacial history during and since the LGM. Quat. Sci. Rev. 100, 31–54.
Andreassen, K., Winsborrow, M., 2009. Signature of ice streaming in bjornoyrenna, Polar North Atlantic, through the Pleistocene and implications for ice-stream dynamics. Ann. Glaciol. 50, 17–26.
Andresen, C.S., Straneo, F., Ribergaard, M.H., Bjørk, A.A., Andersen, T.J., Kuijpers, A., Nørgaard-Pedersen, N., Kjær, K.H., Schjøth, F., Weckström, K., Ahlstrøm, A.P., 2012. Rapid response of helheim glacier in Greenland to climate variability over the past century. Nat. Geosci. 5, 37–41. http://dx.doi.org/10.1038/ngeo1349.
Andrews, J.T., 2000. Icebergs and iceberg rafted detritus (IRD) in the North Atlantic: facts and assumptions. Oceanography 13, 100–108. http://dx.doi.org/10.5670/oceanog.2000.19.
Andrews, J.T., Principato, S.M., 2002. Grain-size characteristics and provenance of ice-proximal glacial marine sediments. Geol. Soc. Lond. Spec. Publ. 203, 305–324.
Andrews, J.T., Vogt, C., 2014. Source to sink: statistical identification of regional variations in the mineralogy of surface sediments in the western Nordic seas (58°N–75°N; 10°W–40°W). Mar. Geol. 357, 151–162.
Andrews, J.T., Domack, E.W., Cunningham, W.L., Leventer, A., Licht, K.J., Jull, A.J.T., DeMaster, D.J., Jennings, A.E., 1999. Problems and possible solutions concerning radiocarbon dating of surface marine sediments, Ross Sea, Antarctica. Quat. Res. 52, 206–216.
Andrews, J.T., Bigg, G.R., Wilton, D.J., 2014. Holocene ice-rafting and sediment transport from the glaciated margin of East Greenland (67–70 degrees N) to the N Iceland shelves: detecting and modelling changing sediment sources. Quat. Sci. Rev. 91, 204–217.
Ashley, G.M., Smith, N.D., 2000. Marine sedimentation at a calving glacier margin. Geol. Soc. Am. Bull. 112, 657–667.
Auffret, G., Zaragosi, S., Dennielou, B., Cortijo, E., Van Rooij, D., Grousset, F., Pujol, C., Eynaud, F., Siegert, M., 2002. Terrigenous fluxes at the Celtic margin during the last glacial cycle. Mar. Geol. 188, 79–108.
Austin, W.E.N., Bard, E., Hunt, J.B., Kroon, D., Peacock, J.D., 1995. The C-14 age of the Icelandic Vedde ash — implications for Younger-Dryas marine reservoir age corrections. Radiocarbon 37, 53–62.
Baeten, N.J., Forwick, M., Vogt, C., Vorren, T.O., 2010. Late Weichselian and Holocene Sedimentary Environments and Glacial Activity in Billefjorden, SvalbardSpecial Publication 344. The Geological Society of London, London, pp. 207–223.
Bailey, I., Hole, G.M., Foster, G.L., Wilson, P.A., Storey, C.D., Trueman, C.N., Raymo, M.E., 2013. An alternative suggestion for the Pliocene onset of major northern hemisphere glaciation based on the geochemical provenance of North Atlantic Ocean ice-rafted debris. Quat. Sci. Rev. 75, 181–194. http://dx.doi.org/10.1016/j.quascirev.2013.06.004.
Balco, G., 2011. Contributions and unrealized potential contributions of cosmogenic-nuclide exposure dating to glacier chronology, 1990–2010. Quat. Sci. Rev. 30, 3–27.
Balco, G., Rovey, C.W., 2010. Absolute chronology for major Pleistocene advances of the Laurentide ice sheet. Geology 38, 795–798.
Ballantyne, C.K., 2002. Paraglacial geomorphology. Quat. Sci. Rev. 21, 1935–2017.
Barclay, D.J., Wiles, G.C., Calkin, P.E., 2009. Holocene glacier fluctuations in Alaska. Quat. Sci. Rev. 28, 2034–2048.
Barrie, J.V., Conway, K.W., 2002. Contrasting glacial sedimentation processes and sea-level changes in two adjacent basins on the Pacific margin of Canada. Geol. Soc. Lond., Spec. Publ. 203, 181–194.
Barrie, J.V., Bornhold, B.D., Conway, K.W., Luternauer, J.L., 1991. Surficial geology of the northwestern Canadian continental-shelf. Cont. Shelf Res. 11, 701–715.
Bart, P.J., Owolana, B., 2012. On the duration of West Antarctic ice sheet grounding events in Ross Sea during the Quaternary. Quat. Sci. Rev. 47, 101–115.
Bartholomaus, T.C., Anderson, R.S., Anderson, S.P., 2007. Response of glacier basal motion to transient water storage. Nat. Geosci. 1, 33–37.
Bartholomew, I., Nienow, P., Mair, D., Hubbard, A., King, M.A., Sole, A., 2010. Seasonal evolution of subglacial drainage and acceleration in a Greenland outlet glacier. Nat. Geosci. 3, 408–411. http://dx.doi.org/10.1038/ngeo863.
Batchelor, C.L., Dowdeswell, J.A., 2014. The physiography of high Arctic cross-shelf troughs. Quat. Sci. Rev. 92, 68–96.
Batchelor, C.L., Dowdeswell, J.A., Hogan, K.A., 2011. Late Quaternary ice flow and sediment delivery through Hinlopen Trough, northern Svalbard margin: submarine landforms and depositional fan. Mar. Geol. 284, 13–27.
Batchelor, C.L., Dowdeswell, J.A., Pietras, J.T., 2013. Seismic stratigraphy, sedimentary architecture and palaeo-glaciology of the Mackenzie trough: evidence for two Quaternary ice advances and limited fan development on the western Canadian Beaufort Sea margin. Quat. Sci. Rev. 65, 73–87.
Batchelor, C.L., Dowdeswell, J.A., Pietras, J.T., 2014. Evidence for multiple Quaternary ice advances and fan development from the Amundsen Gulf cross-shelf trough and slope, Canadian Beaufort Sea margin. Mar. Pet. Geol. 52, 125–143.

Baumann, K.-H., Lackschewitz, K.S., Mangerud, J., Spielhagen, R.F., Wolf-welling, T.C.W., Henrich, R., Kassens, H., 1995. Reflection of Scandinavian ice sheet fluctuations in Norwegian Sea sediments during the past 150,000 years. Quat. Res. 43, 185–197.
Beaud, F., Flowers, G.E., Pimentel, S., 2014. Seasonal-scale abrasion and quarrying patterns from a two-dimensional ice-flow model coupled to distributed and channelized subglacial drainage. Geomorphology 219, 176–191.
Becker, R.A., Tikoff, B., Riley, P.R., Iverson, N.R., 2014. Preexisting fractures and the formation of an iconic American lnadscape: Tuolomne Meadows, Yosemite National Park, USA. GSA Today 24, 4–10. http://dx.doi.org/10.1130/GSATG203A.1.
Benn, D.I., Evans, D.J.A., 2010. Glaciers and Glaciation. 2nd Edition. Hodder Education, London 734 pp.
Benn, D.I., Warren, C.R., Mottram, R.H., 2007. Calving processes and the dynamics of calving glaciers. Earth Sci. Rev. 82, 143–179.
Bennett, M.R., 2003. Ice streams as the arteries of an ice sheet: their mechanics, stability and significance. Earth Sci. Rev. 61, 309–339.
Bentley, C.R., 1987. Antarctic ice streams — a review. J. Geophys. Res. Solid Earth Planets 92 (B9), 8843–8858.
Bentley, M.J., Cofaigh, C.O., Anderson, J.B., Conway, H., Davies, B., Graham, A.G.C., Hillenbrand, C.D., Hodgson, D.A., Jamieson, S.S.R., Larter, R.D., Mackintosh, A., Smith, J.A., Verleyen, E., Ackert, R.P., Bart, P.J., Berg, S., Brunstein, D., Canals, M., Colhoun, E.A., Crosta, X., Dickens, W.A., Domack, E., Dowdeswell, J.A., Dunbar, R., Ehrmann, W., Evans, J., Favier, V., Fink, D., Fogwill, C.J., Glasser, N.F., Gohl, K., Golledge, N.R., Goodwin, I., Gore, D.B., Greenwood, S.L., Hall, B.L., Hall, K., Hedding, D.W., Hein, A.S., Hocking, E.P., Jakobsson, M., Johnson, J.S., Jomelli, V., Jones, R.S., Klages, J.P., Kristoffersen, Y., Kuhn, G., Leventer, A., Licht, K., Lilly, K., Lindow, J., Livingstone, S.J., Masse, G., McGlone, M.S., McKay, R.M., Melles, M., Miura, H., Mulvaney, R., Nel, W., Nitsche, F.O., O'Brien, P.E., Post, A.L., Roberts, S.J., Saunders, K.M., Selkirk, P.M., Simms, A.R., Spiegel, C., Stolldorf, T.D., Sugden, D.E., van der Putten, N., van Ommen, T., Verfaillie, D., Vyverman, W., Wagner, B., White, D.A., Witus, A.E., Zwartz, D., Consortium, R., 2014. A community-based geological reconstruction of Antarctic ice sheet deglaciation since the Last Glacial Maximum. Quat. Sci. Rev. 100, 1–9.
Berger, A.L., Spotila, J.A., 2008. Denudation and deformation in a glaciated orogenic wedge: the St. Elias orogen, Alaska. Geology 36 (7), 523–526.
Berger, A.L., Gulick, S.P.S., Spotila, J.A., Upton, P., Jaeger, J.M., Chapman, J.B., Worthington, L.A., Pavlis, T.L., Ridgway, K.D., Willems, B.A., McAleer, R.J., 2008a. Quaternary tectonic response to intensified glacial erosion in an orogenic wedge. Nat. Geosci. 1, 793–799.
Berger, A.L., Spotila, J.A., Chapman, J.B., Pavlis, T.L., Enkelmann, E., Ruppert, N.A., Buscher, J.T., 2008b. Architecture, kinematics, and exhumation of a convergent orogenic wedge: a thermochronological investigation of tectonic–climatic interactions within the central St. Elias orogen, Alaska. Earth Planet. Sci. Lett. 270, 13–24.
Berger, G.W., Ante, S., Domack, E., 2010. Luminescence from glacimarine sediment-trap samples at the Antarctic Peninsula. Quat. Geochronol. 5, 244–249.
Bergstrøm, B., Olsen, L., Sveian, H., 2005. The Tromsø–Lyngen glacial readvance (early Younger Dryas) at Hinnøya-Ofotfjorden, northern Norway. Norges Geol. Unders. Bull. 445, 73–88.
Bingham, R.G., King, E.C., Smith, A.M., Pritchard, H.D., 2010. Glacial geomorphology: towards a convergence of glaciology and geomorphology. Prog. Phys. Geogr. 34, 327–355.
Bitz, C.M., Battisti, D.S., 1999. Interannual to decadal variability in climate and the glacier mass balance in Washington, western Canada, and Alaska. J. Clim. 12, 3181–3196.
Blum, M.D., Guccione, M.J., Wysocki, D., Robnett, P.C., 2000. Late Pleistocene evolution of the Mississippi valley, southern Missouri to Arkansas. Geol. Soc. Am. Bull. 112, 221–235.
Boldt, K.V., Nittrouer, C.A., Hallet, B., Koppes, M.N., Forrest, B.K., Wellner, J.S., Anderson, J.B., 2013. Modern rates of glacial sediment accumulation along a 15° S–N transect in fjords from the Antarctic Peninsula to southern Chile. J. Geophys. Res. Earth Surf. 118, 1–17. http://dx.doi.org/10.1002/jgrf.20145.
Boulton, G.S., 1979. Process of glacial erosion on different substrata. J. Glaciol. 23, 15–37.
Boulton, G.S., 1986. Push-moraines and glacier-contact fans in marine and terrestrial environments. Sedimentology 33, 677–698.
Boulton, G., Hagdorn, M., 2006. Glaciology of the British Isles ice sheet during the last glacial cycle: form, flow, streams and lobes. Quat. Sci. Rev. 25, 3359–3390.
Boulton, G.S., Dongelmans, P., Punkari, M., Broadgate, M., 2001. Palaeogeology of an ice sheet through a glacial cycle: the European ice sheet through the Weichselian. Quat. Sci. Rev. 20, 591–625.
Boulton, G.S., Lunn, R., Vidstrand, P., Zatsepin, S., 2007. Subglacial drainage by groundwater-channel coupling, and the origin of esker systems: part 1 — glaciological observations. Quat. Sci. Rev. 26, 1067–1090.
Box, J.E., Fettweis, X., Stroeve, J.C., Tedesco, M., Hall, D.K., Steffen, K., 2012. Greenland ice sheet albedo feedback: thermodynamics and atmospheric drivers. Cryosphere 6, 821–839.
Boyd, B.L., Anderson, J.B., Wellner, J.S., Fernández, R.A., 2008. The sedimentary record of glacial retreat, Marinelli Fjord, Patagonia: regional correlations and climate ties. Mar. Geol. 255, 165–178.
Brachfeld, S., Domack, E., Kissel, C., Laj, C., Leventer, A., Ishman, S., Gilbert, R., Camerlenghi, A., Eglinton, L.B., 2003. Holocene history of the Larsen — a ice shelf constrained by geomagnetic paleointensity dating. Geology 31, 749–752.
Braun, J., Zwartz, D., Tomkin, J.H., 1999. A new surface-processes model combining glacial and fluvial erosion. Ann. Glaciol. 28, 282–290.
Briner, J.P., Kaufman, D.S., 2008. Late Pleistocene mountain glaciation in Alaska: key chronologies. J. Quat. Sci. 23, 659–670.
Briner, J.P., Miller, G.H., Davis, P.T., Finkel, R.C., 2006. Cosmogenic radionuclides from fiord landscapes support differential erosion by overriding ice sheets. Geol. Soc. Am. Bull. 118, 406–420.
Cai, J., Powell, R.D., Cowan, E.A., Carlson, P.R., 1997. Lithofacies and seismic-reflection interpretation of temperate glacimarine sedimentation in Tarr Inlet, Glacier Bay, Alaska. Mar. Geol. 143, 5–37.
Carlson, P.R., Molnia, B.F., Kittleson, S.C. and J.C., H., 1977. Distribution of bottom sediments on the continental shelf, northern Gulf of Alaska, Scale 1:500,000. Misc. Field Stud. Map MF-876, U.S. Geological Survey.
Carlson, P.R., Bruns, T.R., Molnia, B.F., Schwab, W.C., 1982. Submarine valleys in the northeatern Gulf of Alaska: characteristics and probable origin. Mar. Geol. 47, 217–242.
Champagnac, J.D., Valla, P.G., Herman, F., 2014. Late-Cenozoic relief evolution under evolving climate: a review. Tectonophysics 614, 44–65.
Chorley, R.J., 1973. The History of the Study of Landforms, or the Developments of Geomorphology. Methuen, London.
Christoffersen, P., Tulaczyk, S., Behar, A., 2010. Basal ice sequences in Antarctic ice streams: exposure of past hydrological conditions and a principle mode of sediment transfer. J. Geophys. Res. 115, F03034.
Church, M., Ryder, J.M., 1972. Paraglacial sedimentation: a consideration of fluvial processes conditioned by glaciation. Geol. Soc. Am. Bull. 83, 3059–3072.
Church, M., Slaymaker, O., 1989. Disequilibrium of Holocene sediment yield in glaciated British Columbia. Nature 337, 452–454.
Chutko, K.J., Lamoureux, S.F., 2008. Identification of coherent links between interannual sedimentary structures and daily meteorological observations in Arctic proglacial lacustrine varves: potentials and limitations. Can. J. Earth Sci. 45, 1–13.
Clark, P.U., Pisias, N.G., 2000. Interpreting iceberg deposits in the deep sea. Science 290, 51–52.
Cofaigh, C.Ó., 2012. Ice sheets viewed from the ocean: the contribution of marine science to understanding modern and past ice sheets. Philos. Trans. R. Soc. A Math. Phys. Eng. Sci. 370, 5512–5539.
Cofaigh, C.Ó., Dowdeswell, J.A., 2001. Laminated sediments in glacimarine environments: diagnostic criteria for their interpretation. Quat. Sci. Rev. 20, 1411–1436.
Cofaigh, C.Ó., Dowdeswell, J.A., Grobe, H., 2001a. Holocene glacimarine sedimentation, inner Scoresby Sund, East Greenland: the influence of fast-flowing ice-sheet outlet glaciers. Mar. Geol. 175, 103–129.
Cofaigh, C.Ó., Dowdeswell, J.A., Pudsey, C.J., 2001b. Late Quaternary iceberg rafting along the Antarctic Peninsula continental rise and in the Weddell and Scotia Seas. Quat. Res. 56, 308–321.
Cofaigh, C.Ó., Taylor, J., Dowdeswell, J.A., Rosell-Mele, A., Kenyon, N.H., Evans, J., Mienert, J., 2002. Sediment reworking on high-latitude continental margins and its implications for palaeoceanographic studies: insights from the Norwegian–Greenland Sea. Geol. Soc. Lond., Spec. Publ. 203, 325–348.
Cofaigh, C.Ó., Taylor, J., Dowdeswell, J.A., Pudsey, C.J., 2003. Palaeo-ice streams, trough mouth fans and high-latitude continental slope sedimentation. Boreas 32, 37–55.
Cofaigh, C.Ó., Dowdeswell, J.A., Evans, J., Kenyon, N.H., Taylor, J., Mienert, J., Wilken, M., 2004. Timing and significance of glacially influenced mass-wasting in the submarine channels of the Greenland basin. Mar. Geol. 207, 39–54.
Cofaigh, C.Ó., Dowdeswell, J.A., Allen, C.S., Hiemstra, J.F., Pudsey, C.J., Evans, J., Evans, D.J.A., 2005. Flow dynamics and till genesis associated with a marine-based Antarctic palaeo-ice stream. Quat. Sci. Rev. 24, 709–740.
Cofaigh, C.Ó., Evans, J., Dowdeswell, J.A., Larter, R.D., 2007. Till characteristics, genesis and transport beneath Antarctic paleo-ice streams. J. Geophys. Res. Earth Surf. 112 (F3).
Cofaigh, C.Ó., Dowdeswell, J.A., Evans, J., Larter, R.D., 2008. Geological constraints on Antarctic palaeo-ice-stream retreat. Earth Surf. Process. Landf. 33, 513–525.
Cofaigh, C.Ó., Dunlop, P., Benetti, S., 2012. Marine geophysical evidence for Late Pleistocene ice sheet extent and recession off northwest Ireland. Quat. Sci. Rev. 44, 147–159.
Cofaigh, C.Ó., Andrews, J.T., Jennings, A.E., Dowdeswell, J.A., Hogan, K.A., Kilfeather, A.A., Sheldon, C., 2013. Glacimarine lithofacies, provenance and depositional processes on a West Greenland trough-mouth fan. J. Quat. Sci. 28, 13–26.
Cofaigh, C.Ó., Davies, B.J., Livingstone, S.J., Smith, J.A., Johnson, J.S., Hocking, E.P., Hodgson, D.A., Anderson, J.B., Bentley, M.J., Canals, M., Domack, E., Dowdeswell, J.A., Evans, J., Glasser, N.F., Hillenbrand, C.D., Larter, R.D., Roberts, S.J., Simms, A.R., 2014. Reconstruction of ice-sheet changes in the Antarctic Peninsula since the Last Glacial Maximum. Quat. Sci. Rev. 100, 87–110.
Cook, S.J., Swift, D.A., 2012. Subglacial basins: their origin and importance in glacial systems and landscapes. Earth Sci. Rev. 115, 332–372.
Cook, C.P., van de Flierdt, T., Williams, T., Hemming, S.R., Iwai, M., Kobayashi, M., Jimenez-Espejo, F.J., Escutia, C., Gonzalez, J.J., Khim, B.-K., McKay, R.M., Passchier, S., Bohaty, S.M., Riesselman, C.R., Tauxe, L., Sugisaki, S., Galindo, A.L., Patterson, M.O., Sangiorgi, F., Pierce, E.L., Brinkhuis, H., Klaus, A., Fehr, A., Bendle, J.A.P., Bijl, P.K., Carr, S.A., Dunbar, R.B., Flores, J.A., Hayden, T.G., Katsuki, K., Kong, G.S., Nakai, M., Olney, M.P., Pekar, S.F., Pross, J., Rohl, U., Sakai, T., Shrivastava, P.K., Stickley, C.E., Tuo, S., Welsh, K., Yamane, M., 2014. Dynamic behaviour of the East Antarctic ice sheet during Pliocene warmth. Nat. Geosci. 6, 765–769.
Cowan, E.A., Powell, R.D., 1990. Suspended sediment transport and deposition of cyclically interlaminated sediment in a temperate glacial fjord, Alaska, U.S.A. In: Dowdeswell, J.A., Scourse, J.D. (Eds.), Glacimarine Environments: Processes and Sediments. Geological Society Special Publication, London, pp. 75–89.
Cowan, E.A., Powell, R.D., 1991. Ice-Proximal Sediment Accumulation Rates in a Temperate Glacial Fjord, Southeastern Alaska. In: Anderson, J.B., Ashley, G.M. (Eds.), Glacial Marine Sedimentation: Paleoclimatic Significance. Geological Society of America, Boulder, CO, pp. 61–73.
Cowan, E.A., Powell, R.D., Smith, N.D., 1988. Rainstorm-induced event sedimentation at the tidewater front of a temperate glacier. Geology 16, 409–412.
Cowan, E.A., Cai, J., Powell, R.D., Clark, J.D., Pitcher, J.N., 1997. Temperate glacimarine varves: an example from Disenchantment Bay, Alaska. J. Sediment. Res. 67, 536–549.
Cowan, E.A., Cai, J., Powell, R.D., Seramur, K.C., Spurgeon, V.L., 1998. Modern tidal rhythmites deposited in a deep-water estuary. Geo-Mar. Lett. 18, 40–48.

Cowan, E.A., Seramur, K.C., Cai, J., Powell, R.D., 1999. Cyclic sedimentation produced by fluctuations in meltwater discharge, tides and marine productivity in an Alaskan fjord. Sedimentology 46, 1109–1126.
Cowan, E.A., Seramur, K.C., Powell, R.D., Willems, B.A., Gulick, S.P.S., Jaeger, J.M., 2010. Fjords as temporary sediment traps: history of glacial erosion and deposition in Muir Inlet, Glacier Bay National Park, southeastern Alaska. Geol. Soc. Am. Bull. 122, 1067–1080. http://dx.doi.org/10.1130/B26595.1.
Cowan, E.A., Christoffersen, P., Powell, R.D., 2012. Sedimentological signature of a deformable bed preserved beneath an ice stream in a late Pleistocene glacial sequence, Ross Sea, Antarctica. J. Sediment. Res. 82, 270–282.
Cowan, E.A., Christoffersen, P., Powell, R.D., Talarico, F.M., 2014. Dynamics of the late plio–Pleistocene West Antarctic ice sheet documented in subglacial diamictites, AND-1B drill core. Glob. Planet. Chang. 119, 56–70.
Cowton, T., Nienow, P., Bartholomew, I., Sole, A., Mair, D., 2012. Rapid erosion beneath the Greenland ice sheet. Geology 40, 343–346.
Creyts, T.T., Clarke, G.K., Church, M., 2013. Evolution of subglacial overdeepenings in response to sediment redistribution and glaciohydraulic supercooling. J. Geophys. Res. Earth Surf. 118, 423–446.
Crossen, K.J., Lowell, T.V., 2010. Holocene history revealed by post-surge retreat; Bering Glacier forelands, Alaska. Geol. Soc. Am. Spec. Pap. 462, 235–250.
Cuffey, K.M., Paterson, W.S.B., 2010. The Physics of Glaciers. 4th edition. Elsevier, New York 704 pp.
Cuffey, K.M., Conway, H., Hallet, B., Gades, A.M., Raymond, C.F., 1999. Interfacial water in polar glaciers and glacier sliding at −17 °C. Geophys. Res. Lett. 26, 751–754. http://dx.doi.org/10.1029/1999GL900096.
Curran, K.J., Hill, P.S., Milligan, T.G., Cowan, E.A., Syvitski, J.P.M., Konings, S.M., 2004. Fine-grained sediment flocculation below the Hubbard Glacier meltwater plume, Disenchantment Bay, Alaska. Mar. Geol. 203, 83–94.
Dahlgren, K.I.T., Vorren, T.O., 2003. Sedimentary environment and glacial history during the last 40 ka of the vøring continental margin, mid-Norway. Mar. Geol. 193, 93–127. http://dx.doi.org/10.1016/S0025-3227(02)00617-5.
Dahlgren, K.I.T., Vorren, T.O., Laberg, J.S., 2002. Late Quaternary glacial development of the mid-Norwegian margin — 65 to 68 degrees N. Mar. Pet. Geol. 19, 1089–1113.
Dahlgren, K.I.T., Vorren, T.O., Stoker, M.S., Nielsen, T., Nygard, A., Sejrup, H.P., 2005. Late Cenozoic prograding wedges on the NW European continental margin: their formation and relationship to tectonics and climate. Mar. Pet. Geol. 22, 1089–1110.
DaSilva, J.L., Anderson, J.B., Stravers, J., 1997. Seismic facies changes along a nearly continuous 24 degrees latitudinal transect: the fjords of Chile and the northern Antarctic Peninsula. Mar. Geol. 143, 103–123.
Davies, M.H., Mix, A.C., Stoner, J.S., Addison, J.A., Jaeger, J., Finney, B., Wiest, J., 2011. The deglacial transition on the southeastern Alaska margin: meltwater input, sea level rise, marine productivity, and sedimentary anoxia. Paleoceanography 26, PA2223. http://dx.doi.org/10.1029/2010PA002051.
Davies-Walczak, M., Mix, A.C., Stoner, J.S., Southon, J.R., Cheseby, M., Xuan, C., 2014. Late glacial to Holocene radiocarbon constraints on North Pacific Intermediate Water ventilation and deglacial atmospheric CO_2 sources. Earth Planet. Sci. Lett. 397, 57–66.
Davis, P.T., Menounos, B., Osborn, G., 2009. Holocene and latest Pleistocene alpine glacier fluctuations: a global perspective. Quat. Sci. Rev. 28, 2021–2033.
Delmas, M., Calvet, M., Gurnell, Y., 2009. Variability of Quaternary glacial erosion rates — a global perspective with special reference to the eastern Pyrenees. Quat. Sci. Rev. 28, 484–498.
DeMaster, D.J., Nelson, T.M., Harden, S.L., Nittrouer, C.A., 1991. The cycling and accumulation of biogenic silica and organic carbon in Antarctic deep-sea and continental margin environments. Mar. Chem. 35, 489–502. http://dx.doi.org/10.1016/S0304-4203(09)90039-1.
Derbyshire, E., 2003. Loess, and the Dust Indicators and Records of Terrestrial and Marine Palaeoenvironments (DIRTMAP) database. Quat. Sci. Rev. 22, 1813–1819.
Deser, C., Holland, M., Reverdin, G., Timlin, M., 2002. Decadal variations in Labrador Sea ice cover and North Atlantic sea surface temperatures. J. Geophys. Res. Oceans 107 (C5) 3-1-3-12.
Desloges, J.R., Gilbert, R., Nielsen, N., Christiansen, C., Rasch, M., Ohlenschlager, R., 2002. Holocene glacimarine sedimentary environments in fiords of Disko Bugt, West Greenland. Quat. Sci. Rev. 21, 947–963.
DeWinter, I., Storms, J., Overeem, I., 2012. Numerical modeling of glacial sediment production and transport during deglaciation. Geomorphology 167-168, 102–114.
Dobson, M., O'Leary, L.R., Veart, M., 1998. Sediment delivery to the Gulf of Alaska: source mechanisms along a glaciated transform margin. In: Stoker, M.S., Evans, D., Cramp, A. (Eds.), Geological Processes on Continental Margins: Sedimentation, Mass-Wasting and StabilitySpecial Publication 129. Geological Society, London, pp. 43–66.
Domack, E.W., 1990. Laminated terrigenous sediments from the Antarctic Peninsula; the role of subglacial and marine processes. In: Dowdeswell, J.A., Scourse, J.D. (Eds.), Glacimarine Environments: Processes and Sediments. Geological Society Special Publication, London, pp. 91–103.
Domack, E.W., Harris, P.T., 1998. A new depositional model for ice shelves, based upon sediment cores from the Ross Sea and the Mac. Robertson shelf, Antarctica. Ann. Glaciol. 27, 281–284.
Domack, E.W., Ishman, S.E., 1993. Oceanographic and physiographic controls on modern sedimentation within Antarctic fjords. Geol. Soc. Am. Bull. 105, 1175–1189.
Domack, E.W., McClennen, C.E., 1996. Accumulation of glacial marine sediments in fjords of the Antarctic Peninsula and their use as late Holocene paleoenvironmental indicators. Antarct. Res. Ser. 70, 135–154.
Domack, E.W., Williams, C.R., 1990. Fine-structure and suspended sediment transport in three Antarctic fjords. Antarct. Res. Ser. 50, 71–89.
Domack, E.W., Foss, D.J.P., Syvitski, J.P.M., McClennen, C.E., 1994. Transport of suspended particulate matter in an Antarctic fjord. Mar. Geol. 121, 161–170.
Domack, E.W., Jacobson, E.A., Shipp, S., Anderson, J.B., 1999. Sedimentologic and stratigraphic signature of the late Pleistocene/Holocene fluctuations of the West Antarctic ice sheet in the Ross Sea: a new perspective. Part 2. Geol. Soc. Am. Bull. 111, 1486–1516.
Dowdeswell, J.A., 1995. Glaciers in the high Arctic and recent environmental change. Phil. Trans. R. Soc. London, Ser. A 352, 321–334.
Dowdeswell, J.A., Bamber, J.L., 2007. Keel depths of modem Antarctic icebergs and implications for sea-floor scouring in the geological record. Mar. Geol. 243, 120–131.
Dowdeswell, J.A., Cromack, M., 1991. Behaviour of a glacier-derived suspended sediment plume in a small Arctic inlet. J. Geol. 99, 111–123.
Dowdeswell, J.A., Fugelli, E.M.G., 2012. The seismic architecture and geometry of grounding-zone wedges formed at the marine margins of past ice sheets. Geol. Soc. Am. Bull. 124, 1750–1761.
Dowdeswell, J.A., Siegert, M.J., 1999. Ice-sheet numerical modeling and marine geophysical measurement of glacier-derived sedimentation on the Eurasian Arctic continental margins. Geol. Soc. Am. Bull. 111, 1080–1097.
Dowdeswell, J.A., Vásquez, M., 2013. Submarine landforms in the fjords of southern Chile: implications for glacimarine processes and sedimentation in a mild glacier-influenced environment. Quat. Sci. Rev. 64, 1–19.
Dowdeswell, J.A., Hamilton, G.S., Hagen, J.O., 1991. The duration of the active phase on surge-type glaciers: contrasts between Svalbard and other regions. J. Glaciol. 37, 388–400.
Dowdeswell, J.A., Kenyon, N.H., Eleverhoi, A., Laberg, J.S., Hollender, F.J., Mienert, J., Siegert, M.J., 1996. Large-scale sedimentation on the glacier-influenced Polar North Atlantic margins: long-range side-scan sonar evidence. Geophys. Res. Lett. 23, 3535–3538.
Dowdeswell, J.A., Elverhøi, A., Spielhagen, R., 1998. Glacimarine sedimentary processes and facies on the Polar North Atlantic margins. Quat. Sci. Rev. 17, 243–272.
Dowdeswell, J.A., Whittington, R.J., Jennings, A.E., Andrews, J.T., Mackensen, A., Marienfeld, P., 2000. An origin for laminated glacimarine sediments through sea-ice build-up and suppressed iceberg rafting. Sedimentology 47, 557–576.
Dowdeswell, J.A., Cofaigh, C.Ó., Taylor, J., Kenyon, N.H., Mienert, J., Wilken, M., 2002. On the architecture of high-latitude continental margins: the influence of ice-sheet and sea-ice processes in the Polar North Atlantic. Geol. Soc. Lond., Spec. Publ. 203, 33–54.
Dowdeswell, J.A., Cofaigh, C.Ó., Pudsey, C.J., 2004. Thickness and extent of the subglacial till layer beneath an Antarctic palaeo-ice stream. Geology 32, 13–16.
Dowdeswell, J.A., Ottesen, D., Rise, L., Craig, J., 2007. Identification and preservation of landforms diagnostic of past ice-sheet activity on continental shelves from three-dimensional seismic evidence. Geology 35, 359–362.
Dowdeswell, J.A., Cofaigh, C.Ó., Noormets, R., Larter, R.D., Hillenbrand, C.D., Benetti, S., Evans, J., Pudsey, C.J., 2008a. A major trough-mouth fan on the continental margin of the Bellingshausen Sea, West Antarctica: the Belgica Fan. Mar. Geol. 252, 129–140.
Dowdeswell, J.A., Ottesen, D., Evans, J., Cofaigh, C.Ó., Anderson, J.B., 2008b. Submarine glacial landforms and rates of ice-stream collapse. Geology 36, 819–822.
Dowdeswell, J.A., Ottesen, D., Rise, L., 2010. Rates of sediment delivery from the Fennoscandian ice sheet through an ice age. Geology 38, 3–6.
Dowdeswell, J.A., Hogan, K.A., Cofaigh, C.Ó., Fugelli, E.M.G., Evans, J., Noormets, R., 2014. Late Quaternary ice flow in a West Greenland fjord and cross-shelf trough system: submarine landforms from Rink Isbrae to Uummannaq shelf and slope. Quat. Sci. Rev. 92, 292–309.
Dühnforth, M., Anderson, R.S., Ward, D., Stock, G.M., 2010. Bedrock fracture control of glacial erosion processes and rates. Geology 38, 423–426.
Dumont, M., Brun, E., Picard, G., Michou, M., Libois, Q., Petit, J.-R., Geyer, M., Morin, S., Josse, B., 2014. Contribution of light-absorbing impurities in snow to Greenland's darkening since 2009. Nat. Geosci. 7, 509–512. http://dx.doi.org/10.1038/ngeo2180.
Egholm, D.L., Nielsen, S.B., Pedersen, V.K., Lesemann, J.-E., 2009. Glacial effects limiting mountain height. Nature 460, 884–887. http://dx.doi.org/10.1038/nature08263.
Egholm, D.L., Pedersen, V.K., Knudsen, M.F., Larsen, N.K., 2012. Coupling the flow of ice, water, and sediment in a glacial landscape evolution model. Geomorphology 141, 47–66.
Eidvin, T., Jansen, E., Riis, F., 1993. Chronology of tertiary fan deposits off the western Barents Sea — implications for the uplife and erosion history of the Barents shelf. Mar. Geol. 112, 109–131.
Eisen, O., Harrison, W.D., Raymond, C.F., 2001. The surges of Variegated Glacier, Alaska, USA, and their connection to climate and mass balance. J. Glaciol. 47, 351–358.
Elverhøi, A., 1984. Glacigenic and associated marine sediments in the Weddell Sea, fjords of Spitsbergen and the Barents Sea: a review. Mar. Geol. 57, 53–88.
Elverhøi, A., Dowdeswell, J.A., Funder, S., Mangerud, J., Stein, R., 1998a. Glacial and oceanic history of the Polar North Atlantic margins: an overview. Quat. Sci. Rev. 17, 1–10.
Elverhøi, A., Hooke, R.L.B., Solheim, A., 1998b. Late Cenozoic erosion and sediment yield from the Svalbard–Barents Sea region: implications for understanding erosion of glacierized basins. Quat. Sci. Rev. 17, 209–241.
Elverhøi, A., de Blasio, F.V., Butt, F.A., Issler, D., Harbitz, C., Engvik, L., Solheim, A., Marr, J., 2002. Submarine mass-wasting on glacially-influenced continental slopes: processes and dynamics. Geol. Soc. Lond., Spec. Publ. 203, 73–87.
Engelhardt, H., Humphrey, N., Kamb, B., Fahnestock, M., 1990. Physical conditions at the base of a fast moving Antarctic ice stream. Science 248, 57–59.
Enkelmann, E., Zeitler, P.K., Garver, J.I., Pavlis, T.L., Hooks, B.P., 2010. The thermochronological record of tectonic and surface process interaction at the Yakutat–North American collision zone in southeast Alaska. Am. J. Sci. 310, 231–260.
Evans, J., Pudsey, C.J., 2002. Sedimentation associated with Antarctic Peninsula ice shelves: implications for palaeoenvironmental reconstructions of glacimarine sediments. J. Geol. Soc. 159, 233–237.
Evans, J., Dowdeswell, J.A., Grobe, H., Niessen, F., Stein, R., Hubberten, H.W., Whittington, R.J., 2002. Late Quaternary sedimentation in kejser franz joseph fjord and the continental margin of East Greenland. Geol. Soc. Lond., Spec. Publ. 203, 149–179.

Eyles, N., Eyles, C.H., 1992. Glacial depositional systems. In: Walker, R.G., James, M.P. (Eds.), Facies Models: Response to Sea Level Change. Geological Association of Canada, pp. 73–100.
Eyles, C.H., Eyles, N., Lagoe, M.B., 1991. The Yakataga Formation; a late Miocene to Pleistocene record of temperate glacial-marine sedimentation in the Gulf of Alaska. In: Anderson, J.B., Ashley, G.M. (Eds.), Glacial Marine Sedimentation: Paleoclimatic Significance. Geological Society of America, Boulder, CO, pp. 159–180.
Fairbanks, R.G., 1989. A 17,000-year glacio-eustatic sea level record: influence of glacial melting rates on the Younger Dryas event and deep ocean circulation. Nature 342, 637–643.
Faleide, J.I., Solheim, A., Fiedler, A., Hjelstuen, B.O., Andersen, E.S., Vanneste, K., 1996. Late Cenozoic evolution of the western Barents Sea–Svalbard continental margin. Glob. Planet. Chang. 12, 53–74.
Fastook, J.L., Hughes, T.J., 2013. New perspectives on paleoglaciology. Quat. Sci. Rev. 80, 169–194.
Fernandez, R.A., Anderson, J.B., Wellner, J.S., Hallet, B., 2011. Timescale dependence of glacial erosion rates: a case study of Marinelli Glacier, Cordillera Darwin, southern Patagonia. J. Geophys. Res. 116 (F1), 1–18. http://dx.doi.org/10.1029/2010JF001685.
Fischer, M.P., Powell, R.D., 1998. A simple model for the influence of push-morainal banks on the calving and stability of glacial tidewater termini. J. Glaciol. 44, 31–41.
Flowerdew, M.J., Tyrrell, S., Riley, T.R., Whitehouse, M.J., Mulvaney, R., Leat, P.T., Marschall, H.R., 2012. Distinguishing east and West Antarctic sediment sources using the Pb isotope composition of detrital K-feldspar. Chem. Geol. 292, 88–102.
Flowerdew, M.J., Tyrrell, S., Peck, V.L., 2013. Inferring sites of subglacial erosion using the Pb isotopic composition of ice-rafted feldspar: examples from the Weddell Sea, Antarctica. Geology 41, 147–150. http://dx.doi.org/10.1130/G33644.1.
Fortuin, J.P.F., Oerlemans, J., 1990. Parameterization of the annual surface temperature and mass balance of Antarctica. Ann. Glaciol. 14, 78–84.
Forwick, M., Vorren, T.O., 2009. Late Weichselian and Holocene sedimentary environments and ice rafting in Isfjorden, Spitsbergen. Palaeogeogr. Palaeoclimatol. Palaeoecol. 280, 258–274.
Fuchs, M., Owen, L.A., 2008. Luminescence dating of glacial and associated sediments: review, recommendations and future directions. Boreas 37, 636–659.
Funder, S., Hjort, C., Landvik, J.Y., Nam, S.I., Reeh, N., Stein, R., 1998. History of a stable ice margin East Greenland during the middle and upper Pleistocene. Quat. Sci. Rev. 17, 77–123.
Gales, J.A., Larter, R.D., Mitchell, N.C., Dowdeswell, J.A., 2013. Geomorphic signature of Antarctic submarine gullies: implications for continental slope processes. Mar. Geol. 337, 112–124.
Garcia, M., Ercilla, G., Alonso, B., Casas, D., Dowdeswell, J.A., 2011. Sediment lithofacies, processes and sedimentary models in the Central Bransfield Basin, Antarctic Peninsula, since the Last Glacial Maximum. Mar. Geol. 290, 1–16.
Garcia, M., Dowdeswell, J.A., Ercilla, G., Jakobsson, M., 2012. Recent glacially influenced sedimentary processes on the East Greenland continental slope and deep Greenland basin. Quat. Sci. Rev. 49, 64–81.
Gilbert, R., Nielsen, N., Desloges, J.R., Rasch, M., 1998. Contrasting glacimarine sedimentary environments of two Arctic fiords on Disko, West Greenland. Mar. Geol. 147, 63–83.
Gilbert, R., Nielsen, N., Moller, H., Desloges, J.R., Rasch, M., 2002. Glacimarine sedimentation in Kangerdluk (Disko Fjord), West Greenland, in response to a surging glacier. Mar. Geol. 191, 1–18.
Gilbert, R., Chong, Å., Dunbar, R.B., Domack, E.W., 2003. Sediment trap records of glacimarine sedimentation at Müller Ice Shelf, Lallemand Fjord, Antarctic Peninsula. Arct. Antarct. Alp. Res. 35, 24–33.
Goehring, B.M., Schaefer, J.M., Schluechter, C., Lifton, N.A., Finkel, R.C., Jull, A.T., Akcar, N., Alley, R.B., 2011. The Rhone glacier was smaller than today for most of the Holocene. Geology 39, 679–682.
Goff, J.A., Lawson, D.E., Willems, B.A., Davis, M., Gulick, S.P.S., 2012. Morainal bank progradation and sediment accumulation in Disenchantment Bay, Alaska: response to advancing Hubbard Glacier. J. Geophys. Res. Earth Surf. 117, F02031. http://dx.doi.org/10.1029/2011JF002312.
Golledge, N.R., Levy, R.H., McKay, R.M., Fogwill, C.J., White, D.A., Graham, A.G.C., Smith, J.A., Hillenbrand, C.-D., Licht, K.J., Denton, G.H., Ackert Jr., R.P., Mass, S.M., Hall, B.L., 2013. Glaciology and geological signature of the Last Glacial Maximum Antarctic ice sheet. Quat. Sci. Rev. 78, 225–247.
Graham, A.G.C., Larter, R.D., Gohl, K., Dowdeswell, J.A., Hillenbrand, C.D., Smith, J.A., Evans, J., Kuhn, G., Deen, T., 2010. Flow and retreat of the late Quaternary Pine Island–Thwaites palaeo-ice stream, West Antarctica. J. Geophys. Res. Earth Surf. (2003–2012) 115 (F3).
Granger, D.E., Lifton, N.A., Willenbring, J.K., 2013. A cosmic trip: 25 years of cosmogenic nuclides in geology. Geol. Soc. Am. Bull. 125, 1379–1402.
Griffith, T.W., Anderson, J.B., 1989. Climatic control of sedimentation in bays and fjords of the northern Antarctic Peninsula. Mar. Geol. 85, 181–204.
Gurnell, A., Hannah, D., Lawler, D., 1996. Suspended sediment yields from glacier basins. Erosion and Sediment Yield: Global and Regional Perspectives. IASH Publication 236, pp. 97–104.
Hagen, J.O., Liestøl, O., Roland, E., Jørgensen, T., 1993. Glacier Atlas of Svalbard and Jan MayenMeddelelser 129. Norsk Polarinstitutt.
Hald, M., Dahlgren, T., Olsen, T.E., Lebesbye, E., 2001. Late Holocene palaeoceanography in Van Mijenfjorden, Svalbard. Polar Res. 20, 23–35.
Hall, B.L., 2009. Holocene glacial history of Antarctica and the sub-Antarctic islands. Quat. Sci. Rev. 28, 2213–2230.
Hallet, B., 1979. A theoretical model of glacial abrasion. J. Glaciol. 23, 29–50.
Hallet, B., 1996. Glacial quarrying: a simple theoretical model. Ann. Glaciol. 22, 1–8.
Hallet, B., Hunter, L., Bogen, J., 1996. Rates of erosion and sediment evacuation by glaciers: a review of field data and their implications. Glob. Planet. Chang. 12, 213–235. http://dx.doi.org/10.1016/0921-8181(95)00021-6.
Hambrey, M.J., Glasser, N.F., 2012. Discriminating glacier thermal and dynamic regimes in the sedimentary record. Sediment. Geol. 251-252, 1–33.
Hanson, M.A., Lian, O.B., Clague, J.J., 2012. The sequence and timing of large late Pleistocene floods from Glacial Lake Missoula. Quat. Sci. Rev. 31, 67–81.
Harbor, J., 1992. Numerical modeling of the deveopment of U-shaped valleys by glacial erosion. Geol. Soc. Am. Bull. 104, 1364–1375.
Harbor, J.M., Hallet, B., Raymond, C.F., 1988. A numerical model of landform development by glacial erosion. Nature 333, 347–349.
Harden, S.L., DeMaster, D.J., Nittrouer, C.A., 1992. Developing sediment geochronologies for high-latitude continental shelf deposits: a radiochemical approach. Mar. Geol. 103, 69–97.
Harris, P.T., Domack, E., Manley, P.L., Gilbert, R., Leventer, A., 1999. Andvord drift: a new type of inner shelf, glacial marine deposystem from the Antarctic Peninsula. Geology 27, 683–686.
Harrison, W.D., Post, A.S., 2003. How much do we really know about glacier surging? Ann. Glaciol. 36, 1–6.
Harrison, W.D., Elsberg, D.H., Echelmeyer, K.A., Krimmel, R.M., 2001. On the characterization of glacier response by a single time-scale. J. Glaciol. 47, 659–664.
Headley, R., Hallet, B., Roe, G., Waddington, E.D., Rignot, E., 2012. Spatial distribution of glacial erosion rates in the St. Elias range, Alaska, inferred from a realistic model of glacier dynamics. J. Geophys. Res. Earth Surf. 117, F03027. http://dx.doi.org/10.1029/2011JF002291.
Headley, R.M., Enkelmann, E., Hallet, B., 2013. Examination of the interplay between glacial processes and exhumation in the Saint Elias Mountains, Alaska. Geosphere 9, 229–241.
Hebbeln, D., Henrich, R., Baumann, K.H., 1998. Paleoceanography of the last interglacial/glacial cycle in the Polar North Atlantic. Quat. Sci. Rev. 17, 125–153.
Hemming, S.R., 2004. Heinrich events: massive late Pleistocene detritus layers of the North Atlantic and their global climate imprint. Rev. Geophys. 42, RG1005. http://dx.doi.org/10.1029/2003RG000128.
Hendy, I.L., Cosma, T., 2008. Vulnerability of the cordilleran ice sheet to iceberg calving during late Quaternary rapid climate change events. Paleoceanography 23, PA2101. http://dx.doi.org/10.1029/2008PA001606.
Henriksen, M., Alexanderson, H., Landvik, J.Y., Linge, H., Peterson, G., 2014. Dynamics and retreat of the Late Weichselian Kongsfjorden ice stream, NW Svalbard. Quat. Sci. Rev. 92, 235–245.
Herman, F., Braun, J., 2008. Evolution of the glacial landscape of the Southern Alps of New Zealand: insights from a glacial erosion model. J. Geophys. Res. Earth Surf. 113, F02009. http://dx.doi.org/10.1029/2007JF000807.
Herman, F., Beaud, F., Champagnac, J.-D., Lemieux, J.-M., Sternai, P., 2011. Glacial hydrology and erosion patterns: a mechanism for carving glacial valleys. Earth Planet. Sci. Lett. 310, 498–508.
Herman, F., Seward, D., Valla, P.G., Carter, A., Kohn, B., Willett, S.D., Ehlers, T.A., 2013. Worldwide acceleration of mountain erosion under a cooling climate. Nature 504, 423–426.
Herman, F., et al., 2015. Erosion by an alpine glacier. Science 350 (6257), 193–195.
Heyman, J., Stroeven, A.P., Harbor, J.M., Caffee, M.W., 2011. Too young or too old: evaluating cosmogenic exposure dating based on an analysis of compiled boulder exposure ages. Earth Planet. Sci. Lett. 302, 71–80.
Hill, P.S., Syvitski, J.P., Cowan, E.A., Powell, R.D., 1998. In situ observations of floc settling velocities in Glacier Bay, Alaska. Mar. Geol. 145, 85–94.
Hillenbrand, C.D., Baesler, A., Grobe, H., 2005. The sedimentary record of the last glaciation in the western Bellingshausen Sea (West Antarctica): implications for the interpretation of diamictons in a polar-marine setting. Mar. Geol. 216, 191–204.
Hillenbrand, C.D., Larter, R.D., Dowdeswell, J.A., Ehrmann, W., Cofaigh, C.Ó., Benetti, S., Graham, A.G.C., Grobe, H., 2010a. The sedimentary legacy of a palaeo-ice stream on the shelf of the southern Bellingshausen Sea: clues to West Antarctic glacial history during the late Quaternary. Quat. Sci. Rev. 29, 2741–2763.
Hillenbrand, C.D., Smith, J.A., Kuhn, G., Esper, O., Gersonde, R., Larter, R.D., Maher, B., Moreton, S.G., Shimmield, T.M., Korte, M., 2010b. Age assignment of a diatomaceous ooze deposited in the western Amundsen Sea embayment after the Last Glacial Maximum. J. Quat. Sci. 25, 280–295.
Hillenbrand, C.D., Bentley, M.J., Stolldorf, T.D., Hein, A.S., Kuhn, G., Graham, A.G.C., Fogwill, C.J., Kristoffersen, Y., Smith, J.A., Anderson, J.B., Larter, R.D., Melles, M., Hodgson, D.A., Mulvaney, R., Sugden, D.E., 2014. Reconstruction of changes in the Weddell Sea sector of the Antarctic ice sheet since the Last Glacial Maximum. Quat. Sci. Rev. 100, 111–136.
Hodgson, D.A., Graham, A.G.C., Roberts, S.J., Bentley, M.J., Cofaigh, C.Ó., Verleyen, E., Vyverman, W., Jomelli, V., Favier, V., Brunstein, D., Verfaillie, D., Colhoun, E.A., Saunders, K.M., Selkirk, P.M., Mackintosh, A., Hedding, D.W., Nel, W., Hall, K., McGlone, M.S., Van der Putten, N., Dickens, W.A., Smith, J.A., 2014. Terrestrial and submarine evidence for the extent and timing of the Last Glacial Maximum and the onset of deglaciation on the maritime-Antarctic and sub-Antarctic islands. Quat. Sci. Rev. 100, 137–158.
Hogan, K.A., Dowdeswell, J.A., Noormets, R., Evans, J., Cofaigh, C.Ó., 2010. Evidence for full-glacial flow and retreat of the Late Weichselian Ice Sheet from the waters around Kong Karls Land, eastern Svalbard. Quat. Sci. Rev. 29 (25–26), 3563–3582.
Hogan, K.A., Dix, J.K., Lloyd, J.M., Long, A.J., Cotterill, C.J., 2011. Seismic stratigraphy records the deglacial history of Jakobshavn Isbrae, West Greenland. J. Quat. Sci. 26, 757–766.
Hogan, K.A., Dowdeswell, J.A., Cofaigh, C.Ó., 2012. Glacimarine sedimentary processes and depositional environments in an embayment fed by West Greenland ice streams. Mar. Geol. 311, 1–16.
Hooke, R.L.B., Elverhøi, E., 1996. Sediment flux from a fjord during glacial periods, Isfjorden, Spitsbergen. Glob. Planet. Chang. 12, 237–249.

Hormes, A., Gjermundsen, E.F., Rasmussen, T.L., 2013. From mountain top to the deep sea — deglaciation in 4D of the northwestern Barents Sea ice sheet. Quat. Sci. Rev. 75, 78–99.
Hughes, T.J., 1992. Theoretical calving rates from glaciers along ice walls grounded in water of variable depths. J. Glaciol. 38, 282–294.
Humphrey, N., Raymond, C.F., 1994. Hydrology, erosion and sediment production in a surging glacier: Variegated Glacier, Alaska, 1982–83. J. Glaciol. 40, 539–552.
Humphrey, N.F., Kamb, B., Fahnestock, M.A., Engelhardt, H., 1993. Characteristics of the bed of the lower Columbia Glacier, Alaska. J. Geophys. Res. 98 (B1), 837–846.
Hunter, L.E., Powell, R.D., Lawson, D.E., 1996a. Flux of debris transported by ice at three Alaskan glaciers. J. Glaciol. 42, 123–135.
Hunter, L.E., Powell, R.D., Lawson, D.E., 1996b. Morainal-bank sediment budgets and their influence on the stability of tidewater termini of valley glaciers entering Glacier Bay, Alaska, U.S.A. Ann. Glaciol. 22, 211–216.
Huybers, K., Roe, G.H., 2009. Spatial patterns of glaciers in response to spatial patterns in regional climate. J. Clim. 22, 4606–4620.
Iken, A., Bindschadler, R., 1986. Combined measurements of subglacial water pressure and surface velocity of findelengletscher, Switzerland: conclusions about drainage system and sliding mechanism. J. Glaciol. 32, 101–119.
Imbrie, J., Hays, J.D., Martinson, D.G., McIntyre, A., Mix, A.C., Morley, J.J., Pisias, N.G., Prell, W.L., Shackleton, N.J., 1984. The orbital theory of Pleistocene climate: support from a revised chronology of the marine delta18O record. Milankovitch and Climate: Understanding the Response to Astronomical Forcing. vol. 1, p. 269.
Ingólfsson, Ó., Landvik, J.Y., 2013. The Svalbard-Barents Sea ice-sheet — historical, current and future perspectives. Quat. Sci. Rev. 64, 33–60.
Iverson, N.R., 1991. Potential effects of subglacial water-pressure fluctuations on quarrying. J. Glaciol. 37, 27–36.
Iverson, N.R., 2012. A theory of glacial quarrying for landscape evolution models. Geology 40, 679–682. http://dx.doi.org/10.1130/G33079.1.
Jaeger, J.M., 2002. Developing high-resolution chronologies in glacimarine sediments: examples from southeastern Alaska. Geol. Soc. Lond., Spec. Publ. 203, 195–214.
Jaeger, J.M., Kramer, B., 2014. A continental shelf sedimentary record of Little Ice Age to modern glacial dynamics: Bering Glacier, Alaska. Cont. Shelf Res. 86, 141–156.
Jaeger, J.M., Nittrouer, C.A., 1999a. Marine record of surge-induced outburst floods from the Bering Glacier, Alaska. Geology 27, 847–850.
Jaeger, J.M., Nittrouer, C.A., 1999b. Sediment deposition in an Alaskan fjord: controls on the formation and preservation of sedimentary structures in icy bay. J. Sediment. Res. 69, 1011–1026.
Jaeger, J.M., Nittrouer, C.A., 2006. A quantitative examination of modern sedimentary lithofacies formation on the glacially influenced Gulf of Alaska continental shelf. Cont. Shelf Res. 26, 2178–2204.
Jaeger, J.M., Nittrouer, C.A., Scott, N.D., Milliman, J.D., 1998. Sediment accumulation along a glacially impacted mountainous coastline: north-east Gulf of Alaska. Basin Res. 10, 155–173.
Jakobsson, M., et al., 2012. The International Bathymetric Chart of the Arctic Ocean (IBCAO) version 3.0. Geophys. Res. Lett. 39, L12609. http://dx.doi.org/10.1029/2012GL052219.
Jakobsson, M., Andreassen, K., Bjarnadottir, L.R., Dove, D., Dowdeswell, J.A., England, J.H., Funder, S., Hogan, K., Ingoolfsson, O., Jennings, A., Larsen, N.K., Kirchner, N., Landvik, J.Y., Mayer, L., Mikkelsen, N., Moller, P., Niessen, F., Nilsson, J., O'Regan, M., Polyak, L., Norgaard-Pedersen, N., Stein, R., 2014a. Arctic Ocean glacial history. Quat. Sci. Rev. 92, 40–67.
Jakobsson, M., Ingólfsson, Ó., Long, A.J., Spielhagen, R.F., 2014b. The dynamic Arctic. Quat. Sci. Rev. 92, 1–8.
Jennings, A.E., Weiner, N.J., 1996. Environmental change on eastern Greenland during the last 1300 years: evidence from foraminifera and lithofacies in Nansen Fjord, 68°N. The Holocene 6, 179–191.
Jerolmack, D.J., Sadler, P., 2007. Transience and persistence in the depositional record of continental margins. J. Geophys. Res. 112, F03S13.
Jiskoot, H., Murray, T., Boyle, P., 2000. Controls on the distribution of surge-type glaciers in Svalbard. J. Glaciol. 46, 412–422.
Joughin, I., Howat, I.M., Alley, R.B., Ekstrom, G., Fahnestock, M., Moon, T., Nettles, M., Truffer, M., Tsai, V.C., 2008. Ice-front variation and tidewater behavior on Helheim and Kangerdlugssuaq Glaciers, Greenland. J. Geophys. Res. 113 (F1), 1–11. http://dx.doi.org/10.1029/2007JF000837.
Joughin, I., Alley, R.B., Holland, D.M., 2012. Ice-sheet response to oceanic forcing. Science 338, 1172–1176. http://dx.doi.org/10.1126/science.1226481.
Kamb, B., Raymond, C.F., Harrison, W.D., Engelhardt, H., Echelmeyer, K.A., Humphrey, N., Brugman, M.M., Pfeffer, T., 1985. Glacier surge mechanism: 1982–1983 surge of Variegated Glacier, Alaska. Science 227, 469–479.
Kawamura, K., Aoki, S., Nakazawa, T., Matsushima, H., Ishidoya, S., Sugawara, S., Lisiecki, L., Raymo, M.E., Severinghaus, J.P., 2008. Accurate chronology of Antarctic climate and greenhouse gas changes over the past 470 ky. Geochim. Cosmochim. Acta 72, A454 A454.
Kempf, P., Forwick, M., Laberg, J.S., Vorren, T.O., 2013. Late Weichselian and Holocene sedimentary palaeoenvironment and glacial activity in the high-Arctic van Keulenfjorden, Spitsbergen. The Holocene 23, 1607–1618.
Kessler, M.A., Anderson, R.S., Briner, J.P., 2008. Fjord insertion into continental margins driven by topographic steering of ice. Nat. Geosci. 1, 365–369.
Kilfeather, A.A., Cofaigh, C.Ó., Lloyd, J.M., Dowdeswell, J.A., Xu, S., Moreton, S.G., 2011. Ice-stream retreat and ice-shelf history in Marguerite Trough, Antarctic Peninsula: sedimentological and foraminiferal signatures. Geol. Soc. Am. Bull. 123, 997–1015.
King, E.L., Haflidason, H., Sejrup, H.P., Lovlie, R., 1998. Glacigenic debris flows on the North Sea trough mouth fan during ice stream maxima. Mar. Geol. 152, 217–246.
Kirchner, N., Greve, R., Stroeven, A.P., Heyman, J., 2011a. Paleoglaciological reconstructions for the Tibetan Plateau during the last glacial cycle: evaluating numerical ice sheet simulations driven by GCM-ensembles. Quat. Sci. Rev. 30, 248–267.
Kirchner, N., Hutter, K., Jakobsson, M., Gyllencreutz, R., 2011b. Capabilities and limitations of numerical ice sheet models: a discussion for earth-scientists and modelers. Quat. Sci. Rev. 30, 3691–3704.
Kirshner, A.E., Anderson, J.B., Jakobsson, M., O'Regan, M., Majewski, W., Nitsche, F.O., 2012. Post-LGM deglaciation in Pine Island Bay, West Antarctica. Quat. Sci. Rev. 38, 11–26.
Knies, J., Matthiessen, J., Vogt, C., Laberg, J.S., Hjelstuen, B.O., Smelror, M., Larsen, E., Andreassen, K., Eidvin, T., Vorren, T.O., 2009. The Plio-Pleistocene glaciation of the Barents Sea–Svalbard region: a new model based on revised chronostratigraphy. Quat. Sci. Rev. 28, 812–829.
Koppes, M.N., Hallet, B., 2002. Influence of rapid glacial retreat on the rate of erosion by tidewater glaciers. Geology 30, 47–50.
Koppes, M., Hallet, B., 2006. Erosion rates during rapid deglaciation in icy bay, Alaska. J. Geophys. Res. Earth Surf. 111 (F2).
Koppes, M., Montgomery, D., 2009. The relative efficacy of fluvial and glacial erosion over modern to orogenic timescales. Nat. Geosci. 2, 644–647.
Koppes, M., Hallet, B., Anderson, J., 2009. Synchronous acceleration of ice loss and glacier erosion, Marinelli Glacier, Tierra del Fuego. J. Glaciol. 55, 207–220. http://dx.doi.org/10.3189/002214309788608796.
Koppes, M., Sylwester, R., Rivera, A., Hallet, B., 2010. Variations in sediment yield over the advance and retreat of a calving glacier, Laguna San Rafael, North Patagonian Icefield. Quat. Res. 73, 84–95. http://dx.doi.org/10.1016/j.yqres.2009.07.006.
Koppes, M., Hallet, B., Rignot, E., Mouginot, J., Wellner, J.S., Boldt, K., 2015. Observed latitudinal variations in erosion as a function of glacier dynamics. Nature 526, 100–103. http://dx.doi.org/10.1038/nature15385.
Krissek, L.A., 1995. Late Cenozoic ice-rafting records from leg 145 sites in the North Pacific: late Miocene onset, late Pliocene intensification, and Pliocene–Pleistocene events. In: Rea, D.K., Basov, I.A., Scholl, D.W., Allan, J.F. (Eds.), Proc. ODP, Sci. Results 145. College Station, TX (Ocean Drilling Program), pp. 179–194. http://dx.doi.org/10.2973/odp.proc.sr.145.118.1995.
Kristensen, L., Benn, D.I., Hormes, A., et al., 2009. Mud aprons in front of Svalbard surge moraines: evidence of subglacial deforming layers or proglacial glaciotectonics? Geomorphology 111, 206–221.
Kristoffersen, Y., Winterhalter, B., Solheim, A., 2000. Shelf progradation on a glaciated continental margin, Queen Maud Land, Antarctica. Mar. Geol. 165, 109–122. http://dx.doi.org/10.1016/s0025-3227(99)00136-x.
Kroon, D., Shimmield, G., Austin, W.E.N., Derrick, S., Knutz, P., Shimmield, T., 2000. Century- to millennial-scale sedimentological–geochemical records of glacial–Holocene sediment variations from the Barra Fan (NE Atlantic). J. Geol. Soc. 157, 643–653.
Kuijpers, A., Dalhoff, F., Brandt, M.P., Hümbs, P., Schott, T., Zotova, A., 2007. Giant iceberg plow marks at more than 1 km water depth offshore West Greenland. Mar. Geol. 246, 60–64.
Laberg, J.S., Vorren, T.O., 1996. The middle and late Pleistocence evolution and the Bear Island trough mouth fan. Glob. Planet. Chang. 12, 309–330.
Laberg, J.S., Eilertsen, R.S., Vorren, T.O., 2009. The palaeo-ice stream in Vestfjorden, north Norway, over the last 35 k.y.: glacial erosion and sediment yield. GSA Bull. 121, 434–447.
Laberg, J.S., Andreassen, K., Knies, J., Vorren, T.O., Winsborrow, M., 2010. Late Pliocene–Pleistocene development of the Barents Sea ice sheet. Geology 38, 107–110.
Landvik, J.Y., Bondevik, S., Elverhi, A., Fjeldskaar, W., Mangerud, J., Siegert, M.J., Salvigsen, O., Svendsen, J.-I., Vorren, T.O., 1998. Last Glacial Maximum of Svalbard and the Barents Sea area: ice sheet extent and configuration. Quat. Sci. Rev. 17, 43–75.
Landvik, J.Y., Ingolfsson, O., Mienert, J., Lehman, S.J., Solheim, A., Elverhoi, A., Ottesen, D., 2005. Rethinking late Weichselian ice-sheet dynamics in coastal NW Svalbard. Boreas 34, 7–24.
Landvik, J.Y., Alexanderson, H., Henriksen, M., Ingolfsson, O., 2014. Landscape imprints of changing glacial regimes during ice-sheet build-up and decay: a conceptual model from Svalbard. Quat. Sci. Rev. 92, 258–268.
Larsen, H.C., Saunders, A.D., Clift, P.D., Beget, J., Wei, W., Spezzaferri, S., Ali, J., Cambray, H., Demant, A., Fitton, G., Fram, M.S., Fukuma, K., Gieskes, J., Holmes, M.A., Hunt, J., Lacasse, C., Larsen, L.M., Lykkeanderson, H., Meltser, A., Morrison, M.L., Nemoto, N., Okay, N., Saito, S., Sinton, C., Stax, R., Vallier, T.L., Vandamme, D., Werner, R., Cliff, P.D., 1994. 7-million years of glaciation in Greenland. Science 264, 952–955.
Larter, R.D., Anderson, J.B., Graham, A.G.C., Gohl, K., Hillenbrand, C.D., Jakobsson, M., Johnson, J.S., Kuhn, G., Nitsche, F.O., Smith, J.A., Witus, A.E., Bentley, M.J., Dowdeswell, J.A., Ehrmann, W., Klages, J.P., Lindow, J., Cofaigh, C.Ó., Spiegel, C., 2014. Reconstruction of changes in the Amundsen Sea and Bellingshausen Sea sector of the West Antarctic ice sheet since the Last Glacial Maximum. Quat. Sci. Rev. 100, 55–86.
Lauritzen, S.-E., 1991. Uranium series dating of speleothems: a glacial chronology for Nordland, Norway, for the last 600 ka. Striae 34, 127–133.
Lawson, D.E., 1993. Glaciohydrologic and Glaciohydraulic Effects on Runoff and Sediment Yield in Glacierized Basins, Monogr. 93–2, Cold Reg. Res. And Eng. Lab. U.S. Army Corps of Eng., Hanover, N. H., USA 108 pp.
Lekens, W.A.H., Sejrup, H.P., Haflidason, H., Petersen, G.O., Hjelstuen, B., Knorr, G., 2005. Laminated sediments preceding Heinrich event 1 in the northern North Sea and southern Norwegian Sea: origin, processes and regional linkage. Mar. Geol. 216, 27–50.
Leventer, A., Dunbar, R., DeMaster, D., 1993. Diatom evidence for late Holocene climatic events in Granite Harbor, Antarctica. Paleoceanography 8, 373–386.
Leventer, A., Domack, E., Dunbar, R., Pike, J., Stickley, C., Maddison, E., Brachfeld, S., Manley, P., McClennen, C., 2006. Marine sediment record from the East Antarctic

margin reveals dynamics of ice sheet recession. GSA Today 16, 4. http://dx.doi.org/10.1130/GSAT01612A.1.
Licht, K.J., Andrews, J.T., 2002. The C-14 record of late Pleistocene ice advance and retreat in the central Ross Sea, Antarctica. Arct. Antarct. Alp. Res. 34, 324–333.
Licht, K.J., Jennings, A.E., Andrews, J.T., Williams, K.M., 1996. Chronology of late Wisconsin ice retreat from the western Ross Sea, Antarctica. Geology 24, 223–226.
Licht, K.J., Dunbar, N.W., Andrews, J.T., Jennings, A.E., 1999. Distinguishing subglacial till and glacial marine diamictons in the western Ross Sea, Antarctica: implications for a Last Glacial Maximum grounding line. Geol. Soc. Am. Bull. 111, 91–103.
Lindow, J., Castex, M., Wittmann, H., Johnson, J.S., Lisker, F., Gohl, K., Spiegel, C., 2014. Glacial retreat in the Amundsen Sea sector, West Antarctica– first cosmogenic evidence from central Pine Island Bay and the Kohler Range. Quat. Sci. Rev. 98, 166–173.
Lingle, C.S., Fatland, D.R., 2003. Does englacial water storage drive temperate glacier surges? Ann. Glaciol. 36, 14–20.
Lisiecki, L.E., Raymo, M.E., 2007. Plio-pleistocene climate evolution: trends and transitions in glacial cycle dynamics. Quat. Sci. Rev. 26, 56–69.
Livingstone, S.J., Cofaigh, C.Ó., Stokes, C.R., Hillenbrand, C.-D., Vieli, A., Jamieson, S.S.R., 2012. Antarctic palaeo-ice streams. Earth Sci. Rev. 111, 90–128.
Lloyd, J.M., 2006. Late Holocene environmental change in Disko Bugt, West Greenland: interaction between climate, ocean circulation and Jakobshavn Isbrae. Boreas 35, 35–49.
Lloyd, J.M., Park, L.A., Kuijpers, A., Moros, M., 2005. Early Holocene palaeoceanography and deglacial chronology of Disko Bugt, West Greenland. Quat. Sci. Rev. 24, 1741–1755.
Lourens, L.J., Becker, J., Bintanja, R., Hilgen, F.J., Tuenter, E., van de Wal, R.S.W., Ziegler, M., 2010. Linear and non-linear response of late Neogene glacial cycles to obliquity forcing and implications for the Milankovitch theory. Quat. Sci. Rev. 29, 352–365.
Lowe, A.L., Anderson, J.B., 2002. Reconstruction of the West Antarctic ice sheet in Pine Island Bay during the Last Glacial Maximum and its subsequent retreat history. Quat. Sci. Rev. 21, 1879–1897.
Lyell, C., 1840. Memoir on the geological evidence of the former existence of glaciers in Forfarshire. Proc. Geol. Soc. Lond. 3, 337–345.
MacGregor, K.R., Anderson, R.S., Waddington, E.D., 2009. Numerical modeling of glacial erosion and headwall processes in alpine valleys. Geomorphology 103, 189–204.
Mackiewicz, N.E., Powell, R.D., Carlson, P.R., Molnia, B.F., 1984. Interlaminated ice-proximal glacimarine sediments in Muir inlet, Alaska. Mar. Geol. 57, 113–147.
Mackintosh, A.N., Verleyen, E., O'Brien, P.E., White, D.A., Jones, R.S., McKay, R., Dunbar, R., Gore, D.B., Fink, D., Post, A.L., Miura, H., Leventer, A., Goodwin, I., Hodgson, D.A., Lilly, K., Crosta, X., Golledge, N.R., Wagner, B., Berg, S., van Ommen, T., Zwartz, D., Roberts, S.J., Vyverman, W., Masse, G., 2014. Retreat history of the East Antarctic ice sheet since the Last Glacial Maximum. Quat. Sci. Rev. 100, 10–30.
Maddison, E., Pike, J., Leventer, A., Domack, E., 2005. Diatom rich sediments from palmer deep, Antarctica: seasonal and sub-seasonal record through the last deglaciation. J. Quat. Sci. 20, 435–446. http://dx.doi.org/10.1002/jqs.947.
Maddison, E., Pike, J., Leventer, A., Dunbar, R., Brachfeld, S., Domack, E., Manley, P., McClennen, C., 2006. Post-glacial seasonal diatom record of the Mertz Glacial Polynya, East Antarctica. Mar. Micropaleontol. 60, 66–88. http://dx.doi.org/10.1016/j.marmicro.2006.03.001.
Mangerud, J., Dokken, T., Hebbeln, D., Heggen, B., Ingolfsson, O., Landvik, J.Y., Mejdahl, V., Svendsen, J.I., Vorren, T.O., 1998. Fluctuations of the Svalbard Barents Sea ice sheet during the last 150000 years. Quat. Sci. Rev. 17, 11–42.
Marcott, S.A., Clark, P.U., Padman, L., Klinkhammer, G.P., Springer, S.R., Liu, Z., Otto-Bliesner, B.L., Carlson, A.E., Ungerer, A., Padman, J., He, F., Cheng, J., Schmittner, A., 2011. Ice-shelf collapse from subsurface warming as a trigger for Heinrich events. Proc. Natl. Acad. Sci. U. S. A. 108, 13415–13419.
Marzeion, B., Cogley, J.G., Richter, K., Parkes, D., 2014. Attribution of global glacier mass loss to anthropogenic and natural causes. Science 345, 919–921.
McClintic, M.A., DeMaster, D.J., Thomas, C.J., Smith, C.R., 2008. Testing the FOODBANCS hypothesis: seasonal variations in near-bottom particle flux, bioturbation intensity, and deposit feeding based on 234Th measurements. Deep-Sea Res. II Top. Stud. Oceanogr. 55, 2425–2437. http://dx.doi.org/10.1016/j.dsr2.2008.06.003.
McKay, R., Browne, G., Carter, L., Cowan, E., Dunbar, G., Krissek, L., Naish, T., Powell, R., Reed, J., Talarico, F., Wilch, T., 2009. The stratigraphic signature of the late Cenozoic Antarctic ice sheets in the Ross Embayment. Geol. Soc. Am. Bull. 121, 1537–1561.
Meier, M.F., Post, A., 1987. Fast tidewater glaciers. J. Geophys. Res. Solid Earth Planets 92 (B9), 9051–9058.
Menounos, B., Osborn, G., Clague, J.J., Luckman, B.H., 2009. Latest Pleistocene and Holocene glacier fluctuations in western Canada. Quat. Sci. Rev. 28, 2049–2074.
Merrand, Y., Hallet, B., 1996. Water and sediment flux during the 1993–94 Bering Glacier surge, Alaska, USA. Ann. Glaciol. 22, 233–240.
Miller, G.H., Wolfe, A.P., Steig, E.J., Sauer, P.E., Kaplan, M.R., Briner, J.P., 2002. The goldilocks dilemma: big ice, little ice, or "just-right" ice in the eastern Canadian Arctic. Quat. Sci. Rev. 21, 33–48.
Milliken, K.T., Anderson, J.B., Wellner, J.S., Bohaty, S.M., Manley, P.L., 2009. High-resolution Holocene climate record from Maxwell Bay, South Shetland Islands, Antarctica. Geol. Soc. Am. Bull. 121, 1711–1725. http://dx.doi.org/10.1130/B26478.1.
Milliman, J.D., Syvitski, J.P.M., 1992. Geomorphic/tectonic control of sediment discharge to the ocean: the importance of small mountainous rivers. J. Geol. 100, 525–544.
Molnia, B.F., 1979. Sedimentation in Coastal Embayments in the Northern Gulf of Alaska, Paper Presented at Offshore Technology Conference, Houston, Tex.
Molnia, B.F., 1983. Glacial Marine Sedimentation. Plenum Press, New York 844 pp.
Molnia, B.F., Post, A., 1995. Holocene history of Bering Glacier, Alaska — a prelude to the 1993–1994 surge. Phys. Geogr. 16, 87–117.
Molnia, B.F., Post, A., 2010. Surges of the Bering Glacier. Geol. Soc. Am. Spec. Pap. 462, 291–316.
Moon, T., Joughin, I., Smith, B., Howat, I., 2012. 21st-century evolution of Greenland outlet glacier velocities. Science 336, 576–578.
Motyka, R.J., O'Neel, S., Connor, C.L., Echelmeyer, K.A., 2003. Twentieth century thinning of Mendenhall Glacier, Alaska, and its relationship to climate, lake calving, and glacier run-off. Glob. Planet. Chang. 35, 93–112.
Motyka, R.J., Truffer, M., Kuriger, E.M., Bucki, A.K., 2006. Rapid erosion of soft sediments by tidewater glacier advance: taku glacier, Alaska, USA. Geophys. Res. Lett. 33. http://dx.doi.org/10.1029/2006GL028467.
Motyka, R.J., Truffer, M., Fahnestock, M., Mortensen, J., Rysgaard, S., Howat, I., 2011. Submarine melting of the 1985 Jakobshavn Isbræ floating tongue and the triggering of the current retreat. J. Geophys. Res. 116 (F1), 1–17. http://dx.doi.org/10.1029/2009JF001632.
Mugford, R.I., Dowdeswell, J.A., 2010. Modeling iceberg-rafted sedimentation in high-latitude fjord environments. J. Geophys. Res. 115, F03024. http://dx.doi.org/10.1029/2009JF001564.
Mugford, R.I., Dowdeswell, J.A., 2011. Modeling glacial meltwater plume dynamics and sedimentation in high-latitude fjords. J. Geophys. Res. 116 (F1), 1–20. http://dx.doi.org/10.1029/2010JF001735.
Mulder, T., Syvitski, J., 1995. Turbidity currents generated at river mouths during exceptional discharges to the world oceans. J. Geol. 103, 285–299.
Muñoz, Y.P., Wellner, J.S., Anderson, J.B., Minzoni, R., Fernández, R.A., 2014. Holocene Accumulation Rates in Antarctic Peninsula Fjords from Millennial to Recent Timescales. GSA Annual Meeting, Vancouver, British Columbia.
Murray, T., Strozzi, T., Luckman, A., Jiskoot, H., Christakos, P., 2003. Is there a single surge mechanism? Contrasts in dynamics between glacier surges in Svalbard and other regions. J. Geophys. Res. Solid Earth 108 (B5), 15.
Muskett, R.R., Lingle, C.S., Sauber, J.M., Post, A.S., Tangborn, W.V., Rabus, B.T., 2008. Surging, accelerating surface lowering and volume reduction of the Malaspina Glacier system, Alaska, USA, and Yukon, Canada, from 1972 to 2006. J. Glaciol. 54, 788–800.
Nesje, A., Dahl, S.O., Thun, T., Nordli, O., 2008. The 'Little Ice Age' glacial expansion in western Scandinavia: summer temperature or winter precipitation? Clim. Dyn. 30, 789–801.
Nick, F.M., van der Veen, C.J., Oerlemans, J., 2007. Controls on advance of tidewater glaciers: results from numerical modeling applied to Columbia Glacier. J. Geophys. Res. 112 (F3), 1–11. http://dx.doi.org/10.1029/2006JF000551.
Nielsen, T., De Santis, L., Dahgren, K.I.T., Kuijpers, A., Laberg, J.S., Nygård, A., Praeg, D., Stoker, M.S., 2005. A comparison of the NW European glaciated margin with other glaciated margins. Mar. Pet. Geol. 22, 1149–1183.
Noormets, R., Dowdeswell, J.A., Larter, R.D., Cofaigh, C.Ó., Evans, J., 2009. Morphology of the upper continental slope in the Bellingshausen and Amundsen Seas — implications for sedimentary processes at the shelf edge of West Antarctica. Mar. Geol. 258, 100–114.
Nygård, A., Sejrup, H.P., Haflidason, H., Bryn, P., 2005. The glacial North Sea fan, southern Norwegian margin: architecture and evolution from the upper continental slope to the deep-sea basin. Mar. Pet. Geol. 22, 71–84.
Nygård, A., Sejrup, H.P., Haflidason, H., Lekens, W.A.H., Clark, C.D., Bigg, G.R., 2007. Extreme sediment and ice discharge from marine-based ice streams: new evidence from the North Sea. Geology 35, 395–398.
O'Neel, S., Pfeffer, W.T., Krimmel, R.M., Meier, M., 2005. Evolving force balance at Columbia Glacier, Alaska, during its rapid retreat. J. Geophys. Res. 110, 1–18. http://dx.doi.org/10.1029/2005JF000292.
Oerlemans, J., 2005. Extracting a climate signal from 169 glacier records. Science 308, 675–677.
Ohkouchi, N., Eglinton, T.I., 2008. Compound-specific radiocarbon dating of Ross Sea sediments: a prospect for constructing chronologies in high-latitude oceanic sediments. Quat. Geochronol. 3, 235–243.
Olsen, L., Sveian, H., Bergstrøm, B., 2001. Rapid adjustments of the western part of the Scandinavian ice sheet during the mid- and late Weichselian — a new model. Nor. J. Geol. 81, 93–118.
Ottesen, D., Dowdeswell, J.A., 2006. Assemblages of submarine landforms produced by tidewater glaciers in Svalbard. J. Geophys. Res. Earth Surf. 111 (F1). http://dx.doi.org/10.1029/2005JF000330.
Ottesen, D., Dowdeswell, J.A., 2009. An inter-ice-stream glaciated margin: submarine landforms and a geomorphic model based on marine-geophysical data from Svalbard. Geol. Soc. Am. Bull. 121, 1647–1665.
Ottesen, D., Dowdeswell, J.A., Rise, L., 2005. Submarine landforms and the reconstruction of fast-flowing ice streams within a large Quaternary ice sheet: the 2500-km-long Norwegian–Svalbard margin (57 degrees–80 degrees N). Geol. Soc. Am. Bull. 117, 1033–1050.
Ottesen, D., Dowdeswell, J.A., Landvik, J.Y., Mienert, J., 2007. Dynamics of the late Weichselian ice sheet on Svalbard inferred from high-resolution sea-floor morphology. Boreas 36, 286–306.
Ottesen, D., Dowdeswell, J.A., Benn, D.I., Kristensen, L., Christiansen, H.H., Christensen, O., Hansen, L., Lebesbye, E., Forwick, M., Vorren, T.O., 2008a. Submarine landforms characteristic of glacier surges in two Spitsbergen fjords. Quat. Sci. Rev. 27, 1583–1599.
Ottesen, D., Stokes, C.R., Rise, L., Olsen, L., 2008b. Ice-sheet dynamics and ice streaming along the coastal parts of northern Norway. Quat. Sci. Rev. 27, 922–940.
Parish, T.R., Bromwich, D.H., 2007. Reexamination of the near-surface airflow over the Antarctic continent and implications on atmospheric circulations at high southern latitudes. Mon. Weather Rev. 135, 1961–1973.
Patterson, M.O., McKay, R., Naish, T., Escutia, C., Jimenez-Espejo, F.J., Raymo, M.E., Meyers, S.R., Tauxe, L., Brinkhuis, H., Integrated Ocean Drilling Expedition 318 Scientists, 2014. Orbital forcing of the East Antarctic ice sheet during the Pliocene and early Pleistocene. Nat. Geosci. 7, 841–847.

Pedersen, V.K., Egholm, D.L., 2013. Glaciations in response to climate variations preconditioned by evolving topography. Nature 493, 206–210.
Pedersen, J.B.T., Kroon, A., Jakobsen, B.H., Mernild, S.H., Andersen, T.J., Andresen, C.S., 2013. Fluctuations of sediment accumulation rates in front of an Arctic delta in Greenland. The Holocene 23, 860–868.
Pedersen, V.K., Huismans, R.S., Herman, F., Egholm, D.L., 2014. Controls of initial topography on temporal and spatial patterns of glacial erosion. Geomorphology 223, 96–116.
Pelto, M.S., Warren, C.R., 1991. Relationship between tidewater glacier calving velocity and water depth at the calving front. Ann. Glaciol. 15, 115–118.
Pelto, M.S., Higgins, S.M., Hughes, T.J., Fastook, J.L., 1990. Modeling mass-balance changes during a glaciation cycle. Ann. Glaciol. 14, 238–241.
Pfeffer, W.T., 2007. A simple mechanism for irreversible tidewater glacier retreat. J. Geophys. Res. 112, 1–12. http://dx.doi.org/10.1029/2006JF000590.
Phillips, A.C., Smith, N.D., Powell, R.D., 1991. Laminated sediments in prodeltaic deposits, Glacier Bay, Alaska. In: Anderson, J.B., Ashley, G.M. (Eds.), Glacial Marine Sedimentation; Paleoclimatic Significance. Geological Society America Special Paper 261, pp. 51–60.
Pierce, E.L., Hemming, S.R., Williams, T., van de Flierdt, T., Thomson, S.N., Reiners, P.W., Gehrels, G.E., Brachfeld, S.A., Goldstein, S.L., 2014. A comparison of detrital U–Pb zircon, $^{40}Ar/^{39}Ar$ hornblende, $^{40}Ar/^{39}Ar$ biotite ages in marine sediments off East Antarctica: implications for the geology of subglacial terrains and provenance studies. Earth-Sci. Rev. 138, 156–178.
Pimentel, S., Flowers, G.E., 2010. A numerical study of hydrologically driven glacier dynamics and subglacial flooding. Proc. R. Soc. A Math. Phys. Eng. Sci. 467, 537–558.
Plassen, L., Vorren, T.O., Forwick, M., 2004. Integrated acoustic and coring investigation of glacigenic deposits in Spitsbergen fjords. Polar Res. 23, 89–110.
Plink-Bjorklund, P., Ronnert, L., 1999. Depositional processes and internal architecture of late Weichselian ice-margin submarine fan and delta settings. Sedimentology 46, 215–234.
Powell, R.D., 1981. A model for sedimentation by tidewater glaciers. Ann. Glaciol. 2, 129–134.
Powell, R.D., 1983. Glacial-marine sedimentation processes and lithofacies of temperate tidewater glaciers, Glacier Bay, Alaska. In: Molnia, B.F. (Ed.), Glacial Marine Sedimentation. Plenum Press, New York, pp. 185–232.
Powell, R.D., 1984. Glacimarine processes and inductive lithofacies modelling of ice shelf and tidewater glacier sediments based on Quaternary examples. Mar. Geol. 57, 1–52.
Powell, R.D., 1990. Glacimarine processes at grounding line fans and their growth to ice-contact deltas. In: Dowdeswell, J.A., Scourse, J.D. (Eds.), Glacimarine Environments: Processes and Sediments. Geological Society Special Publication, London, pp. 53–74.
Powell, R.D., 1991. Grounding-line systems as second-order controls on fluctuations of tidewater termini of temperate glaciers. In: Anderson, J.B., Ashley, G.M. (Eds.), Glacial Marine Sedimentation: Paleoclimatic Significance. Geological Society of America, Special Paper, Boulder, CO, pp. 75–93.
Powell, R.D., Cooper, J.M., 2002. A glacial sequence stratigraphic model for temperate, glaciated continental shelves. Geol. Soc. Lond., Spec. Publ. 203, 215–244.
Powell, R., Domack, E., 1995. Modern glaciomarine environments. In: Menzies, J.J. (Ed.), Modern Glacial Environments: Processes, Dynamics, and Sediments. Butterworth-Heinemann, Oxford, pp. 445–486.
Powell, R.D., Domack, E., 2002. Modern glaciomarine environments. In: Menzies, J. (Ed.), Modern and Past Glacial Environments. Butterworth-Heinemann, Boston, pp. 361–389.
Powell, R.D., Molnia, B.F., 1989. Glacimarine sedimentary processes, facies and morphology of the south southeast Alaska shelf and fjords. Mar. Geol. 85, 359–390.
Powell, R.D., Dawber, M., McInnes, J.N., Pyne, A.R., 1996. Observations of the grounding-line area at a floating glacier terminus. Ann. Glaciol. 22, 217–223.
Praetorius, S.K., Mix, A.C., 2014. Synchronization of North Pacific and Greenland climates preceded abrupt deglacial warming. Science 345, 444–448.
Prior, D.B., Bornhold, B.D., Johns, M.W., 1986. A sand-transporting fjord-bottom channel system. Geology 14, 581–584.
Prior, D.B., Bornhold, B.D., Wiseman, W.J., Lowe, D.R., 1987. Turbidity current activity in a British Columbia fjord. Science 237, 1330–1333.
Pritchard, H., Murray, T., Luckman, A., Strozzi, T., Barr, S., 2005. Glacier surge dynamics of Sortebrae, East Greenland, from synthetic aperture radar feature tracking. J. Geophys. Res. Earth Surf. 110 (F3), 13. http://dx.doi.org/10.1029/2004JF000233.
Radi, T., de Vernal, A., 2008. Last Glacial Maximum (LGM) primary productivity in the northern North Atlantic ocean. Can. J. Earth Sci. 45, 1299–1316.
Raymond, C.F., 1987. How do glaciers surge — a review. J. Geophys. Res. Solid Earth Planets 92 (B9), 9121–9134.
Rebesco, M., Camerlenghi, A., Geletti, R., Canals, M., 2006. Margin architecture reveals the transition to the modern Antarctic ice sheet ca. 3 Ma. Geology 34, 301–304.
Rebesco, M., Laberg, J.S., Pedrosa, M.T., Camerlenghi, A., Lucchi, R.G., Zgur, F., Wardell, N., 2014. Onset and growth of trough-mouth fans on the north-western Barents Sea margin — implications for the evolution of the Barents Sea/Svalbard ice sheet. Quat. Sci. Rev. 92, 227–234.
Reece, R.S., Gulick, S.P.S., Horton, B.K., Christeson, G.L., Worthington, L.L., 2011. Tectonic and climatic influence on the evolution of the surveyor fan and channel system, Gulf of Alaska. Geosphere 7, 830–844.
Refsnider, K.A., Miller, G.H., Frechette, B., Rood, D.H., 2013. A chronological framework for the Clyde Foreland Formation, Eastern Canadian Arctic, derived from amino acid racemization and cosmogenic radionuclides. Quat. Geochronol. 16, 21–34.
Reyes, A.V., Carlson, A.E., Beard, B.L., Hatfield, R.G., Stoner, J.S., Winsor, K., Welke, B., Ullman, D.J., 2014. South Greenland ice-sheet collapse during marine isotope stage 11. Nature 510, 525–528.
Rignot, E., Koppes, M.N., Velicogna, I., 2010. Rapid submarine melting of the calving faces of West Greenland glaciers. Nat. Geosci. 3, 1–5. http://dx.doi.org/10.1038/ngeo765.
Rignot, E., Mouginot, J., Morlighem, M., Seroussi, H., Scheuchl, B., 2014. Widespread, rapid grounding line retreat of Pine Island, Thwaites, Smith, and Kohler glaciers, West Antarctica, from 1992 to 2011. Geophys. Res. Lett. 41, 3502–3509.
Riihimaki, C.A., MacGregor, K.R., Anderson, R.S., Anderson, S.P., Loso, M.G., 2005. Sediment evacuation and glacial erosion rates at a small alpine glacier. J. Geophys. Res. 110, 1–17. http://dx.doi.org/10.1029/2004JF000189.
Roe, G.H., 2005. Orographic precipitation. Annu. Rev. Earth Planet. Sci. 33, 645–671.
Roe, G.H., Baker, M.B., 2014. Glacier response to climate perturbations: an accurate linear geometric model. J. Glaciol. 60, 670–684.
Roksandic, M.M., 1979. Geology of the continental shelf off West Greenland between 61°150 N and 64°000 N: an interpretation of sparker seismic and echosounder data. Grønl. Geol. Unders. 92, 15.
Romans, B.W., Castelltort, S., Covault, J.A., Fildani, A., Walsh, J.P., 2016. Environmental signal propagation in sedimentary systems across timescales. Earth Sci. Rev. 153, 7–29 (this volume).
Rosenheim, B.E., Day, M.B., Domack, E., Schrum, H., Benthien, A., Hayes, J.M., 2008. Antarctic sediment chronology by programmed-temperature pyrolysis: methodology and data treatment. Geochem. Geophys. Geosyst. 9. http://dx.doi.org/10.1029/2007gc001816.
Rother, H., Fink, D., Shulmeister, J., Mifsud, C., Evans, M., Pugh, J., 2014. The early rise and late demise of New Zealand's Last Glacial Maximum. Proc. Natl. Acad. Sci. 111, 11630–11635.
Ruddiman, W.F., 1977. Late Quaternary deposition of ice-rafted sand in the sub-Polar North Atlantic (40–60°N). Geol. Soc. Am. Bull. 88, 1813–1827.
Salcedo-Castro, J., Bourgault, D., Bentley, S.J., deYoung, B., 2013. Non-hydrostatic modeling of cohesive sediment transport associated with a subglacial buoyant jet in glacial fjords: a process-oriented approach. Ocean Model. 63, 30–39. http://dx.doi.org/10.1016/j.ocemod.2012.12.005.
Schoof, C., 2010. Ice-sheet acceleration driven by melt supply variability. Nature 468, 803–806. http://dx.doi.org/10.1038/nature09618.
Schumann, K., Völker, D., Weinrebe, W.R., 2012. Acoustic mapping of the Ilulissat Ice Fjord mouth, West Greenland. Quat. Sci. Rev. 40, 78–88.
Shackleton, N.J., 1987. Oxygen isostopes, ice volume and sea level. Quat. Sci. Rev. 6, 183–190.
Sheaf, M.A., Serpa, L., Pavlis, T.L., 2003. Exhumation rates in the St. Elias Mountains, Alaska. Tectonophysics 367, 1–11.
Shipp, S.S., Wellner, J.S., Anderson, J.B., 2002. Retreat signature of a polar ice stream: subglacial geomorphic features and sediments from the Ross Sea, Antarctica. Geol. Soc. Spec. Publ. 203, 277–304.
Shuster, D.L., Ehlers, T.A., Rusmore, M.E., Farley, K.A., 2005. Rapid glacial erosion at 1.8 Ma revealed by $^{4}He/^{3}He$ thermochronometry. Science 310, 1668–1670.
Siegert, M.J., 1993. Numerical modelling studies of the Svalbard–Barents Sea ice sheet. Unpublished Ph.D. Thesis, University of Cambridge.
Siegert, M.J., Dowdeswell, J.A., 1995. Numerical modeling of the late Weichselian Svalbard–Barents Sea ice sheet. Quat. Res. 43, 1–13.
Siegert, M.J., Dowdeswell, J.A., 2002. Late Weichselian iceberg, surface-melt and sediment production from the Eurasian ice sheet: results from numerical ice-sheet modelling. Mar. Geol. 188, 109–127.
Siegert, M.J., Dowdeswell, J.A., 2004. Numerical reconstructions of the Eurasian ice sheet and climate during the late Weichselian. Quat. Sci. Rev. 23, 1273–1283.
Siegert, M.J., Dowdeswell, J.A., Melles, M., 1999. Late Weichselian glaciation of the Eurasian high Arctic. Quat. Res. 52, 273–285.
Simon, Q., St-Onge, G., Hillaire-Marcel, C., 2012. Late Quaternary chronostratigraphic framework of deep Baffin Bay glaciomarine sediments from high-resolution paleomagnetic data. Geochem. Geophys. Geosyst. 13, 24. http://dx.doi.org/10.1029/2012GC004272.
Simon, Q., Hillaire-Marcel, C., St-Onge, G., Andrews, J.T., 2014. Northeastern laurentide, western Greenland and southern innuitian ice stream dynamics during the last glacial cycle. J. Quat. Sci. 29, 14–26.
Smith, L.M., Andrews, J.T., 2000. Sediment characteristics in iceberg dominated fjords, Kangerlussuaq region, East Greenland. Sediment. Geol. 130, 11–25.
Smith, N.D., Phillips, A.C., Powell, R.D., 1990. Tidal drawdown: a mechanism for producing cyclic sediment laminations in glaciomarine deltas. Geology 18, 10–13.
Solheim, A., Faleide, J.I., Andersen, E.S., Elverhoi, A., Forsberg, C.F., Vanneste, K., Uenzelmann-Neben, G., Channell, J.E.T., 1998. Late Cenozoic seismic stratigraphy and glacial geological development of the East Greenland and Svalbard Barents Sea continental margins. Quat. Sci. Rev. 17, 155–184.
St. John, K.E.K., Krissek, L.A., 1999. Regional patterns of Pleistocene ice-rafted debris flux in the North Pacific. Paleoceanography 14, 653–662.
Steffen, K., Box, J., 2001. Surface climatology of the Greenland ice sheet: Greenland climate network 1995–1999. J. Geophys. Res.-Atmos. 106 (D24), 33951–33964.
Stock, J.D., Montgomery, D.R., 1999. Geologic constraints on bedrock river incision using the stream power law. J. Geophys. Res. Solid Earth 104 (B3), 4983–4993.
Stokes, C.R., Clark, C.D., 2001. Palaeo-ice streams. Quat. Sci. Rev. 20, 1437–1457.
Stokes, C.R., Tarasov, L., 2010. Ice streaming in the Laurentide ice sheet: a first comparison between data-calibrated numerical model output and geological evidence. Geophys. Res. Lett. 37. http://dx.doi.org/10.1029/2009GL040990.
Stokes, C.R., Clark, C.D., Darby, D.A., Hodgson, D., 2005. Late Pleistocene ice export events into the Arctic Ocean from the M'clure strait ice stream, Canadian Arctic archipelago. Glob. Planet. Chang. 49, 139–162.
Stoner, J.S., Channell, J.E.T., Hillaire-Marcel, C., Kissel, C., 2000. Geomagnetic paleointensity and environmental record from Labrador sS core MD95-2024: global marine sediment and ice core chronostratigraphy for the last 110 kyr. Earth Planet. Sci. Lett. 183, 161–177.
Straneo, F., Heimbach, P., 2013. North Atlantic warming and the retreat of Greenland's outlet glaciers. Nature 504, 36–43.

Striberger, J., Bjorck, S., Benediktsson, I.O., Snowball, I., Uvo, C.B., Ingolfsson, O., Kjaer, K.H., 2011. Climatic control of the surge periodicity of an Icelandic outlet glacier. J. Quat. Sci. 26, 561–565.
Stroeven, A.P., Fabel, D., Hatterstrand, C., Harbor, J.A., 2002. Relict landscape in the Centre of the Fennoscandian glaciation: cosmogenic radionuclide evidence of tors preserved through multiple glacial cycles. Geomorphology 44, 145–154.
Svendsen, J.I., Mangerud, J., 1997. Holocene glacial and climatic variations on Spitsbergen, Svalbard. The Holocene 7, 45–57.
Svendsen, J.I., Mangerud, J., Elverhoi, A., Solheim, A., Schuttenhelm, R.T.E., 1992. The late Weichselian Glacial Maximum on Western Spitsbergen inferred from offshore sediment cores. Mar. Geol. 104, 1–17.
Svendsen, J.I., Astakov, V.I., Bolshiyanov, D.Y., Demidov, I., Dowdeswell, J.A., Gataullin, V., Hjort, C., Hubberten, H.W., Larsen, E., Mangerud, J., Melles, M., Moller, P., Saarnisto, M., Siegert, M.J., 1999. Maximum extent of the Eurasian ice sheets in the Barents and Kara Sea region during the Weichselian. Boreas 28, 234–242.
Svendsen, H., Beszczynska-Møller, A., Hagen, J.O., et al., 2002. The physical environment of Kongsfjorden–Krossfjorden, an Arctic fjord system in Svalbard. Polar Res. 21, 133–166.
Svendsen, J.I., Alexanderson, H., Astakhov, V.I., Demidov, I., Dowdeswell, J.A., Funder, S., Gataullin, V., Henriksen, M., Hjort, C., Houmark-Nielsen, M., Hubberten, H.W., Ingolfsson, O., Jakobsson, M., Kjaer, K.H., Larsen, E., Lokrantz, H., Lunkka, J.P., Lysa, A., Mangerud, J., Matiouchkov, A., Murray, A., Moller, P., Niessen, F., Nikolskaya, O., Polyak, L., Saarnisto, M., Siegert, C., Siegert, M.J., Spielhagen, R.F., Stein, R., 2004. Late Quaternary ice sheet history of northern Eurasia. Quat. Sci. Rev. 23, 1229–1271.
Swift, D.A., Nienow, P.W., Hoey, T.B., 2005. Basal sediment evacuation by subglacial meltwater: suspended sediment transport from haut glacier d'arolla, Switzerland. Earth Surf. Process. Landf. 30, 867–883. http://dx.doi.org/10.1002/esp.1197.
Swift, D.A., Persano, C., Stuart, F.M., Gallagher, K., Whitham, A., 2008. A reassessment of the role of ice sheet glaciation in the long-term evolution of the East Greenland fjord region. Geomorphology 97, 109–125.
Syvitski, J.P.M., 1989. On the deposition of sediment within glacier-influenced fjords: oceanographic controls. Mar. Geol. 85, 301–329.
Syvitski, J.P.M., Shaw, J., 1995. Sedimentology and geomorphology of fjords. In: Perillo, G.M.E. (Ed.), Geomorphology and Sedimentology of Estuaries: Developments in Sedimentology. Elsevier, New York, pp. 113–178.
Syvitski, J.P.M., Burrell, D.C., Skei, J.M., 1987. Fjords: Processes and Products. Springer Verlag, New York 379 pp.
Syvitski, J.P.M., Andrews, J.T., Dowdeswell, J.A., 1996. Sediment deposition in an iceberg-dominated glacimarine environment, East Greenland: basin fill implications. Glob. Planet. Chang. 12, 251–270.
Szczucinski, W., Zajaczkowski, M., Scholten, J., 2009. Sediment accumulation rates in subpolar fjords — impact of post-Little Ice Age glaciers retreat, Billefjorden, Svalbard. Estuar. Coast. Shelf Sci. 85, 345–356. http://dx.doi.org/10.1016/j.ecss.2009.08.021.
Taylor, J., Dowdeswell, J.A., Kenyon, N.H., Cofaigh, C.Ó., 2002a. Late Quaternary architecture of trough-mouth fans: debris flows and suspended sediments on the Norwegian margin. Geol. Soc. Lond., Spec. Publ. 203, 55–71.
Taylor, J., Dowdeswell, J.A., Siegert, M.J., 2002b. Late Weichselian depositional processes, fluxes, and sediment volumes on the margins of the Norwegian Sea (62–75°N). Mar. Geol. 188, 61–77.
Taylor, J., Tranter, M., Munhoven, G., 2002c. Carbon cycling and burial in the glacially influenced Polar North Atlantic. Paleoceanography 17 (1). http://dx.doi.org/10.1029/2001PA000644.
Thompson, L.G., Mosley-Thompson, E., Arnao, B.M., 1984. El-Nino Southern Oscillation events recorded in the stratigraphy of the tropical Quelccaya ice cap, Peru. Science 226, 50–53.
Thomson, S.N., Brandon, M.T., Tomkin, J.H., Reiners, P.W., Vásquez, C., Wilson, N.J., 2010. Glaciation as a destructive and constructive control on mountain building. Nature 467, 313–317. http://dx.doi.org/10.1038/nature09365.
Tomkin, J.H., 2007. Coupling glacial erosion and tectonics at active orogens: a numerical modeling study. J. Geophys. Res. Earth Surf. (2003–2012) 112 (F2).
Tomkin, J.H., 2009. Numerically simulating alpine landscapes: the geomorphologic consequences of incorporating glacial erosion in surface process models. Geomorphology 103, 180–188.
Tomkin, J.H., Braun, J., 2002. The influence of alpine glaciation on the relief of tectonically active mountain belts. Am. J. Sci. 302, 169–190.
Tremblay, M.M., Shuster, D.L., Balco, G., 2014. Cosmogenic noble gas paleothermometry. Earth Planet. Sci. Lett. 400, 195–205.
Tripati, A.K., Eagle, R.A., Morton, A., Dowdeswell, J.A., Atkinson, K.L., Bahe, Y., Dawber, C.F., Khadun, E., Shaw, R.M.H., Shorttle, O., Thanabalasundaram, L., 2008. Evidence for glaciation in the northern hemisphere back to 44 Ma from ice-rafted debris in the Greenland Sea. Earth Planet. Sci. Lett. 265, 112–122.
Truffer, M., Motyka, R.J., Harrison, W.D., Echelmeyer, K.A., Fisk, B., Tulaczyk, S., 1999. Subglacial drilling at Black Rapids Glacier, Alaska, USA: drilling method and sample descriptions. J. Glaciol. 45, 495–505.
Tulaczyk, S.B., Scherer, R.P., Clark, C.D., 2001. A ploughing model for the origin of weak tills beneath ice steams: a qualitative treatment. Quat. Int. 86, 59–70.
Van der Veen, C., 1996. Tidewater calving. J. Glaciol. 42, 375–385.
Vorren, T.O., Laberg, J.S., 1997. Trough mouth fans — palaeoclimate and ice-sheet monitors. Quat. Sci. Rev. 16, 865–881.
Vorren, T.O., Hald, M., Lebesbye, E., 1988. Late Cenozoic environments in the Barents Sea. Paleoceanography 3, 601–612.
Vorren, T.O., Richardsen, G., Knutsen, S., Henriksen, E., 1991. Cenozoic erosion and sedimentation in the western Barents Sea. Mar. Pet. Geol. 8, 317–340.
Vorren, T.O., Laberg, J.S., Blaume, F., Dowdeswell, J.A., Kenyon, N.H., Mienert, J., Rumohr, J., Werner, F., 1998. The Norwegian Greenland Sea continental margins: morphology and late Quaternary sedimentary processes and environment. Quat. Sci. Rev. 17, 273–302.
Walton, M.A.L., Gulick, S.P.S., Reece, R.S., Barth, G.A., Christeson, G.L., Van Avendonk, H.J.A., 2014. Dynamic response to strike–slip tectonic control on the deposition and evolution of the Baranof Fan, Gulf of Alaska. Geosphere 10, 680–691.
Warren, C., Aniya, M., 1999. The calving glaciers of southern South America. Glob. Planet. Chang. 22, 59–77.
Warren, C.R., Glasser, N.F., Harrison, S., Winchester, V., Kerr, A.R., Rivera, A., 1995. Characteristics of tidewater calving at Glaciar San Rafael, Chile. J. Glaciol. 41, 273–289.
Wellner, J.S., Lowe, A.L., Shipp, S.S., Anderson, J.B., 2001. Distribution of glacial geomorphic features on the Antarctic continental shelf and correlation with substrate: implications for ice behavior. J. Glaciol. 47, 397–411.
Wellner, J.S., Heroy, D.C., Anderson, J.B., 2006. The death mask of the Antarctic ice sheet: comparison of glacial geomorphic features across the continental shelf. Geomorphology 75, 157–171.
Wiles, G.C., Post, A., Muller, E.H., Molnia, B.F., 1999. Dendrochronology and late Holocene history of Bering Piedmont Glacier, Alaska. Quat. Res. 52, 185–195.
Wiles, G.C., Barclay, D.J., Calkin, P.E., Lowell, T.V., 2008. Century to millennial-scale temperature variations for the last two thousand years indicated from glacial geologic records of Southern Alaska. Glob. Planet. Chang. 60, 115–125.
Wilken, M., Mienert, J., 2006. Submarine glacigenic debris flows, deep-sea channels and past ice-stream behaviour of the East Greenland continental margin. Quat. Sci. Rev. 25, 784–810.
Willems, B.A., Powell, R.D., Cowan, E.A., Jaeger, J.M., 2011. Glacial outburst flood sediments within Disenchantment Bay, Alaska: implications of recognizing marine jökulhlaup deposits in the stratigraphic record. Mar. Geol. 284, 1–12.
Winsborrow, M.C.M., Clark, C.D., Stokes, C.R., 2010. What controls the location of ice streams? Earth Sci. Rev. 103, 45–59.
Winsor, K., Carlson, A.E., Rood, D.H., 2014. Be-10 dating of the narsarsuaq moraine in southernmost Greenland: evidence for a late Holocene ice advance exceeding the Little Ice Age maximum. Quat. Sci. Rev. 98, 135–143.
Yanites, B.J., Ehlers, T.A., 2012. Global climate and tectonic controls on the denudation of glaciated mountains. Earth Planet. Sci. Lett. 325–326, 63–75.
Yoon, H., Park, B., Domack, E., 1998. Distribution and dispersal pattern of suspended particulate matter in Maxwell Bay and its tributary Marian Cove, in the South Shetland Islands, West Antarctica. Mar. Geol. 152, 261–275.